

NPS ARCHIVE

1997.09  
CURRAN, P.

# NAVAL POSTGRADUATE SCHOOL Monterey, California



## THESIS

EXPLORING A CHROMATIC OBLIQUE EFFECT

by  
Paul G. Curran

September, 1997

Thesis Advisor:  
Second Reader:

William K. Krebs  
Samuel E. Buttrey

Thesis  
C9535

Approved for public release; distribution is unlimited.

DUDLEY KNOX LIBRARY  
NAVAL POSTGRADUATE SCHOOL  
MONTEREY CA 93943-5101

**DUDLEY KNOX LIBRARY  
NAVAL POSTGRADUATE SCHOOL  
MONTEREY, CA 93943-5101**

# REPORT DOCUMENTATION PAGE

Form Approved  
OMB No. 0704-0188

Public reporting burden for this collection of information is estimated to average 1 hour per response, including the time for reviewing instruction, searching existing data sources, gathering and maintaining the data needed, and completing and reviewing the collection of information. Send comments regarding this burden estimate or any other aspect of this collection of information, including suggestions for reducing this burden, to Washington headquarters Services, Directorate for Information Operations and Reports, 1215 Jefferson Davis Highway, Suite 1204, Arlington, VA 22202-4302, and to the Office of Management and Budget, Paperwork Reduction Project (0704-0188) Washington DC 20503.

1. AGENCY USE ONLY (Leave blank)		2. REPORT DATE September 1997	3. REPORT TYPE AND DATES COVERED Master's Thesis	
4. TITLE AND SUBTITLE <b>EXPLORING A CHROMATIC OBLIQUE EFFECT</b>			5. FUNDING NUMBERS	
6. AUTHOR(S) Curran, Paul G.				
7. PERFORMING ORGANIZATION NAME(S) AND ADDRESS(ES) Naval Postgraduate School Monterey, CA 93943-5000			8. PERFORMING ORGANIZATION REPORT NUMBER	
9. SPONSORING / MONITORING AGENCY NAME(S) AND ADDRESS(ES)			10. SPONSORING / MONITORING AGENCY REPORT NUMBER	
11. SUPPLEMENTARY NOTES The views expressed in this thesis are those of the author and do not reflect the official policy or position of the Department of Defense or the U.S. Government.				
12a. DISTRIBUTION / AVAILABILITY STATEMENT Approved for public release; distribution is unlimited.			12b. DISTRIBUTION CODE	
13. ABSTRACT (maximum 200 words) For centuries, military forces have used camouflage to obscure potential targets from the enemy. Because the eye is fairly adept at picking out edges, colors, and bright areas, camouflage is often used to degrade these qualities from human detection. The purpose of this thesis was to investigate the role of certain spatial, temporal, and chromatic features on the human visual system and how these features may aid the quest for better camouflage. Methods: Test patterns were spatio-temporal raised cosines of varying orientation (horizontal or vertical and oblique), spatial frequency (1, 3, and 7 cpd), and modulated at 2.0 Hz. Color contrast thresholds were determined from 16 different red-green color mixture ratios. This methodology eliminates the problems with luminance artifacts and the need to determine exact equiluminance. Results: The data formed an ellipse with the half-length measuring color discrimination and the half-width measuring brightness discrimination. A maximum likelihood method was used to fit the data. Three of the four subjects showed a 3 cpd chromatic oblique effect, while the 1 and 7 cpd achromatic and chromatic oblique effect was inconsistent across subjects. Conclusions: While real-world objects are more complex than laboratory stimuli, knowledge of spatial and chromatic qualities that inhibit detection will aid the quest for better camouflage.				
14. SUBJECT TERMS Oblique Effect, Ellipse, Camouflage			15. NUMBER OF PAGES 105	16. PRICE CODE
17. SECURITY CLASSIFICATION OF REPORT Unclassified	18. SECURITY CLASSIFICATION OF THIS PAGE Unclassified	19. SECURITY CLASSIFICATION OF ABSTRACT Unclassified	20. LIMITATION OF ABSTRACT UL	

NSN 7540-01-280-5500

Standard Form 298 (Rev. 2-89)  
Prescribed by ANSI Std. Z39-18



**Approved for public release; distribution is unlimited**

**EXPLORING A CHROMATIC OBLIQUE EFFECT**

Paul G. Curran  
Major, United States Marine Corps  
B.S., United States Naval Academy, 1987

Submitted in partial fulfillment of the  
requirements for the degree of

**MASTER OF SCIENCE IN OPERATIONS RESEARCH**

from the

**NAVAL POSTGRADUATE SCHOOL**  
**September 1997**



## ABSTRACT

For centuries, military forces have used camouflage to obscure potential targets from the enemy. Because the eye is fairly adept at picking out edges, colors, and bright areas, camouflage is often used to degrade these qualities from human detection. The purpose of this thesis was to investigate the role of certain spatial, temporal, and chromatic features on the human visual system and how these features may aid the quest for better camouflage. Methods: Test patterns were spatio-temporal raised cosines of varying orientation (horizontal or vertical and oblique), spatial frequency (1, 3, and 7 cpd), and modulated at 2.0 Hz. Color contrast thresholds were determined from 16 different red-green color mixture ratios. This methodology eliminates the problems with luminance artifacts and the need to determine exact equiluminance. Results: The data formed an ellipse with the half-length measuring color discrimination and the half-width measuring brightness discrimination. A maximum likelihood method was used to fit the data. Three of the four subjects showed a 3 cpd chromatic oblique effect, while the 1 and 7 cpd achromatic and chromatic oblique effect was inconsistent across subjects. Conclusions: While real-world objects are more complex than laboratory stimuli, knowledge of spatial and chromatic qualities that inhibit detection will aid the quest for better camouflage.

The following table shows the results of the experiment. The data indicates that the reaction rate is directly proportional to the concentration of the reactants. This is consistent with the proposed mechanism, which suggests that the reaction is first order with respect to both reactants. The rate constant,  $k$ , is determined to be  $0.025 \text{ s}^{-1}$ .

Concentration of A (M)	Concentration of B (M)	Initial Rate (M/s)
0.10	0.10	0.0025
0.20	0.10	0.0050
0.10	0.20	0.0050
0.20	0.20	0.0100

The reaction is first order with respect to both reactants, A and B. The rate constant,  $k$ , is  $0.025 \text{ s}^{-1}$ .



## TABLE OF CONTENTS

I.	INTRODUCTION .....	1
II.	BACKGROUND .....	3
III.	METHODS .....	25
	A. SUBJECTS .....	25
	B. APPARATUS .....	25
	C. STIMULI .....	26
	D. PROCEDURE .....	27
IV.	RESULTS .....	29
	A. CLASS-I TYPE ELLIPSES .....	34
	B. CLASS-II AND CLASS-III TYPE ELLIPSES .....	35
	C. STATISTICAL TESTS .....	35
V.	CONCLUSIONS .....	43
	APPENDIX A. S-PLUS CODE .....	45
	APPENDIX B. EXAMPLES .....	71
	LIST OF REFERENCES .....	75
	BIBLIOGRAPHY .....	81
	INITIAL DISTRIBUTION LIST .....	89



## ACKNOWLEDGMENT

The author would like to thank Professors Krebs and Buttrey for their extensive guidance and time commitments. Professor Essock and Mike Sinai at the University of Louisville and LCDR Don Lawson were also instrumental in the completion of this thesis. More importantly I would like to thank my wife Paige for her unwavering support which enabled this thesis to be completed.



## EXECUTIVE SUMMARY

For centuries, military forces have used camouflage to obscure potential targets from the enemy. Because the eye is fairly adept at picking out edges, colors, and bright areas, these are the qualities that camouflage seeks to degrade. The purpose of this thesis was to investigate the effects of certain spatial, temporal, and chromatic features on the human visual system and how these features may aid the quest for better camouflage.

Camouflage targets tend to match their backgrounds both in color and structure. Netting or paint can make detection of a potential target more difficult by reducing chromatic contrast. They can also reduce structural contrast by reducing sharp edge effects. This is evident in the "stealth" design in which the lack of defined edges helps reduce the radar signature. By removing defined edges, and thus high spatial frequency components, the visual signature is also reduced since "stealth" ships and aircraft generally have backgrounds consisting primarily of low frequencies (sea and sky). The perception aspects of this real world example can be simplified by examining less complex stimuli in the laboratory. For example, camouflage design would be affected if it were known that oblique chromatic lines were more difficult to detect than horizontal or vertical chromatic lines.

It has been shown that horizontal and vertical achromatic lines are easier to detect than oblique achromatic lines. This phenomenon is known as the "oblique effect," which in this case is an achromatic oblique effect. Several studies have shown that the magnitude of the oblique effect is largest with high spatial and a low temporal frequency sinusoidal gratings. Previous researchers have used this knowledge to design experiments testing for a chromatic oblique effect, but have had problems with luminance artifacts due to the difficulty of obtaining exact equiluminance. By adapting the methodology of an earlier researcher the problem of determining exact equiluminance was avoided and an experiment to test for a chromatic oblique effect was designed.

The experiment was conducted concurrently at the Naval Postgraduate School (NPS) and the University of Louisville, Kentucky (UL). Four subjects, 2 NPS and 2 UL, volunteered for this experiment. All subjects had normal (20/20), or corrected to normal, acuity and color

vision. Stimuli were presented by a VisionWorks computer graphics system (Vision Research Graphics, Inc.) on an IDEK MF-8521 high resolution color monitor (21" X 20" of viewable area). The monitor had a resolution of 800 by 600 pixels ( $x=75.02$  and  $y=74.92$  pixels/degree), 98.9 Hz frame-rate, mean chromaticity of  $r = 0.334$ ,  $g = 0.336$ ,  $b = 0.300$  (1931 CIE), and a maximum luminance of 100 cd/m<sup>2</sup>. The University of Louisville's apparatus and procedure were identical to the Naval Postgraduate School's, except that the stimuli were displayed on a 17" Nanao Flexscan F2.21 color monitor. Subjects viewed the monitor from 1.5 meters and were positioned by an adjustable chinrest.

Sinusoidal gratings were presented within a spatially windowed circular test field that subtended  $7.59^\circ$  of visual angle. The Gaussian window was truncated at  $\pm 1$  standard deviations for both  $x$  and  $y$  directions. The test patterns were one-dimensional spatio-temporal sinusoids of varying orientation (principal and oblique), spatial frequency (1.0, 3.0, and 7.0 cycles/degree), and color contrast. Test patterns for each subject consisted of two orientations, principal ( $0^\circ$  and  $90^\circ$ ) and oblique ( $45^\circ$  and  $135^\circ$ ). For each subject, maximum sensitivity for each orientation within the principal and oblique grouping was chosen. All sinusoids were raised cosines temporally modulated at 2.0 Hz. The sinusoid pattern was presented in a 1500 msec interval with contrast ramped on and off according to a linear window. (Contrast peaked at 202 msec and fell at 1304 msec. Color contrast was computed by different ratios of percent red and green. Sixteen different sinusoidal red-green color mixtures were generated by changing the red phosphor only, green phosphor only, or by changing the red and green guns in fixed proportions. Color contrast was defined according to the Michelson formula. Thresholds were determined by a sequential two-alternative forced choice adaptive psychometric procedure, QUEST. Threshold was defined at 75 percent correct. A total of 480 trials, 30 trials per condition, were randomly presented within each session. A session (~ 45 minutes) consisted of one sinusoidal condition with 16 different red-green color mixtures. A subject had to complete six sessions to contribute one set of 16 thresholds for each condition.

Numerous surveys of differential thresholds have been carried out, but one of the more extensive ones was completed by D.L. MacAdam. The data from this survey was elliptical (the

closed curves connecting the thresholds were elliptical in shape). It was shown that the errors of thresholds about these closed curves were Normally distributed, therefore the curves should be ellipses, as they appeared to be.

The elliptical properties of the experimental data were used to fit ellipses using the method of maximum likelihood a nested F-test (which is only approximate, because of non-linearity) was used to examine the significance of the different orientations. Results of this test showed that the chromatic oblique effect was inconsistent across the spatial frequencies of 1, 3 and 7 cycles/degree (cpd). The lack of a 1 cpd chromatic oblique effect was due to the insensitivity of the chromatic channel at the lower spatial frequencies. Two of the four subjects showed a graphical 7 cpd chromatic oblique effect, but this was non-significant. Chromatic aberration may have been a factor. Three of the four subjects showed a 3 cpd chromatic oblique effect with two significant and the third marginally significant. It is predicted that the marginally significant subject would show significance with additional trials.

The main value of this study is the tool it provides for further investigation of a chromatic oblique effect without the problems associated with luminance artifacts. Additionally, further investigation of a chromatic oblique effect will likely provide knowledge of spatial and chromatic qualities that inhibit detection. Knowledge of these qualities will aid the quest for better camouflage





# I. INTRODUCTION

The continual decline of the military budget has necessitated the increased protection of current and future war-fighting assets. This increase, coupled with public expectation of zero or close-to-zero casualties, has forced the services to reassess the way they conduct operations. Today's political climate necessitates this reassessment since the potential loss of public support for military actions generally increases with the number of American casualties.

A cruise missile attack is an effective method used to minimize civilian and friendly casualties. For example, cruise missile attacks were successful against Iraq's military targets during the Gulf War. Although the cruise missile is an effective weapon, it is an expensive resource for the United States military inventory. A less expensive alternative is an air strike, but the disadvantage of an air strike is the increased likelihood of aircrew casualties and missed targets. Ideally, the aviator would like to enter the threat zone undetected, thereby increasing the probability of locating the target without becoming engaged by the enemy.

The ability to avoid detection is a distinct advantage during battle. For centuries, the element of surprise has resulted in a quick and decisive destruction of forces. For example, the U.S. Air Force F-117 "stealth" fighter was responsible for much of the precision bombing during the Gulf War. Because their aircraft was nearly invisible within the Iraqi air defenses, pilots had additional time to accurately drop bombs on target. This near-invisibility must extend beyond the visible spectrum since today's battlefields are equipped with electro-optical sensors that often extend the range and increase the probability of detecting potential threats. Electro-optical sensors make detection possible through visual, infrared, thermal and other means. For example, shielding hot parts of a vehicle is part of the vehicle's thermal camouflage as it tries to disperse its thermal signature.

But, even with these technological advances, a large threat to operations, and to reconnaissance operations in particular, is often the most common sensor--an enemy's eyes. Prior to the start of the Gulf ground war, U. S. forces had reconnaissance teams operating in the interior of Kuwait. These teams used their speed and camouflage to prevent detection and capture. If their camouflage had been inadequate, capture and death would have been likely,

delaying the start of the ground offensive. While the saying “if they can't see you, they can't hurt you” is no longer true, the likelihood of being hurt is reduced when the enemy cannot see you.

To make the enemy's task of detection more difficult, camouflage is used. Since detection has traditionally been associated with *visual* detection, camouflage is generally thought of as making the visual detection of personnel or any potential target more difficult. It is in this sense that camouflage will be discussed.

Camouflage has many different applications, ranging from the clothes and face paint of an infantryman to the netting used to cover tanks and vehicles to the paint used on larger platforms such as aircraft and ships. Since the eye is fairly adept at picking out edges and bright areas, camouflage is often used to break up edges and to cover or conceal bright areas. All objects possess certain unique qualities of shape and color. In order to deceive a sensor, the object must blend with the background. An invisible object would match the background, while an easily identifiable target would contain noticeable spatial, temporal, or chromatic features. By manipulating the spatial, temporal and chromatic features, an object can be made more difficult to detect. Knowledge of the range of these features will aid military designers in their quest for better camouflage.

To understand how to make detection more difficult, one must also understand the sensors that will be used. Since, in this discussion, the primary sensors are the enemies' eyes, either directly or through some sort of image intensifying mechanism, a working knowledge of how the eye works and what cues it uses to accomplish detection is essential.

## II. BACKGROUND

The ability to perceive an object is an unconscious, automatic process. The world is filled with a variety of sensory information that stimulates our senses. This information is obtained through visual, auditory, tactile and olfactory inputs. We use our senses to collect this information and translate it into meaningful units of sensory awareness. This information is then relayed to the brain, resulting in the formation of perceptions. The brain then categorizes this sensory data and compares it to past experiences. Thus, perceptions are a culmination of sensory inputs that are organized into a meaningful representation of the outside world. The study of perception involves a complete understanding of the description of objects, appearances and events in the outside world (Sekuler and Blake, 1994). In brief, sensation and perception refer to a sequence of events: stimulation of an external object; machinery to capture this information; and translation of this information into electrical energy to form an experience. Perceptual experiences guide our actions in the world. This thesis investigates the different techniques of manipulating visual sensory input to change the appearance or perception of an object. (Sekuler and Blake, 1994)

The basic function of the eye is to capture visual sensory input or light and focus it on the retina, a thin layer of receptor cells located in the back of the eye. The light must pass through these retinal cells before reaching the photoreceptors, which convert the light into an electrical signal. This process of converting an external stimulus into a neural signal is called transduction. These neural signals are then sent through the network of retinal cells, which, in turn, are sent to the brain (Figure 2.1).

The human retina contains two major classes of photoreceptors, rods and cones. There are approximately 8 million cones and 120 million rods. The fovea, located at the center of the retina, has the greatest concentration of cones. The cones are sensitive to daylight and provide high-acuity color vision, while the rods are used for night viewing and are thought to be achromatic. Between five and ten percent of the total cone population are sensitive to short

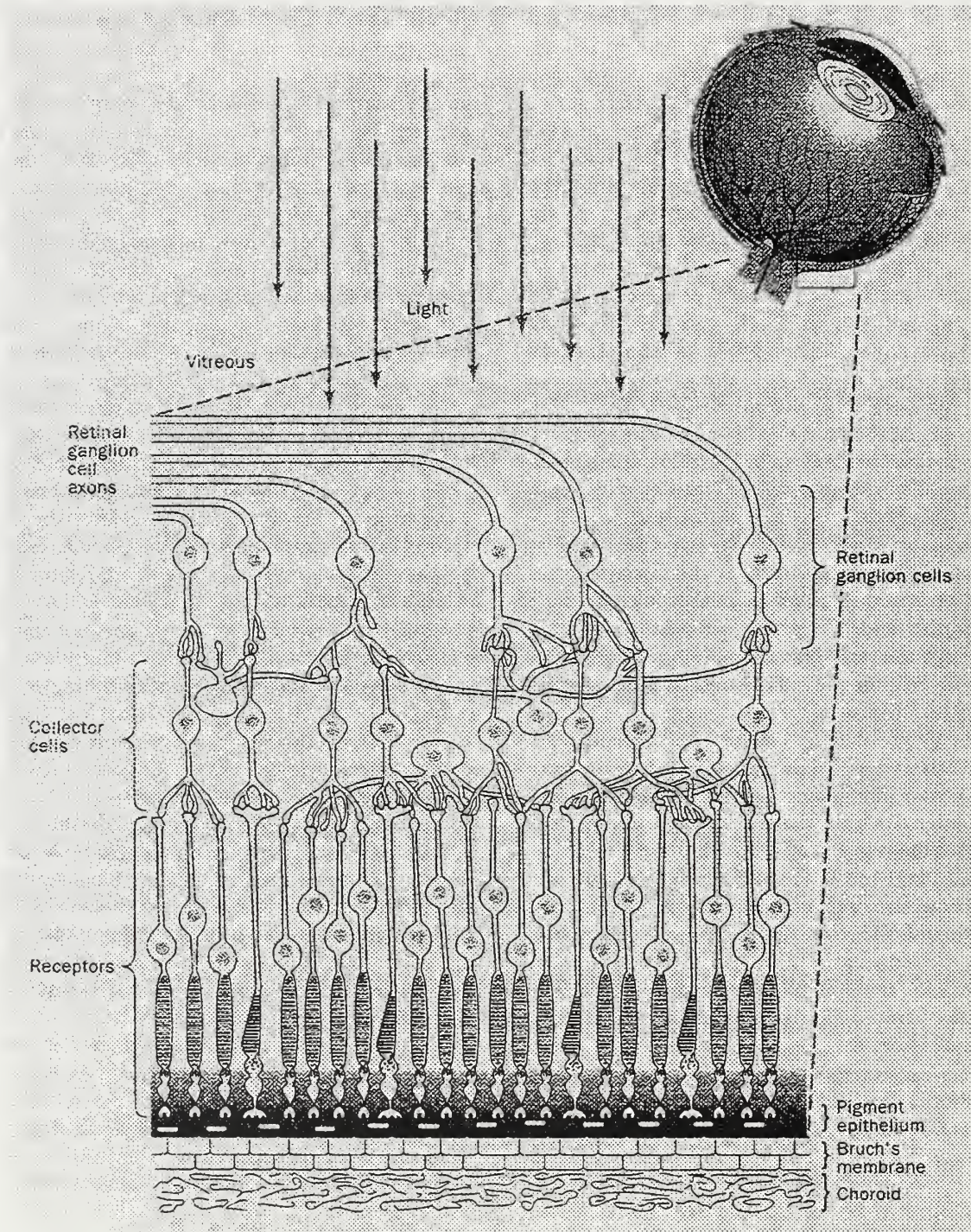


Figure 2.1. A cross section of the human retina. From Sekuler and Blake [1994].

wavelengths, with a peak sensitivity of 420nm. This cone class is referred to as S or blue cones. A few S cones are located at the fovea, but the largest concentration of S cones forms a ring around the fovea. This large concentration of cones tapers off with increasing distance (eccentricity) from the fovea. The remaining cone population is sensitive to middle (peak sensitivity of 530nm) and long wavelengths (peak sensitivity of 565nm). The long-wavelength (L or red) cones outnumber the middle-wavelength (M or green) cones two to one. The R and G cone distribution is randomly mixed throughout the retina, with the greatest concentration located inside the fovea. (Tovee, 1996)

While he did not directly identify cones, Thomas Young believed that the retina contained three receivers that were sensitive to a limited number of light vibrations. These receivers are now known as cones. Young also is responsible for one of the first explanations of how we perceive color. Earlier, Newton had demonstrated that white light could be split by a prism into a spectrum of colored lights. He found that recombining some of these colored lights resulted in the original white light. Newton mixed and subtracted colors, but he did not attempt to explain how we perceive color. Young, however, postulated that color perception is due to the vibrations of light interacting with the retina. The three receivers in the retina were broadly tuned with overlapping sensitivities. Helmholtz confirmed and elaborated Young's color theory by showing that there are three types of receivers (cones or photoreceptors) in the human retina, and that each type contains a different pigment. The spectral sensitivity of the cone is determined by the absorption spectrum of its photopigment. (McIlwain, 1996)

Young hypothesized that there were three broadly tuned receivers in the retina because, he reasoned, a single broadly-tuned receiver could not provide enough information about the wavelength of light. If there were two receivers, then there would be one particular frequency that excited both receivers equally, and thus white light would be produced (intersection of the curves in Figure 2.2b). Since Young did not observe white light in the color spectrum produced by a prism, he concluded that the visual system must have three broadly tuned receivers. A single cone pigment cannot discriminate between changes in wavelength and changes in the intensity of light. A cone can only increase or decrease its

output, so its signal is ambiguous as to whether the change is due to a shift in the light's wavelength or to a change in its intensity. This type of response is explained by the principle of univariance. For example, a retina that contains one cone class may give the same response to two different wavelengths, while a two-cone class retina may excite the receptors in different ratios (Figure 2.2). Therefore, the retina needs at least two cone types to distinguish between changes in wavelengths. Primate vision can discriminate millions of colors with three cone types, whereas non-primate mammals, which usually have two cone types, cannot. These mammals tend to rely much more heavily upon auditory and olfactory sensory inputs to survive. (Tovee, 1996)

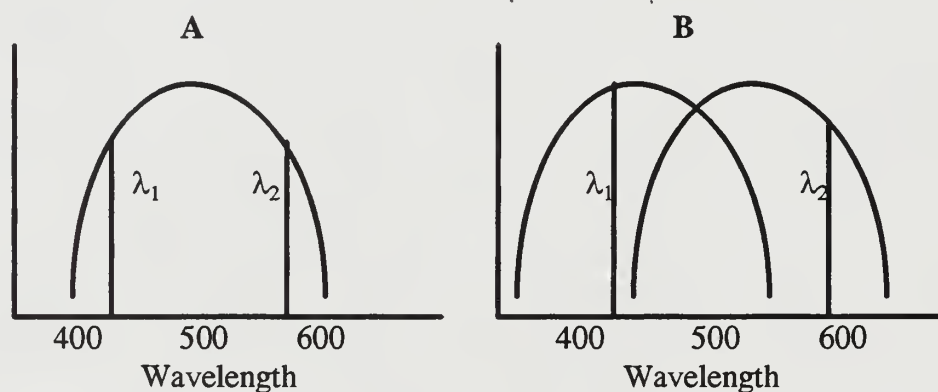


Figure 2.2. Wavelength discrimination by (a) a one-class retina and (b) a two-class retina. A retina that contains one cone pigment responds more or less with the same energy for some wavelength within its spectral sensitivity--the principle of univariance. A retina that contains two cone pigments will have different responses depending upon the location of the two wavelengths. From McIlwain [ 1996].

The Young-Helmholtz trichromatic theory accounts for many, but not all, of the phenomena associated with color vision. The theory predicts that a signal comprised of a certain combination of long and medium wavelengths cannot be distinguished from a specific third wavelength (yellow), but it does not account for the fact that the signal appears yellow rather than red-green or green-red. Additionally, the phenomenon where an object's color appears to vary depending on the colors viewed immediately before viewing the object (successive color contrast) or on the colors surrounding the object (simultaneous color

contrast), cannot be accounted for. A theory that does account for both these phenomena and those explained by the Young-Helmoltz theory is known as the opponent-color theory. (McIlwain, 1996)

The opponent-color theory was first introduced in 1878 by Hering and has been furthered through the work of Hurvitch and Jameson. Hering postulated that there were three visual processes, two chromatic and one achromatic. The processes consist of three antagonistic or opponent pairings. These pairings are red-green and yellow-blue for the chromatic processes and black-white for the achromatic process. Such opponent pairs are well explained by the center-surround or on-center and off-center type ganglion cells consisting of the aforementioned pairings. These opponent pairs account for the fact that the colors in these pairings cannot be seen at the same time; thus, there are no reddish-green hues. The inputs from the S, M and L cones in the first diagram of Figure 2.3 display in a simplified way how these inputs are combined to form a signal that we perceive as blue. The second diagram in the Figure is identical to the first, except that the weightings of these signals result in the perception of yellow instead of blue. Intermediate weightings of the signals displayed result in our perception of many more colors than the six shown in Figure 2.3. (Tovee, 1996)

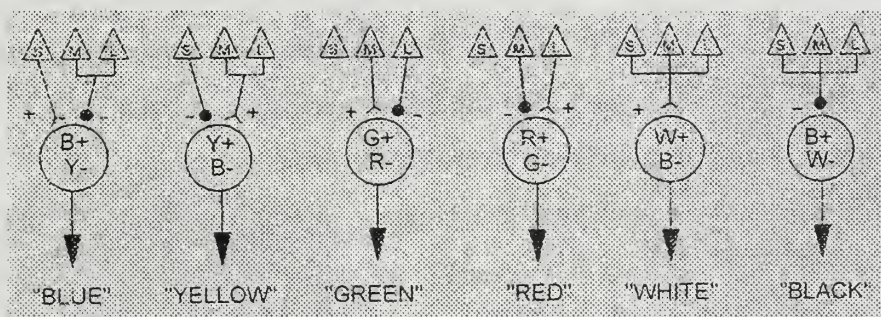


Figure 2.3. Simplified hypothetical display for a model based on color opponency. From McIlwain [1996].

The cones relay their information by synapsing onto ganglion cells, whose axons travel through the optic nerves to the visual cortex located in the back of the brain. The human eye contains approximately one million ganglion cells. The input of 128 million photoreceptor signals has been reduced to an output produced by these one million ganglion cells. In 1938,

Hartline discovered that the retinal ganglion cells of the frog were comprised of two concentrically shaped ring-like areas on the retina (Figure 2.4). He found that certain ganglion cells increased their electrical energy when a light was passed through their center or inner ring and decreased their electrical energy when a light was passed through the outer ring. Hartline called these ON-center ganglion cells. Cells that respond vigorously to a dark center and a light edge are called OFF-center ganglion cells. A network of such ON-center and OFF-center cells is responsible for providing edge detection as well as orientation information. Hartline's work laid the foundation for later work by Devalois (1958), who discovered that primate ganglion cells behaved in a similar manner. (Sekuler and Blake, 1996)

The morphological and physiological properties of primate ganglion cells are divided into three categories: large size  $P_\alpha$  or A cells, small size  $P_\beta$  or B cells, and  $P_\gamma$  or W-like cells. Livingstone and Hubel (1988) classify two major types of ganglion cells,  $P_\alpha$  and  $P_\beta$  cells, and their projections to different cortical regions within the primate visual system.  $P_\alpha$  cells (ten percent of ganglion cells) have high conduction velocities, transient responses, no color sensitivities, high contrast sensitivity and very good temporal frequency modulation.  $P_\beta$  cells (80 percent of ganglion cells) have lower conduction velocities, sustained responses, low contrast sensitivity, color opponency and moderate temporal resolution. Both  $P_\alpha$  and  $P_\beta$  neurons are segregated into two different pathways which project to different locations within the lateral geniculate nucleus (LGN), V1, and higher cortical regions within the primate cortex (Livingstone and Hubel, 1984). Refer to Figure 2.5 for a graphical representation of the visual pathway. (Merigan, 1989)

The magnocellular pathway (M pathway) receives input from  $P_\alpha$  ganglion cells that project first to layers 1-2 of the LGN. Cells in the magnocellular geniculate layers project to layer 4C $_\alpha$  of the primary visual cortex. From layer 4C $_\alpha$  they project to layer 4B, which, in turn, projects to visual area 2 and to the medial superior temporal area (Tovee, 1996). This pathway is thought to involve spatial awareness, that is, 'where' an object is located in space. Alternatively, the parvocellular pathway (P-pathway) receives input from  $P_\beta$  ganglion cells and first projects to layers 3-6 of the LGN. Cells in the parvocellular



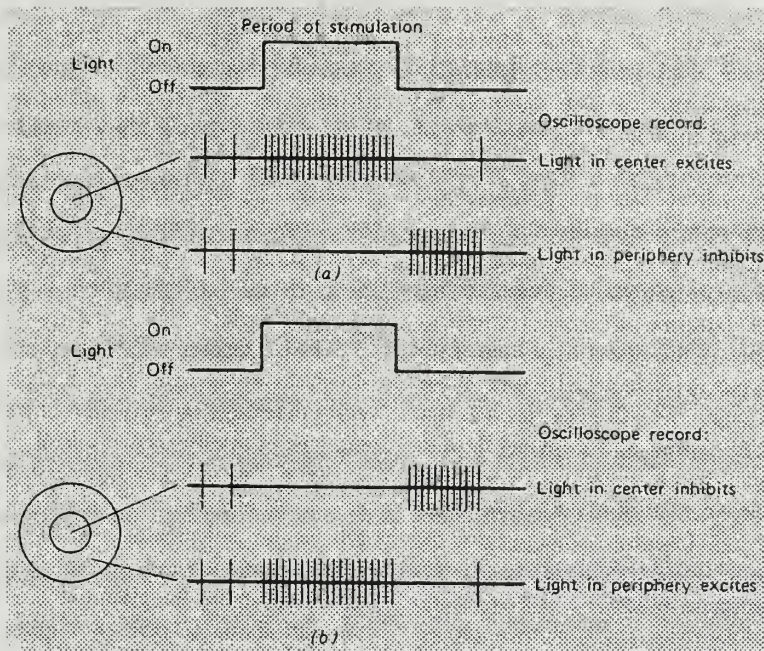


Figure 2.4. Receptive field layout of a retinal ganglion cell with (a) an “ON” center excitatory and “OFF” periphery inhibitory and (b) an “OFF” center excitatory and “ON” periphery inhibitory. From Schiffman [1996].

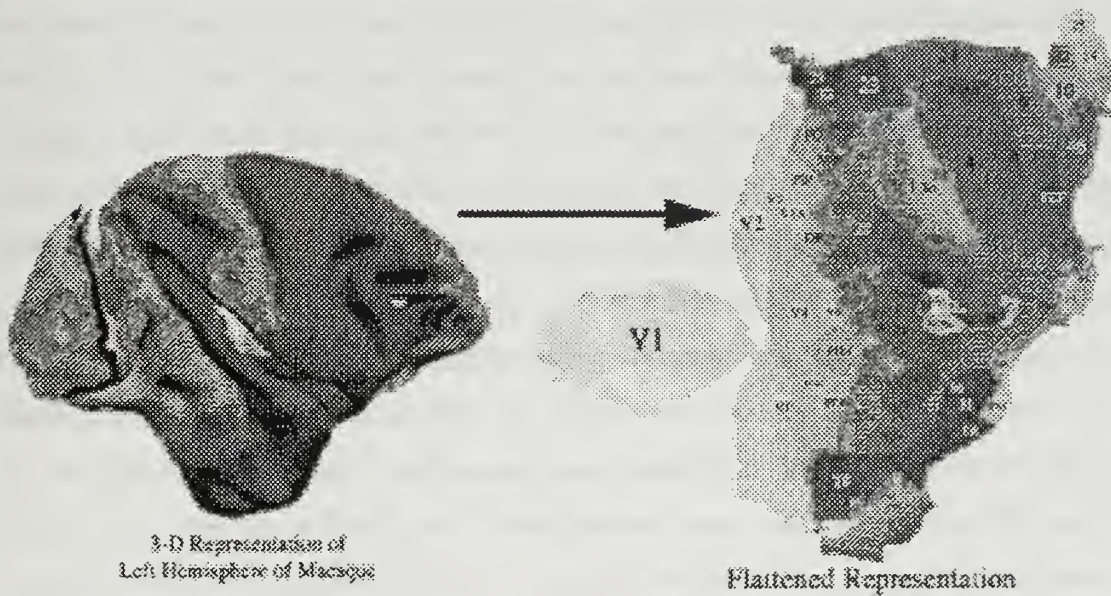


Figure 2.5. Images were obtained from Dr. Van Essen’s laboratory home page, Washington University, St. Louis, Mo.

geniculate layers project to layer  $4C_{\beta}$  in the primary visual cortex. From layer  $4C_{\beta}$  they, in turn, project to layers 2 and 3. From these two layers, information is sent to visual area 2, layer 4, and then to the inferior temporal cortex (Tovee, 1996). The inferior temporal cortex is thought to be concerned about the 'what' of an object. In summary, a crude but simple classification of the P and M pathways can be characterized as the 'what and where' of objects that an observer perceives. (Livingstone and Hubel, 1988)

Scientists have learned about the P and M pathways and their contributions to vision through studies that observed one pathway after the other pathway had been made inoperative by lesioning it. In 1990, Schiller and Logothetis created lesions in the P or M pathway of monkeys and then conducted various tests, including color perception, texture perception, acuity, pattern perception, flicker perception, and contrast perception. The results of these tests indicate that particular functions do tend to be associated with a specific pathway. In general, the P pathway is associated with color perception, texture perception, pattern perception, acuity, and contrast perception, whereas the M pathway is associated with flicker and motion perception. While only parvocellular lesions had an effect on the monkey's ability to discriminate between subtle color differences, these same lesions did not affect the monkey's ability to detect a single large target whose color differed from its background, even when the target was equiluminous with its background. This implies that the M pathway is capable of conducting some gross color information and can do so at isoluminance. While lesions in the M pathway resulted in a deficit of flicker perception, this was universally true for high temporal frequencies only. For low temporal frequencies, lesions in the M pathway had no effect, thus demonstrating that the P pathway is capable of transmitting low temporal frequency information. (Sekuler and Blake, 1994)

The P pathway also provides information to bloblike regions of the visual cortex. Unlike most ganglion cells, the cells in these bloblike regions are not at all concerned about orientation. These cells called blobs exhibit color opponency in a manner similar to that of the ON and OFF center cells. However, these cells turn ON and OFF in response to a specific chromatic illumination instead of an overall illuminance (Sekuler and Blake, 1994). Having this

basic physiological background, we can now focus on possible physiological explanations for a phenomenon known as the “oblique effect.”

It is well documented that horizontal and vertical lines are easier to see than lines at oblique angles, a phenomenon known as the “oblique effect” (Campbell, Kulikowski and Levinson., 1966; Appelle, 1972). This phenomenon has been observed in a variety of visual tasks. Essock (1980) divided the oblique effect into two classes. Oblique effects arising from basic visual functions such as detection, acuity, and other measures of sensitivity are termed Class I oblique effects. The Class I oblique effect is not caused by a bias in the optics of the eye (Campbell and Kulikowski, 1966), but is thought to result from the orientation bias of the P-cells located in the visual cortex (Lennie, 1974). Several studies have shown that an oblique effect is most observable when a stimulus with a high spatial frequency and a low temporal frequency is presented to the fovea (Maffei and Fiorentini, 1973; Berkley, Kitterle and Watkins, 1975; Camissa, Blake and Lema, 1977).

Class II oblique effects arise from tasks that require subsequent processing of stimulus information. For example, a task measuring the detection threshold of a stimulus oriented either obliquely or non-obliquely would result in a Class I oblique effect. When an observer must press one of two buttons indicating whether two simultaneously-presented stimuli of various orientations are the same, or whether they are different, the result would be a Class II oblique effect. This Class II oblique effect would be the result of encoding or further processing of stimulus information required for task completion. An important distinction, however, is that the Class I oblique effect discussed above results from achromatic stimuli. For chromatic stimuli, the results are not clear and leave uncertainty as to whether an oblique effect exists (Kelly, 1975b; Murasagi and Cavanagh, 1989). This thesis explores a Class I oblique effect and will be specific as to whether this oblique effect is a result of achromatic or chromatic stimuli. (Essock, 1980)

There are various hypotheses explaining why the oblique effect exists. One suggests that the world we live in, especially urban areas, contains more stimuli oriented horizontally or vertically as opposed to obliquely; thus, visual experience plays a role in determining sensitivity (Annis and Frost, 1973). However, the oblique effect has been demonstrated with infants as

young as six weeks old (Leehy, Moskowitz-Cook, Brill and Held, 1975). It seems unlikely that the visual experience of infants would be sufficient to account for the oblique effect. To further confuse the issue, it has been shown that with extensive practice detecting diagonal lines, observers may improve their oblique sensitivity until it is equal to their sensitivity for detecting horizontal and vertical lines (Mayers, 1983; Krebs, 1992). A more widely accepted hypothesis suggests that more cells are tuned to vertical and horizontal stimuli than to oblique stimuli.

Similarly disputed is whether the oblique effect is a retinal or a neural phenomenon. Campbell and Kulikowski (1966) and Mitchel and Muir (1967) used lasers to bypass the optics of the eye by projecting stimuli directly onto the retina. The oblique effect was obtained in both studies. Other studies involving head tilt (Rock and Heimer, 1957; Attneave and Reid, 1968) further investigated whether the oblique effect was a retinal phenomenon. When subjects viewed tilted stimuli with their heads tilted the same amount as the stimuli, the stimuli were retinally upright, but phenomenally oblique. (“Phenomenally” describes the stimuli’s orientation in the visual frame of reference of the subject [Lasaga and Garner, 1983]. The phenomenal frame of reference in this case would be gravitational.) Other, similar studies have adopted an arbitrary frame of reference (Rock and Heimer, 1957). In a study by Attneave and Reid (1968), subjects were told to think of the top of their heads as vertical, regardless of whether or not they were tilted. For head-tilt experiments in which subjects had their heads tilted 45 degrees, stimuli that were horizontal/vertical were retinally oblique, but were phenomenally upright. Unless otherwise instructed, subjects tended to adopt a phenomenal frame of reference rather than a retinal frame of reference. Therefore, when a subject’s head was tilted 45 degrees, an oblique effect was obtained for oblique stimuli, even though these stimuli were not retinally oblique (Attneave and Olsen, 1967). However, when subjects were told to think of the top of their heads as vertical, regardless of their 45 degree head tilt, they displayed an oblique effect for stimuli that were gravitationally upright, but retinally oblique (Attneave and Reid, 1968). In light of these studies, the oblique effect is highly unlikely to be a retinal phenomenon.

Another possible cause of the oblique effect is a neural phenomenon. This hypothesis, and that the origin of this neural phenomenon arises in the P pathway, seem credible even without the additional evidence provided by Rabin's (1992 and 1994) work with Visual Evoked Potentials (VEPs). The P pathway is responsible for acuity information and, thus, spatial information and is capable of processing low frequency temporal information. The Class I oblique effect has been observed primarily at high spatial frequencies and low temporal frequencies.

While the origin of the Class I achromatic oblique effect has been disputed, the dispute about a Class I chromatic oblique effect is not over its origin, but over its very existence. One of the earliest articles discussing the Class I oblique effect and chromaticity is a 1975 study by D. H. Kelly.

The stimuli Kelly used in the experiment were striped luminous-contrast gratings flickering sinusoidally. A grating is a pattern of adjacent light and dark bars or stripes, and a sinusoidal grating, shown in Figure 2.6, has a gradual transition from light areas to dark areas with no sharp edges (Schiffman, 1996). The gratings were presented horizontally, vertically,

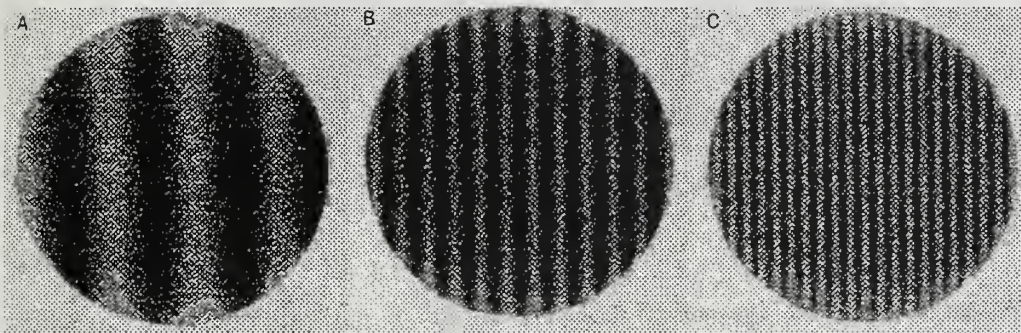


Figure 2.6. Sinusoidal gratings. Wide stripes correspond to low spatial frequencies. As the spatial frequency increases the stripes become thinner.

and at angles of 45 and 135 degrees (obliquely). A plot of the mean threshold at each orientation for various temporal frequencies ranging from approximately 1-40 hertz is shown in Figure 2.7. As the figure shows, the thresholds for the oblique presentations are consistently

lower than those for the non-oblique presentations for all temporal frequencies. This result is consistent with previous results. (Kelly, 1975)

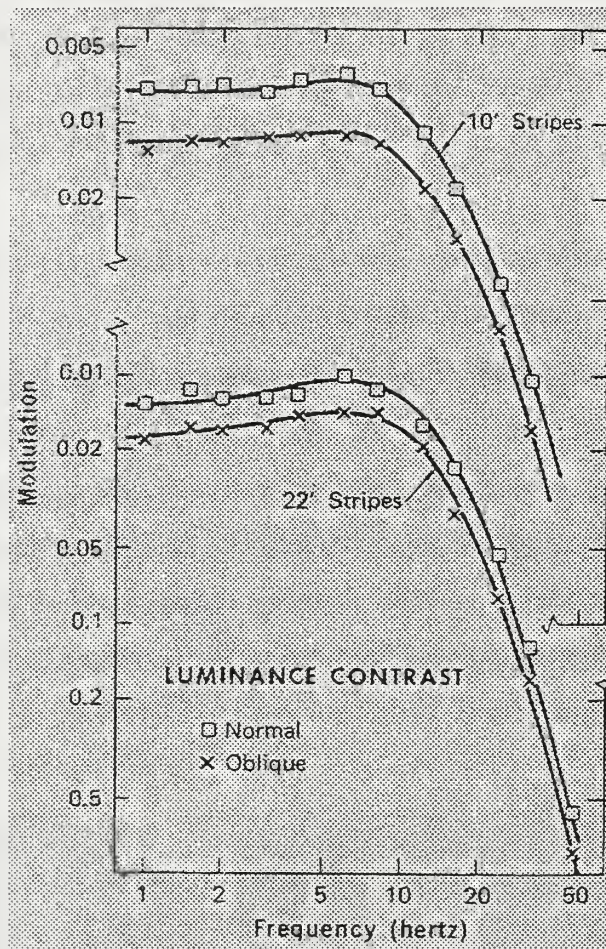


Figure 2.7. Achromatic sine-wave flicker sensitivity curves.  $10' = 3$  cpd and  $22' = 1.36$  cpd. From Kelly [1975].

Although this result was consistent, Kelly wanted to test the hypothesis that luminous contrast was a necessary condition for the oblique effect. He repeated the experiment, but changed the stimulus to a red-green equiluminous grating. The thresholds obtained, presented in Figure 2.8, showed that for the 10-minute stripes, an oblique effect was present for temporal frequencies under approximately 10 hertz. However, for the 22-minute stripes, no oblique effect was observed. This is due to the luminous grating sensitivity decreasing with decreasing spatial frequency, whereas chromatic grating sensitivity remains constant (Kelly, 1975). Kelly

concluded that the oblique effect for the 10-minute stripes was probably a hybrid response resulting from a spurious luminous component. This spurious luminous component was likely

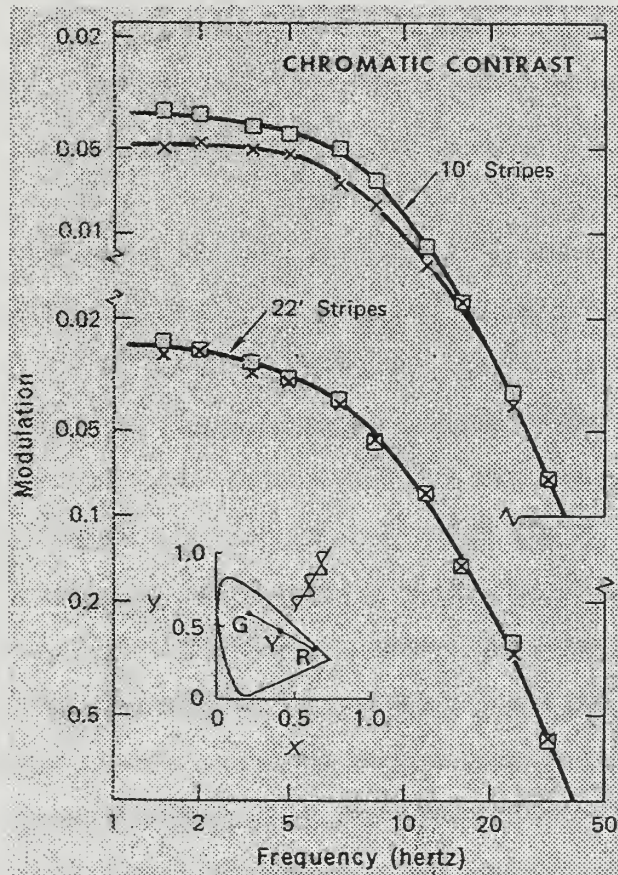


Figure 2.8. Chromatic sine-wave flicker sensitivity curves. From Kelly [1975].

a result of the stimuli not being isoluminant for the observer. Obtaining exact isoluminance is not an easy task. (Kelly, 1975)

Kelly provided a study that could be used directly in the dispute over a possible Class I chromatic oblique effect. Other studies were used indirectly and provided better tools or research methods. One such study by Mullen (1985) had important implications for future vision research in this area.

Mullen's article, "The Contrast Sensitivity of Human Colour Vision to Red-Green and Blue-Yellow Chromatic Gratings," described an innovation with her experimental design which led to measurements without any type of chromatic aberration. By using a large field size, she was able to measure thresholds for low spatial frequencies without the reduction in luminous sensitivity shown to occur with spatial frequencies below approximately four cycles/deg. Instead of using only one chromatic intensity value for all specific spatial frequencies, as had often been done before, Mullen used a number of selected points. This provided more accuracy. These factors combined to give the chromatic contrast sensitivity function (CSF) obtained for red-green gratings a much different look than previously thought. The CSF still had the same basic shape, but the cutoff for high frequencies occurred much earlier at approximately 10-12 cycles/deg. (Mullen, 1985)

The CSF is a method used to describe the visual system's sensitivity to sinusoidal waveforms. Contrast, as defined in a CSF, is a relative measure that is computed rather than measured. Contrast, the difference between stimuli elements, is formally defined as the amplitude of a waveform relative to its mean. Therefore, at a mean luminance level of .5 cd/m<sup>2</sup>, a sinusoidal grating with a contrast of 50 percent would have a trough of .25 and a peak of .75 cd/m<sup>2</sup>. This same waveform at a mean luminance level of 500 cd/m<sup>2</sup> would still have a contrast of 50 percent if its peak were at 750 and its trough were at 250 cd/m<sup>2</sup> (Schiffman, 1996). The use of sensitivity (1/threshold contrast) in CSF is similar to everyday usage; therefore, a low detection threshold is equivalent to high sensitivity. (Schiffman, 1996)

A CSF for spatial frequency is shown in Figure 2.9. Peak sensitivity is found at approximately three cycles per degree (cpd), with approximately 50 cpd being the cutoff for high frequency acuity.

Prior to Mullen's work, studies with red-green stimuli used frequencies more than 20 cpd and suggested resolution above 25 cpd (Mullen, 1985). Mullen's work provided a template for further research. It is not by coincidence that Murasagi and Cavanagh's 1989 article dealing with the chromatic oblique effect, and using red-green stimuli, chose spatial frequencies under the 10-12 cpd cutoff proposed by Mullen.



This article by Murasagi and Cavanagh further explored earlier work by Kelly regarding the oblique effect for luminous, as well as chromatic, stimuli. Kelly had postulated the absence of an oblique effect for chromatic channels if the opponent-color

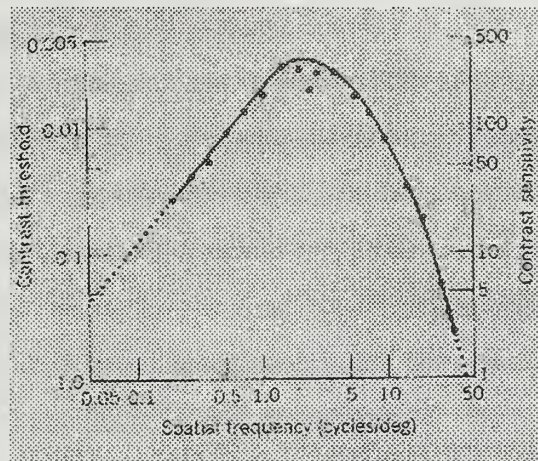


Figure 2.9. Contrast Sensitivity Function. From [Schiffman, 1996].

pathways for humans, like those in monkeys, were not orientation selective. However, research published the same year as Kelly's article (Poggio, Baker, Mansfield, Sillito and Grigg, 1975), as well as additional research a few years later (Michael, 1978), revealed that monkeys might possess orientation selectivity in their chromatic channel. The possibility of the chromatic channel analyzing orientation independently of the luminous channel led the authors to design an experiment to test this possibility in humans by determining if an oblique effect obtained with chromatic stimuli differed from that obtained with strictly achromatic stimuli. (Murasagi and Cavanagh, 1986)

To test this possibility, the researchers used a constant temporal frequency of 2 Hz and spatial frequencies of 2, 4 and 8 cpd were used. The stimuli were sinusoidal gratings. The gratings were presented at oblique (45 and 135 degrees) and non-oblique (0 and 90 degrees) angles. Axial chromatic aberration was taken into account by having the subjects view the stimuli through an achromatizing lens. A revised ascending method of limits was used to determine thresholds for both luminance and chromatic stimuli. Since the production of an isoluminant stimulus is a non-trivial matter, with isoluminance varying slightly from subject to subject, Murasagi and Cavanagh used stimuli in five different areas

in the neighborhood of equiluminance. The maximum threshold for the spatiotemporal region they were investigating was assumed to occur at equiluminance. They made this assumption because a chromatic grating with no luminous component should be the hardest to detect, as detection is by color alone rather than by color and luminance.

A significant main effect of orientation was present for all observers, as was a significant three-way interaction between grating types. Spatial frequency and orientation effects were present for three of the four observers. This showed that, for three of the four observers, the effects of the four orientations at certain spatial frequencies were different for achromatic and chromatic stimuli.

Like Kelly, Murasagi and Cavanagh have possible problems with spurious luminous components. By taking five measurements in the neighborhood of equiluminance, the contribution of these components has probably been reduced. However, if the actual isoluminance point were in a region between the areas they picked, then a luminous component would be present in their stimuli. Additionally, while spatial frequencies of 2, 4 and 8 cpd were used, a chromatic oblique effect was present only at 8 cpd for three of the four observers. At 8 cpd, chromatic aberration is a factor. The researchers used an achromatizing lens to account for axial chromatic aberration, but they did not take into account lateral chromatic aberration. *Post hoc* analysis minimized the possibility of this being a factor. As the authors themselves state, any slight misalignment between a subject and the achromatizing lens would result in a spurious luminance component. (Murasagi and Cavanagh, 1986)

During the same time frame as the Murasagi and Cavanagh work, Bradley, Switkes and De Valois, were also exploring Kelly's earlier work. The authors designed an experiment to compare the visual processing of chromatic and luminance information. The prolonged viewing or adaptation of a sinusoidal grating desensitizes the observer to similar gratings, especially when the similarity is in orientation or spatial frequency. However, this desensitivity is not present for gratings with orientations differing by approximately 45 degrees or spatial frequencies differing by 1.5 octaves. Thus, this adaptation has been termed selective.

The effects of selective adaptation have been used as psychophysical evidence for the presence of spatial frequency-selective and orientation-selective neurons in the human visual system. However, the behavior of cells displaying selective adaptation for spatial frequency when measured psychophysically has not always been consistent with their physiology. Thorell, De Valois, and Albrecht (1984) observed neurons that displayed different spatial frequency tuning depending on whether the stimulus contained luminance or color. They observed low-pass tuning for chromatic gratings, but band-pass tuning for luminance gratings. Additional studies by Livingstone and Hubble (1984) and Lennie, Sclar and Krauskopf (1985) found that cells in the visual cortex that responded to isoluminant color contrast did not display selective adaptation for orientation or spatial frequency. (Bradley, Switkes and De Valois, 1988)

Bradley et al. (1988) set out to explore this inconsistency with spatial frequency adaptation and orientation for chromatic gratings. The zero contrast condition for all gratings was a uniform yellow field with a chromaticity that was adjusted for each observer's differing sensitivity to red and green phosphor emissions. This varying of the zero contrast condition enabled presentation of the red-green sinusoidal gratings at each observer's isoluminance axis. Both isochromatic and isoluminant gratings were presented and were viewed through an achromatizing lens. To overcome problems associated with making repeated measurements of a decaying effect, the researchers used a long initial adaptation period followed by alternation of a brief stimulus presentation with a brief adaptation period. The stimuli used for adapting was a 2 cpd grating, run separately for each of the four possible conditions of horizontal or vertical and luminance or chromatic. For a spatial frequency of 2 cpd, thresholds for luminance gratings were similar in both pre- and post-adaptation trials for oblique angles and showed the desensitivity expected at horizontal and vertical angles. However, while the pre-adaptation data for chromatic gratings at this frequency did not show an oblique effect, an oblique effect was evident in the post-adaptation data. (Bradley, et al., 1988)

A similar experiment varying spatial frequency while keeping orientation constant confirmed that, for varying spatial frequencies, a specific spatial frequency adaptation

effect can be observed for sinusoidal luminous gratings. This experiment was repeated with chromatic gratings, and a specific spatial frequency adaptation effect was also observed with sinusoidal chromatic gratings. The results of this study along with previous psychophysical studies demonstrating the parallels between the data for luminance and color (De Valois and Switkes, 1983; Switkes and De Valois, 1983; and Ware and Mitchell, 1974) suggest that for the beginning stages of human vision, color and luminance are processed in a similar manner. (Bradley, et al., 1988)

In addition to the numerous psychophysical studies on the oblique effect, other studies have been conducted electrophysiologically. When studying primates or other animals, collecting data is often not possible through psychophysical means. Although an animal may not be able to verbalize or react, a response may still be obtained electrophysiologically. By electrically stimulating an individual cell, it is possible to monitor the cell output. VEPs provide an additional method of studying the role of chromatic patterns in perception (Rabin, 1994). In Rabin's 1992 paper "VEP's in Three-Dimensional Color Space," a Class I oblique effect at isoluminance or a chromatic oblique effect was shown at the spatial frequency of 1 cpd. Psychophysically, the Class I oblique effect for luminance or chromaticity is typically not obtained at low spatial frequencies.

The Class I oblique effect for achromatic stimuli has been obtained under a number of different conditions. It has been demonstrated psychophysically (Campbell and Kulikowski, 1966; Camisa, et al., 1977) and electrophysiologically (Maffei and Campbell, 1970; Rabin, Switkes, Crognale, Schneck and Adams, 1994). Electrophysiologically the oblique effect is evident by comparing the output of microelectrodes for oblique and non-oblique stimuli. These microelectrodes monitor the VEPs of cells as they are exposed to different stimuli. Psychophysically, the Class I oblique effect is evident by comparing the responses of subjects for oblique and non-oblique stimuli. A Class I chromatic oblique effect could be measured the same way. However, the Class I oblique effect for chromatic stimuli has not been obtained under various conditions, and whether such an oblique effect actually exists is a matter of debate. To participate in this debate, it is necessary to understand how the information that the eye collects is processed. One explanation is that

the eye uses a process similar to Fourier analysis so named after the nineteenth century mathematician responsible for this analysis.

Jean Baptiste Fourier studied how heat flows through an object when it is heated up and found that heat behaved in waves. He modeled these waves using complex equations, and discovered that they consist of periodic waveforms. Fourier found that any quantity that changed in a complex manner over time could be converted into a series of simple sinusoidal functions. Each sinusoidal pattern could be defined by its period, frequency, and angular velocity. This process is now known as Fourier analysis. (Who is Fourier?, 1995)

Fourier analysis can be used to analyze a natural scene by decomposing it into a sum of a series of sinusoidal components, each having a different spatial frequency, amplitude, and orientation. Vision scientists believe that the human visual system uses a process similar to Fourier analysis to process visual imagery. The human eye receives different intensities of light reflected from an object. These light intensities pass through the cornea and filter down into the photoreceptors. The photoreceptors then send an electrical signal to the brain, where these neural responses are categorized into specific spatial channels. Psychologists believe that this sensory input is transformed into a neural response, which is then categorized into a perceptual experience. If the visual system passes the image, and this image corresponds to a perceptual experience, then the observer can recognize the object. However, if your cornea is degraded--e.g., a cataract--high spatial frequency sinusoidal waves will not pass through the lens and be sent to the brain. A degraded signal such as this or a lack of a similar perceptual experience may result in failure to recognize the object. The absence of high spatial frequencies will cause the image to appear blurry. In some cases, the amplitude of those missing high spatial frequencies can be increased so that these signals can be sent to the brain.

Scene (Figure 2.10) can be broken down into many different visual components by Fourier analysis or other tools. These components or parameters include color, orientation, and spatial qualities and include the scene as a whole, as well as for the individual objects that comprise the scene. By manipulating the parameters of an object

(e.g., armored personnel carrier [APC]) in a scene, it is possible to camouflage this object. This may be done by changing the object's color to match that of its background through

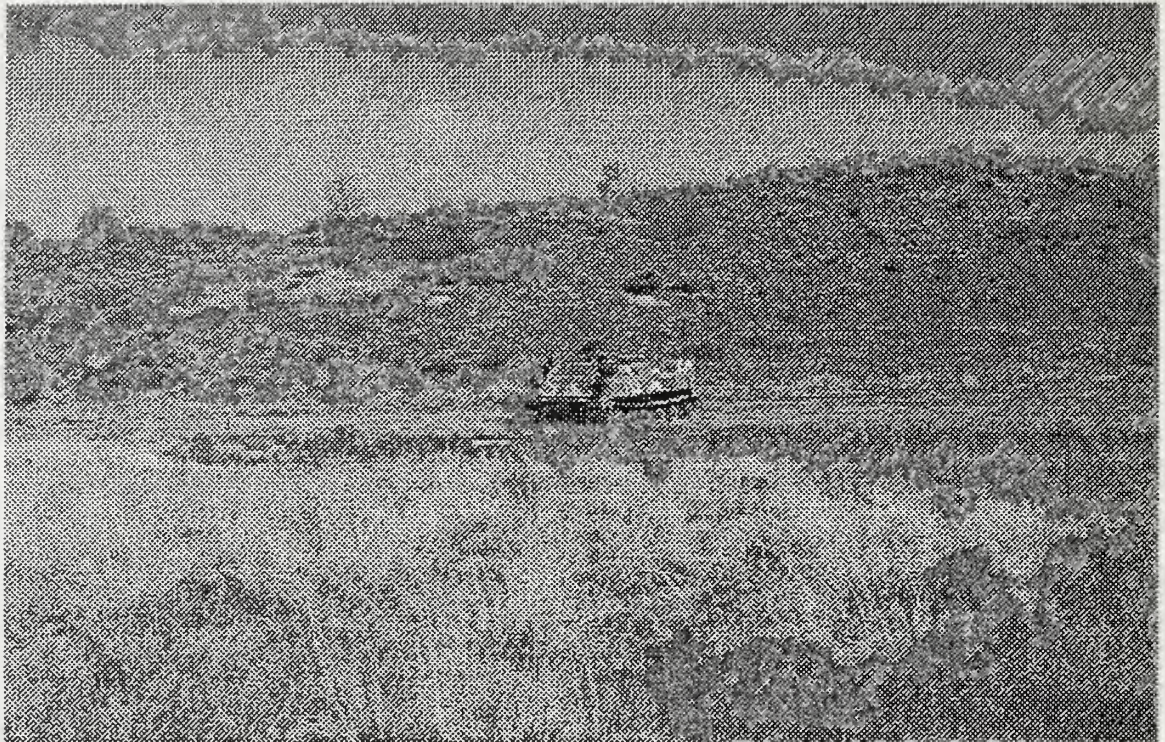


Figure 2.10. Armored Personnel Carrier

temporary means such as netting, or by more permanent means such as paint. A Fourier analysis shows the spatial composition of the scene. The low spatial frequencies are located in the center of Figure 2.11, and the high spatial frequencies are found in the corner regions of the figure. The high spatial regions result from the edges of the APC. These high spatial frequencies contrast with the low spatial frequencies found elsewhere in the scene. Netting would reduce these high spatial frequencies and would also lessen the edge effect evident in Figure 2.12, thereby enhancing the APC's camouflage.

We have looked at a scene's color, orientation, and spatial information and how these parameters can be manipulated to achieve better camouflage. The parameters manipulated in the experiment in this thesis are spatial and orientation. Since the Class I oblique effect has been primarily observed at low temporal and high spatial frequencies, a temporal frequency of 2 Hz and spatial frequencies of 1, 3 and 7 cpd were chosen. The

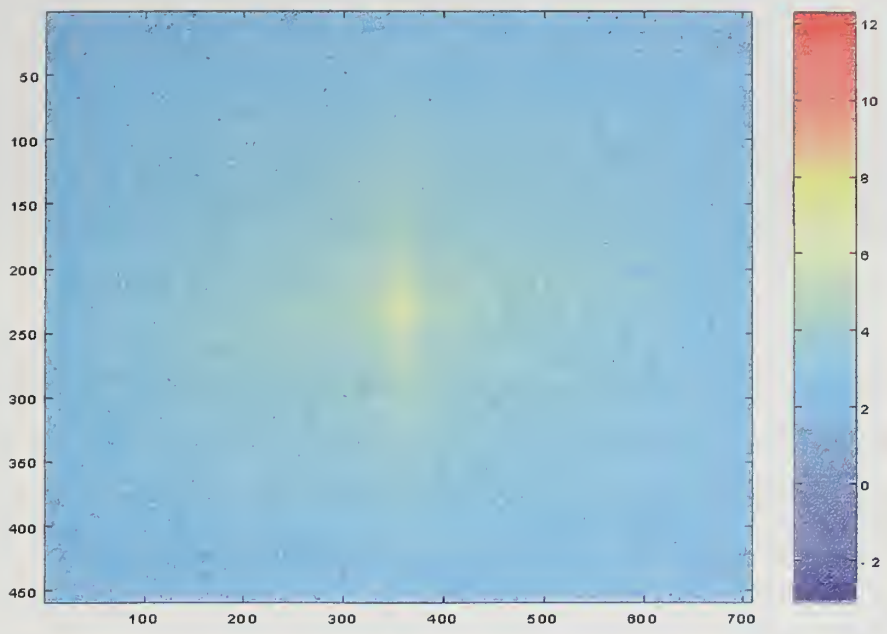


Figure 2.11. Fast Fourier Transformation on the APC.







Figure 2.12. High-pass filter of the APC originally shown in Figure 2.10.

red-green spatial CSF begins to decrease at frequencies greater than 1 cpd; therefore the frequencies of 3 and 7 were chosen knowingly, trading off sensitivity for the advantages of a higher spatial frequency where there would be a higher likelihood of observing an oblique effect. Frequencies higher than 7 cpd were not chosen due to increasing effects of chromatic aberration.

A Class I chromatic oblique effect was expected to be observed at spatial frequencies of 3 and 7 cpd. Psychophysically, the Class I oblique effect has not been readily observed at spatial frequencies as low as 1 cpd and accordingly a Class I chromatic oblique effect was not expected to be observed at this spatial frequency.



### III. METHODS

#### A. SUBJECTS

The experiment was conducted concurrently at the Naval Postgraduate School (NPS) and the University of Louisville, Kentucky (UL). Four subjects, 2 NPS and 2 UL, volunteered for this experiment. All subjects had normal (20/20), or corrected to normal, acuity and color vision. Color vision was verified with pseudo-isochromatic plates. Two of the four subjects (1 NPS and 1UL) were naive as to the purpose of the experiment. The other two subjects, the author and the remaining UL subject, were experienced psychophysical observers. All subjects signed an informed consent and were briefed on the ethical conduct for subject participation specified in the Protection of Human Subjects, SECNAV Instruction 3900.39B. Subjects were screened for uncorrected astigmatic errors by determining spatial resolution limits for  $0^\circ$ ,  $45^\circ$ ,  $90^\circ$ , and  $135^\circ$ .

#### B. APPARATUS

Stimuli were presented by a VisionWorks computer graphics system (Vision Research Graphics, Inc.) on an IDEK MF-8521 high resolution color monitor (21" X 20" of viewable area) equipped with an non-glare, anti-reflect, P-22 phosphor. The monitor had a resolution of 800 by 600 pixels ( $x=75.02$  and  $y=74.92$  pixels/degree), 98.9 Hz frame-rate, mean chromaticity of  $r = 0.334$ ,  $g = 0.336$ ,  $b = 0.300$  (1931 CIE), and a maximum luminance of 100 cd/m<sup>2</sup>. Refer to Table 3.1 for the chromaticity and luminance coordinates for each phosphor. The University of Louisville's apparatus and procedure were identical to the Naval Postgraduate School's, except that the stimuli were displayed on a 17" Nanao Flexscan F2.21 color monitor. Subjects viewed the monitor from 1.5 meters and were positioned by an adjustable chinrest. A small floor lamp (2.6 cd/m<sup>2</sup>) was positioned behind the monitor to reduce screen glare.

	CIE			Luminance (cd/m <sup>2</sup> )
	x	y	z	
Red phosphor	.617	.345	.038	24.0
Green phosphor	.334	.581	.085	88.7
Blue phosphor	.162	.081	.757	12.7

Table 3.1. Chromaticity and luminance of monitor

### C. STIMULI

Sinusoidal gratings were presented within a spatially windowed circular test field that subtended  $7.59^\circ$  of visual angle. The Gaussian window was truncated at  $\pm 1$  standard deviations for both x and y directions. The test patterns were one-dimensional spatio-temporal sinusoids of varying orientation (principal and oblique), spatial frequency (1.0, 3.0, and 7.0 cycles/degree), and color contrast. Test patterns for each subject consisted of two orientations, principal ( $0^\circ$  and  $90^\circ$ ) and oblique ( $45^\circ$  and  $135^\circ$ ). For each subject, maximum sensitivity for each orientation within the principal and oblique grouping was chosen. All sinusoids were raised cosines temporally modulated at 2.0 Hz. The sinusoid pattern was presented in a 1500 msec interval with contrast ramped on and off according to a linear window. (Contrast peaked at 202 msec and fell at 1304 msec).

Color contrast was computed by different ratios of percent red and green (Sellers et al., 1986). The monitor was controlled by a Cambridge Research Systems VSG 2/4 video board that was linearized to 10 bits of resolution per gun. The outputs of each gun were linearized by means of stored look-up table file. Sixteen different sinusoidal red-green color mixtures were generated by changing the red phosphor only, green phosphor only, or by changing the red and green guns in fixed proportions. Color contrast was defined according to the (Michelson) formula shown in Equation 3.1. Blue gun was held constant in all quadrants. Red and green gun values were used in the determination of red and green contrast as shown in Equations 3.2 and 3.3.

contrast	=	$(\text{peak} - \text{trough}) / (\text{peak} + \text{trough})$	3.1
red contrast	=	$(\text{red gun value} - 50) / 50$	3.2
green contrast	=	$(\text{green gun value} - 50) / 50$	3.3

#### D. PROCEDURE

Thresholds were determined by a two-alternative forced choice adaptive psychometric procedure, QUEST (Watson and Pelli, 1983). Threshold was defined at 75 percent correct. A total of 480 trials, 30 trials per condition, were randomly presented within each session. A session (~ 45 minutes) consisted of one sinusoidal condition with 16 different red-green color mixtures. A subject had to complete six sessions to contribute one threshold point for all conditions.

At the beginning of each session, subjects dark-adapted for approximately five minutes before initiating the first experimental trial. Three of the four subjects were tested monocularly, while the fourth subject (UL) was tested binocularly. At the beginning of each trial, the subject was instructed to focus on a fixation cross (.19° by .13°) located in the center of the screen. The subject initiated the first trial with a keyboard response, the fixation cross extinguished followed by presentation of the first interval, 121 msec ISI, and then presentation of the second interval. The subject's task was to detect which interval contained the sinusoidal grating. The next trial followed 250 msec after the subject's keyboard response.

Color contrast thresholds were determined from 16 different color-mixture ratios. The sixteen different ratios could be divided into four different percent red and green quadrants. Quadrant one started with 100 percent green and 0 percent red, quadrant two started at 100 percent red and 0 percent green, quadrant three started at -100 percent green and 0 percent red, and quadrant four started at -100 percent green and 0 percent red. The red-green ratios within each quadrant were 0.0, 0.5, 1.0, and 2.0. The thresholds from these red-green ratios will form an ellipse with the half-length of the axis

measuring color discrimination and the half-width of the axis measuring brightness discrimination (Sellers, 1986).

## IV. RESULTS

Many researchers have carried out experiments to determine visual sensitivity to color differences. One way of determining these differing sensitivities is through differing values of International Commission on Illuminance (ICI or, more commonly, CIE, for the French translation) primaries (Kaiser and Boynton, 1996). These primaries allow all colors to be specified in terms of three numbers representing the red, green and blue primaries. The color-matching type experiment is set up to test if an observer can discriminate between a chosen color and another color similar to this color. Color-matching experiments have looked at the standard deviations of color-matchings for representative colors throughout the color spectrum. These standard deviations are directly related to the corresponding just-noticeable difference of colors. (Brown and MacAdam, 1949)

Numerous surveys of differential thresholds have been carried out, but W. D. Wright (1941) and D.L. MacAdam (1942) completed two of the more extensive surveys. “MacAdam plotted the results of the survey on the chromaticity diagram in terms of the standard deviation of color-matching in several directions for selected colors.”(Brown and MacAdam, 1949) The figures resulting from this survey formed closed curves on the diagram and the closed curves were elliptical in shape. (Brown and MacAdam, 1949)

In a later paper, Silberstein and MacAdam discussed that the errors of these closed curves were Normally distributed. They deduced that the curves should be ellipses, as they appeared to be. They further expostulated that if the variations were not confined to chromaticity, the closed curves would form ellipsoids rather than ellipses. Using the assumption that the probability of making a match that falls within a specific region of color space, near the target color, was not changed by any change of primaries, Silberstein proved the standard deviation figures to be ellipsoids. (Brown and MacAdam, 1949)

The fact that there was a theoretical explanation for MacAdam’s ellipses and not just an empirical observation was interesting. However, the discrimination ellipsoids of Brown and MacAdam were obtained for a bipartite field only. Noorlander, Heuts and Koenderink (1979 and 1980) and Noorlander and Koenderink (1983) furthered the work of Brown and MacAdam by

extending their methodology from a simple bipartite field to more complicated stimuli by varying temporal and spatial frequencies. When three primaries are used discrimination ellipsoids are obtained. However, if just two primaries are used, such as red and green, than a cross-section of a discrimination ellipse is obtained. Neurlander, Heuts and Koenderink (1980) did this by obtaining discrimination ellipses for a number of different spatial and temporal frequencies. The lengths of the major and minor axes of these ellipses, as well as their orientation, are highly dependent on both the spatial and temporal frequencies.

The finding that the cross-section of a discrimination ellipsoid is an ellipse was also used by Sellers et al. (1986) in a study of congenital and acquired color defects. However, in the Sellers et al. paper, the axes of their graphs were not primaries as in Brown and MacAdam's or Neurlander, Heuts and Koenderink's, but were percent red contrast and percent green contrast. Even without knowledge of discrimination ellipsoids, the fact that Sellers et al.'s data form an ellipse can be explained by examining the following model. The central dashed line in Figure 4.1 is the equiluminance axis. Assume there are two luminance processes for detecting the brightening and darkening of a spot. The thresholds of these processes are displayed in Figure 4.1 with dashed lines and are labeled "BRIGHT" and "DARK." Similarly, the processes for detecting color are labeled "RED1" and "GREEN1." ("RED2" and "GREEN2" refer to two different thresholds.) As a first approximation, the visual threshold will be determined by whichever process has the lowest threshold. Therefore, this will be the parallelogram bounded by the four lines "BRIGHT," "DARK," "RED1," AND "GREEN1." A phenomenon known as probability summation accounts for the rounding of the corners of the parallelogram, and an ellipse is formed. Probability summation occurs near the corners of the parallelogram and can be thought of as a sum of two processes, e.g. "BRIGHT" and "RED1." For example, if the probability of either of the processes detecting a stimulus is .5, then if both processes are independent, the probability of either of them (or both) detecting a stimuli is .75. Thus, a contour connecting points where the probability of detection is .5 will exclude the corners of the parallelogram (Graham, 1989). (Sellers, 1986)

A ratio can be determined by dividing the length of the major axis by the length of the minor axis. For ellipses with a ratio greater than four, the major axis nearly coincides with the equiluminance axis. The angle of discrepancy between the equiluminous axis and the major axis



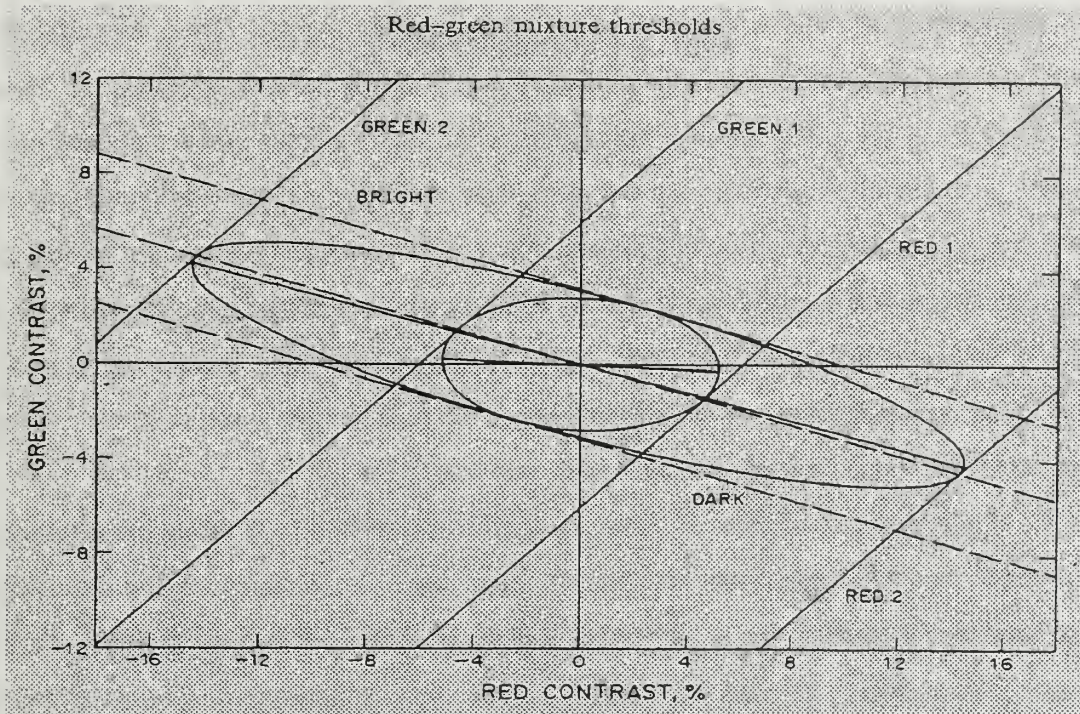


Figure 4.1. Detection model. From Sellers et al.[1986].

varies approximately as the inverse square of the length/width ratio. Therefore, elongated ellipses have a major axis that nearly coincides with their equiluminous axis. (Sellers et al., 1986)

The paper by Sellers et al. (1986) is extremely important to this thesis in that its methodology provided a foundation for the methodology used in this thesis. Using percent red contrast as the x-value and percent green contrast as the y-value, thresholds were determined for 16 different rays. For each ray, the proportion of percent red contrast to percent green contrast is constant along the ray. When plotted, the thresholds form an ellipse where the half-length of the major axis is a useful measure of color discrimination, and the half-width is a useful measure of brightness discrimination. Sellers et al. were interested in length and orientation, since they used these values for classification of color deficient subjects. Major axis length and orientation are important in this thesis. However, the crucial fact that Sellers et al.'s methodology resulted in data that theoretically forms ellipses is the crucial item. Data points from rays in the vicinity of isoluminance will have high leverage since they will be close to the end of the major axis, but they do not need to be at isoluminance.

The subjects run in this experiment did not have any color defects. Thus, collecting data on these subjects for classification purposes was not an exceptionally interesting endeavor. However, the possibility of using this methodology to explore a chromatic oblique effect was interesting. If oblique and non-oblique sensitivities are the same, and if oblique and non-oblique information is processed in an identical manner, then the ellipse obtained from a subject responding to non-oblique (horizontal or vertical) chromatic stimuli and the ellipse obtained from the same subject at the same temporal and spatial parameters, but with oblique chromatic stimuli, should be identical. A “spurious” luminous component is not a problem. Since the data points theoretically form an ellipse, the requirement for a point exactly at isoluminance no longer holds.

The elliptical nature of the data has been used to fit ellipses to the data by the method of maximum likelihood. A well-known result from linear regression informs us that the method of maximum likelihood is identical to the method of least squares in this case (Larsen and Marx, 1986). The programs used here to fit ellipses minimize the sum of the squared error. Assistant Professor Professor Samuel Buttrey of the Naval Postgraduate School in Monterey, CA. created these programs, their sub-programs and other programs of use. He created these programs, which are found in Appendix A, using the statistical package S-Plus.

The following terminology will be used to describe ellipses and their parameters (Figure 4.2).

terminology	definition
$a$	half-length of the major axis of an ellipse
$b$	half-length of the minor axis of an ellipse
$\theta$	angle as measured from the x-axis to the major axis of an ellipse
$x_i$	x-coordinate for data point $i$ . X-axis is percent red contrast
$y_i$	y-coordinate for data point $i$ . Y-axis is percent green contrast
$x_c$	x-coordinate for the center of an ellipse
$y_c$	y-coordinate for the center of an ellipse
$r_i$	distance from $(x_c, y_c)$ to a point on the ellipse along the ray
$\epsilon_i$	error term
$t_i$	polar angle of $r_i$

## Five-Parameter Ellipse

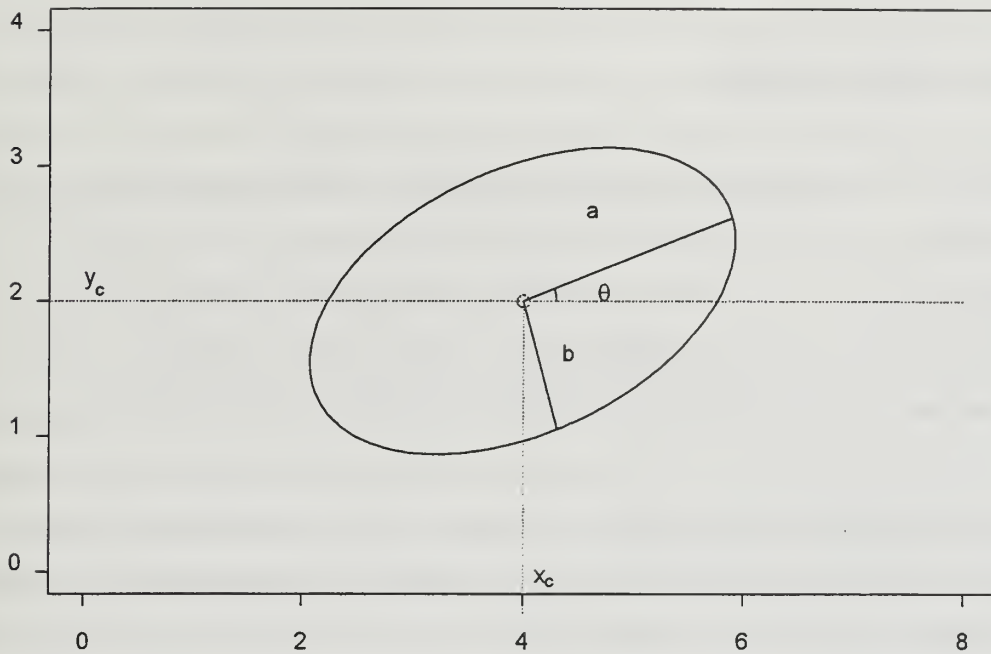


Figure 4.2. Five parameter ellipse. Created by Professor Samuel Buttrey.

The parameters for the true ellipse are unknown, but they may be estimated from the data. Three models were used to represent the underlying ellipse, and ellipses will be classified according to the method in which they were modeled. The polar angle relative to the coordinate  $t_i$  is fixed at the start of the experiment and is determined by  $\tan(t_i) = y_i/x_i$ . The sixteen values for  $t_i$  in degrees are  $(0, \pm 30, \pm 45, \pm 60, \pm 90, \pm 120, \pm 135, \pm 150, 180)$ . Each of these ellipses possesses an equiluminous axis along which, by definition, luminance is constant. The exact determination of this equiluminous axis is difficult, but for ellipses with an  $a/b$  ratio greater than four, this equiluminous axis is closely approximated by the major axis of the ellipse (Sellers, et al., 1986). A ray that coincides with the equiluminous axis will vary in color along  $r_i$ , but will have a constant luminosity. Any ray that is not aligned with the equiluminous axis will have a constant red to green percent contrast ratio along the

ray, but luminosity will not be constant along the ray. Both  $x$  and  $y$  values can be positive or negative.

## A. CLASS I-TYPE ELLIPSES

The Class I-type ellipse has five estimated parameters. These parameters are  $\alpha$ ,  $b$ ,  $\theta$ ,  $x_o$ , and  $y_o$ . The predicted  $r_i$  or  $\hat{r}_i$ , is a function of the estimated parameters and  $\hat{r}_i = f(\alpha, b, \theta, x_o, y_o, t_i)$ . The actual model used is  $r_i = \hat{r}_i + \epsilon_i$ . Here  $\epsilon_i$  are independent identically distributed (iid) and  $N(0, \sigma^2)$ . The function  $f(\alpha, b, \theta, x_o, y_o, t_i)$  is complicated and can be found in Appendix A (ell.pred). The objective function is the sum of the squared differences between the observed  $r_i$  and the predicted  $\hat{r}_i$ . Data were collected from both oblique and non-oblique stimuli; the class I-type ellipse is an ellipse that is obtained by fitting an ellipse to all of the data for a specific spatial frequency. For example, Subject One completed five runs at each condition. Each run results in the calculation of a threshold along each ray; thus, 16 thresholds were determined for this subject on five different sessions. This resulted in 80 data points for the non-oblique condition and 80 data points for the oblique condition for each of the three spatial frequencies used. Class I-type ellipses are fitted to the combined data of a subject at a specific spatial frequency. For Subject One, 160 data points were used, and an ellipse was fitted by the method of maximum likelihood. In the past, the ellipses obtained in this manner have been forced to have their center at the origin (Sellers, et al., 1986). However, much better fitting ellipses are obtained by allowing the center not to be pinned to the origin. The centers obtained for most subjects were generally close to the origin. The fact that a better fit was obtained by letting the ellipse be centered at coordinates other than the origin may be an indicator that centers may have some sort of bivariate distribution across subjects, or it may be an effect caused by the monitor. However, data from UL were definitely not centered on the origin and tended to have a center in the second quadrant. The ellipse programs in Appendix A allow the ellipse center to be pinned at the origin (fit.center=F) or to “float” (fit.center=T), but it did not make sense to pin the center to the origin when some of the actual ellipse centers obtained were definitely not at the origin.

## B. CLASS-II TYPE AND CLASS-III TYPE ELLIPSES

The Class-II Type ellipse has six (program ellipse.II) and the Class-III Type ellipse has seven (program ellipse.III) estimated parameters. The models for the  $\hat{r}_i$  for the three classes of ellipses are shown below. The model for Class-II Type ellipses may be changed so that it is  $f(a, b + \delta_b, \theta, x_c,$  and  $y_c)$  by changing which.type from one to two in the program ellipse.II.

$$\hat{r}_i(\text{class I type ellipses}) = f(a, b, \theta, x_c, y_c) \quad 4.1$$

$$\hat{r}_i(\text{class II type ellipses}) = f(a + \delta_a, b, \theta, x_c, y_c) \quad 4.2$$

$$\hat{r}_i(\text{class III type ellipses}) = f(a + \delta_a, b + \delta_b, \theta, x_c, y_c) \quad 4.3$$

The Class-II Type and Class-III Type ellipses use the information of whether the data were from an oblique or non-oblique condition. An ellipse is then fitted to the data, but the additional information of whether the data were from an oblique condition or a non-oblique condition is used to determine a  $\delta_a$  and/or a  $\delta_b$ . This is done by fitting a Class-II or Class-III Type ellipse to the data. Actually, two ellipses are fit to the data, one to the non-oblique data and one to the oblique data; but a common ellipse center and theta are maintained for both ellipses. If the sum of the objective functions for the ellipse fitted to the non-oblique data and the ellipse fitted to the oblique data is smaller than the objective function for the ellipse fitted to all of the data, then there will be a  $\delta_a$  and/or a  $\delta_b$ . If the  $\delta_a$  or  $\delta_b$  are small (This will be quantified in the next section.), then this orientation information does not significantly improve the fit of the ellipse. If the  $\delta_a$  and  $\delta_b$  are large, then this additional information significantly improves the fit of the ellipse.

## C. STATISTICAL TESTS

A complete discussion of the statistical test used for comparing ellipses can be found on pages 103-104 of Bates and Watts (1988). This test is an approximation, due to non-linearity, of an F-test. The derivation of this  $F$  statistic and how it is obtained are shown in Table 4.1 and Equation 4.4 respectively. For this experiment, the full model consists of Class-III type ellipses, and the partial

model consists of Class-II type ellipses. The full and partial models were chosen this way because of interest in the significance of the difference in the length of the major axis between non-oblique and oblique data.

Source	Sum of Squares	Degrees of Freedom	Mean Square	F Ratio
Extra parameters	$S_e = S_p - S_f$	$\nu_e = P_f - P_p$	$s_e^2 = S_e / \nu_e$	$s_e^2 / s_f^2$
Full model	$S_f$	$\nu_f = N - P_f$	$s_f^2 = S_f / \nu_f$	
Partial Model	$S_p$	$N - P_p$		

Table 4.1. Extra sum of squares analysis. From Bates and Watts [1988].

$$\frac{S_e/\nu_e}{S_f/\nu_f} \approx F_{\nu_e, \nu_f, N-P_p} \quad 4.4$$

If the equiluminous axis is identical to the major axis of an ellipse, then if the length of the major axis for oblique stimuli is greater than the length of the major axis for non-oblique stimuli, a chromatic oblique effect has been observed. Additionally, if the length of the ellipse minor axis for oblique stimuli is greater than the length of the minor axis for non-oblique stimuli, a luminous oblique effect has been observed. For ellipses with a major axis to minor axis ratio of four or greater, the equiluminous axis is closely approximated by the major axis (Sellers et al., 1986). The ellipses obtained generally had a ratio less than four, but the major axis was still used as the equiluminous axis as a rough approximation.

Four subjects took part in this experiment. Data from Subjects One and Three were collected at the NPS, while data from Subjects Two and Four were collected at UL. The data for these subjects at a spatial frequency of one cpd and both oblique and non-oblique orientations are shown in Figure 4.3. The measurements for  $a$ ,  $b$ ,  $\theta$ ,  $x_c$  and  $y_c$  are shown on the individual graphs and are displayed in Table 4.2, as well.

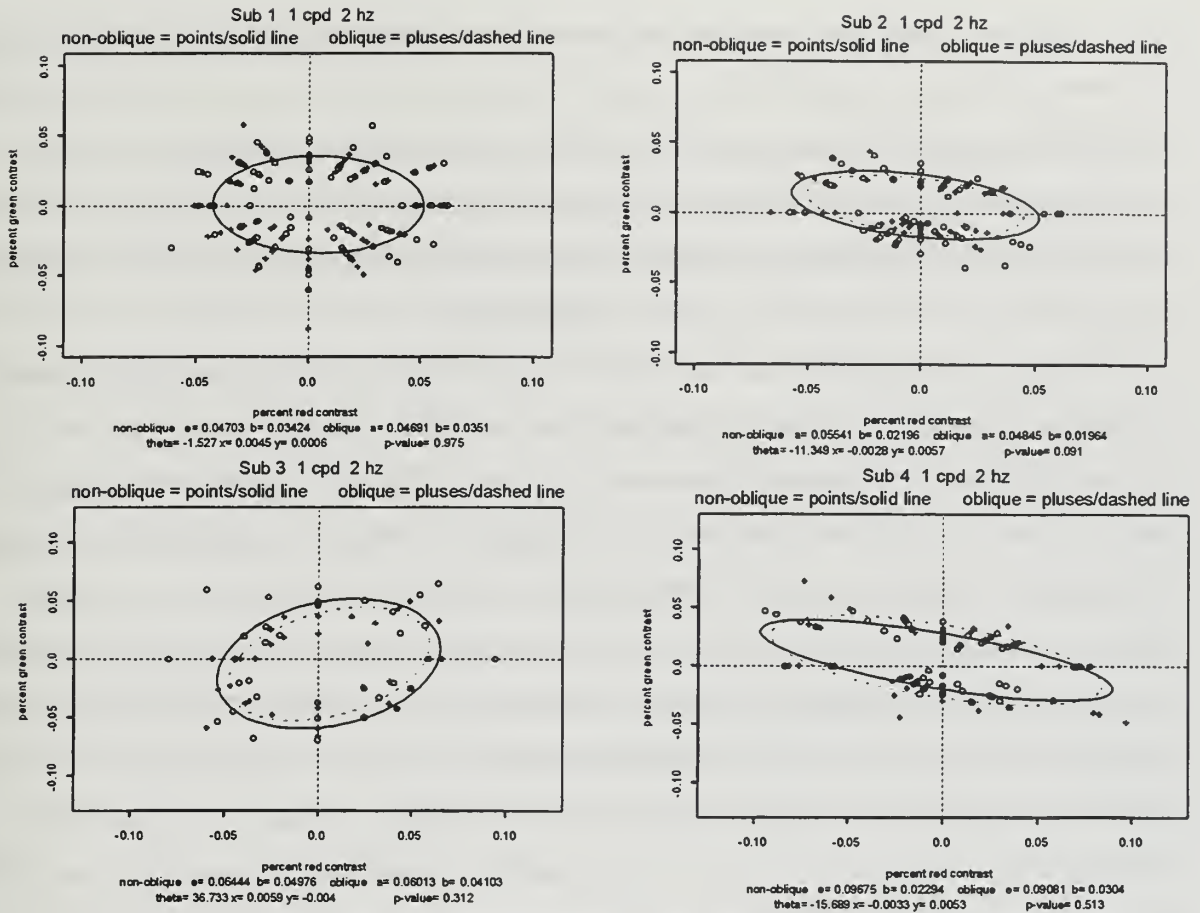


Figure 4.3. Ellipses and values for Subjects 1-4 at 1 cpd

Ellipse Type	Subj	a	b	theta	center.x	center.y	delta.a	delta.b	*p-value
non-oblique	1	0.04703	0.03424	-1.5274	0.00447	0.00064			
oblique	1	0.04691	0.0351	-1.5274	0.00447	0.00064	-0.0001	0.0009	0.975
non-oblique	2	0.05541	0.02196	-11.349	-0.0028	0.00569			
oblique	2	0.04845	0.01964	-11.349	-0.0028	0.00569	-0.007	-0.0023	0.091
non-oblique	3	0.06444	0.04976	36.733	0.00593	-0.004			
oblique	3	0.06013	0.04103	36.733	0.00593	-0.004	-0.0043	-0.0087	0.312
non-oblique	4	0.09675	0.02294	-15.689	-0.0033	0.00525			
oblique	4	0.09081	0.0304	-15.689	-0.0033	0.00525	-0.0059	0.0075	0.513
*Ho	delta.a=0								
Ha	delta.a<>0								

Table 4.2. Ellipse values for Subjects 1-4 at 1 cpd

The p-values were obtained by the F-test approximation discussed in the models section; however, an example is shown below for further clarification. For Subject One the ellipse from the non-oblique data and the ellipse from the oblique data are almost identical, whereas for Subjects Two and Three the opposite of a chromatic oblique effect (oblique ellipses with shorter  $a$ 's than non-oblique ellipses) is displayed and for Subject Four, a chromatic oblique effect is shown. However, with an alpha of .05, none of these results are significant.

Here is an example of how the p-values were calculated. Subject 1 completed 5 runs at all conditions. For each run, a total of 16 thresholds were calculated, so for a spatial frequency of 1 cpd a total of 80 oblique data points and 80 non-oblique data points were collected for this subject. The data was input to the program ellipse.III, and the ellipse center was allowed to float or not be pinned to the origin. From the output of this program, the objective function value is obtained. This objective function value is the sum of the squared error ( $SS_{III}$  for Class-III Type ellipses). This value is subtracted from the objective function value obtained from the output of a Class-II Type ellipse obtained with the same data,  $SS_{II}$ . The difference is then divided by the difference in the number of estimated parameters, or degrees of freedom, between the two classes of ellipses. This is the numerator for the equation. There is only one additional estimated parameter for Class-III Type ellipses, compared to Class-II Type ellipses, so this number is a one. Finally, the denominator is the value of the objective function obtained from the Class-III Type ellipse output divided by its degrees of freedom. For Class-III Type ellipses, seven parameters are estimated, so the 160 degrees of freedom for subject One decreased to 153 degrees of freedom. The resulting fraction is shown in equation 4.5. This fraction is referred to the  $F$  distribution with 1 and 153 degrees of freedom. Thus the fraction is approximately an  $F$  random variable with degrees of freedom given by 1 and 153,

$$\frac{(SS_{II} - SS_{III})/(1)}{SS_{III}/153} \quad 4.5$$

if the hypothesis that the ellipses differ only by  $\delta_a$ , and if iid Normal errors are true. A p-value is then calculated through tables or statistical programs. P-values for other subjects were calculated



similarly, with the degrees of freedom reflecting the number of observations the subject had for that condition.

The data for subjects at a spatial frequency of three cpd and both oblique and orientations are shown in Figure 4.4. The measurements for  $a$ ,  $b$ ,  $\theta$ ,  $x_c$  and  $y_c$  are shown on the individual graphs and are displayed in Table 4.3, as well. A chromatic oblique effect is shown for Subjects One, Two and Three and is significant for Subjects One and Two.

The data for the subjects at a spatial frequency of seven cpd and both oblique and non-oblique orientations are shown in Figure 4.5. The measurements for  $a$ ,  $b$ ,  $\theta$ ,  $x_c$  and  $y_c$  are shown on the individual graphs, and are displayed in Table 4.4. An achromatic oblique effect is expected here and is evidenced by  $\delta_b > 0$  leading to larger  $b$  values for oblique ellipses compared to the  $b$  values for non-oblique ellipses. A peculiarity of the program that determines the  $\delta$  values is that if the  $\delta$  value is negative and if it is larger in magnitude than the value to be added to, then the signs of both values must be reversed. The hypothesis of  $\delta_b > 0$  was tested in a manner similar to  $\delta_a > 0$ , and all subjects displayed an achromatic oblique effect. This achromatic oblique effect was significant for Subjects One, Two and Four. A chromatic oblique effect is shown for Subjects One and Two, but is not significant for either.

The data collected from the subjects were extremely variable. This variability is not only from subject to subject, but also from day to day and run to run. To display some of this variability, Table 4.5 shows p-values (uncorrected for multiple comparisons) for a subject's run at a specific condition against all of the other runs at this identical condition.

In summary, at one cpd neither an achromatic nor a chromatic oblique effect was shown. At three cpd a chromatic oblique effect was shown for three subjects and was significant for two of them. At seven cpd both achromatic and chromatic oblique effects were shown. All four subjects showed an achromatic oblique effect and this oblique effect was significant for three of them. Only two of the four subjects showed a chromatic oblique effect, but neither of the p-values were significant.

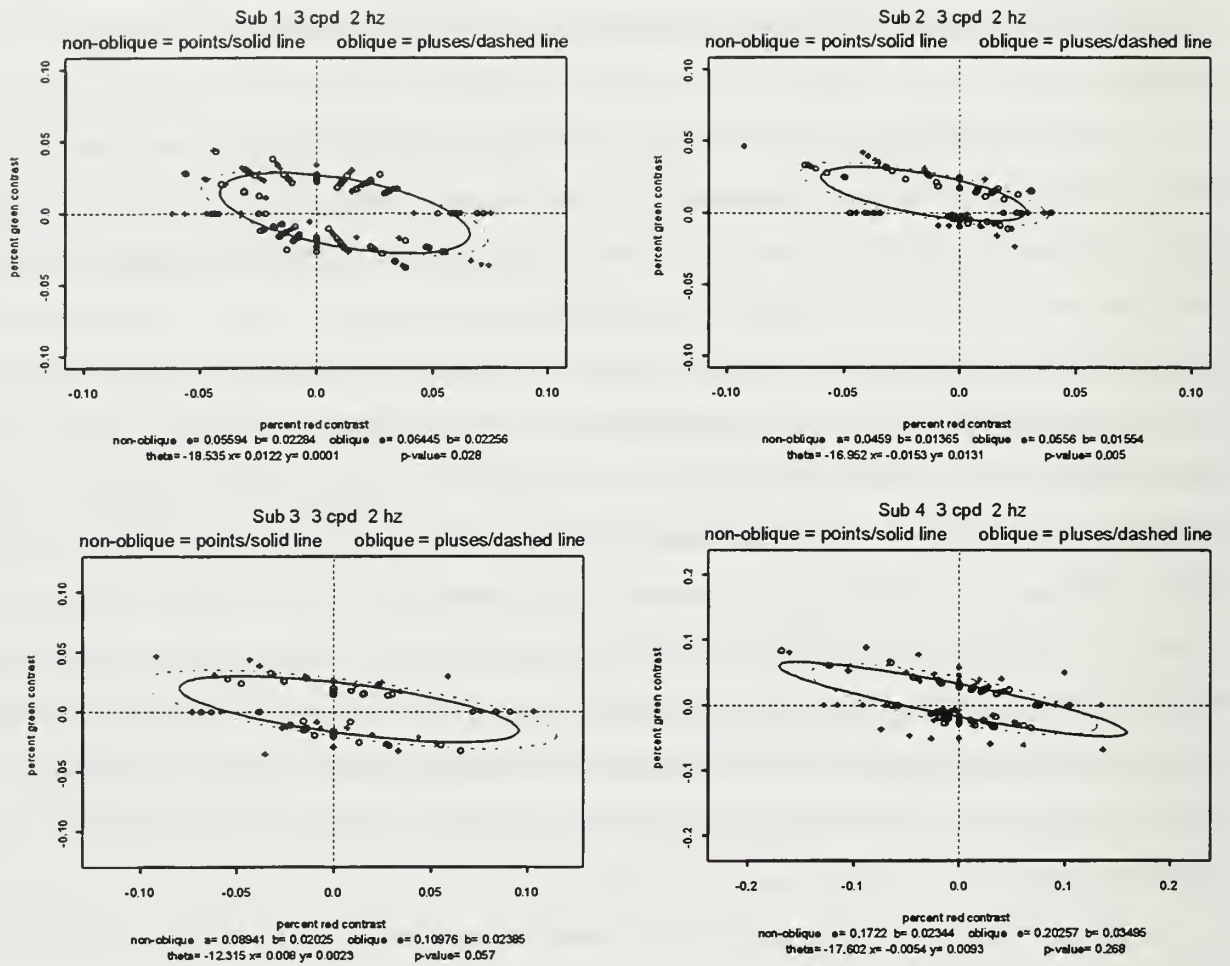


Figure 4.4. Ellipses and values for Subjects 1-4 at 3 cpd

Ellipse Type	Subj	a	b	theta	center.x	center.y	delta.a	delta.b	*p-value
non-oblique	1	0.05594	0.02284	-0.3235	0.01224	0.0001			
oblique	1	0.06445	0.02256	-0.3235	0.01224	0.0001	0.0085	-0.0003	0.028
non-oblique	2	0.0459	0.01365	-0.2959	-0.0153	0.01315			
oblique	2	0.0556	0.01554	-0.2959	-0.0153	0.01315	0.0097	0.0019	0.005
non-oblique	3	0.08941	0.02025	-0.2149	0.00796	0.00232			
oblique	3	0.10976	0.02385	-0.2149	0.00796	0.00232	0.0203	0.0036	0.057
non-oblique	4	0.1722	0.02344	-0.3072	-0.0054	0.0093			
oblique	4	0.14182	0.03495	-0.3072	-0.0054	0.0093	-0.0304	-0.0584	0.268
*Ho delta.a=0									
Ha delta.a<>0									

Table 4.3. Ellipses and values for Subjects 1-4 at 3 cpd

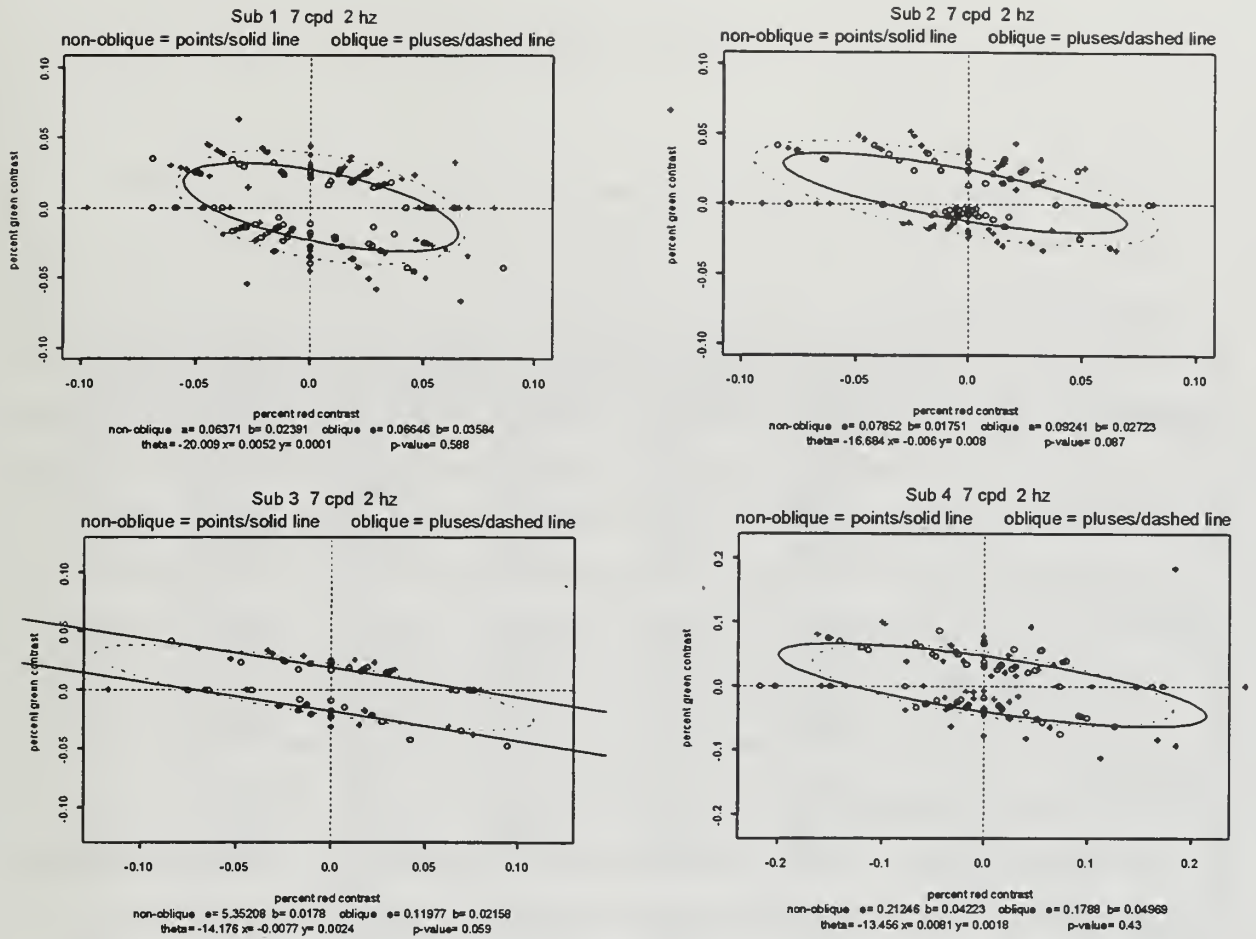


Figure 4.5. Ellipses and values for Subjects 1-4 at 7 cpd

Ellipse Type	Subj	a	b	theta	center.x	center.y	delta.a	delta.b	*p-value
non-oblique	1	0.06371	0.02391	-0.3492	0.00517	0.00012			
oblique	1	0.06646	0.03584	-0.3492	0.00517	0.00012	0.0028	0.0119	0.588
non-oblique	2	0.07852	0.01751	-0.2912	-0.006	0.00799			
oblique	2	0.09241	0.02723	-0.2912	-0.006	0.00799	0.0139	-0.0447	0.087
non-oblique	3	5.35208	0.0178	-0.2474	-0.0077	0.00238			
oblique	3	0.11978	0.02158	-0.2474	-0.0077	0.00238	-5.2323	-0.0394	0.059
non-oblique	4	0.21246	0.04223	-0.2349	0.00806	0.00179			
oblique	4	0.1788	0.04969	-0.2349	0.00806	0.00179	-0.0337	0.0075	0.43
*Ho	delta.a=0								
Ha	delta.a<>0								

Table 4.4. Ellipses and values for Subjects 1-4 at 7 cpd

	run	1 cpd		3 cpd		7 cpd	
		non-oblique	oblique	non-oblique	oblique	non-oblique	oblique
Subject 1	1	0.359	0.436	<b>0.000</b>	0.562	<b>0.000</b>	0.397
	2	0.056	0.199	0.242	0.048	0.191	0.393
	3	0.818	0.544	0.680	<b>0.000</b>	0.558	0.933
	4	0.399	0.673	0.152	0.181	0.529	<b>0.001</b>
	5	0.066	0.831	0.722	0.141	0.762	0.975
Subject 2	1	0.065	0.695	0.812	0.758	<b>0.000</b>	<b>0.000</b>
	2	0.070	0.800	<b>0.005</b>	0.620	0.899	0.146
	3	0.222	0.019	0.900	0.014	0.462	0.013
	4	<b>0.002</b>	<b>0.004</b>	<b>0.002</b>	0.676	<b>0.000</b>	0.126
Subject 3	1	<b>0.000</b>	0.604	0.021	0.759	0.834	0.217
	2	0.770	0.033	0.796	0.095	<b>0.006</b>	0.231
	3	0.226	0.017	0.079	<b>0.001</b>	0.101	<b>0.004</b>
Subject 4	1	0.320	0.752	0.057	0.394	<b>0.000</b>	0.071
	2	0.777	0.258	0.546	0.042	0.513	<b>0.000</b>
	3	0.397	0.926	0.415	<b>0.000</b>	0.136	<b>0.000</b>
	4	0.620	n/a	n/a	0.659	<b>0.003</b>	n/a

Table 4.5. P-values for comparing one subjects run against their other runs at that same condition. P-values have not been corrected for multiple comparisons. Bold values are less than  $.05/(\text{number of runs at that condition})$ .

## V. CONCLUSIONS

The purpose of this thesis was to investigate the human visual system's ability to detect certain simple targets. This thesis investigated how an object's spatial, temporal, and color features affected humans' detection of objects. The results showed that certain spatial and chromatic qualities do, indeed, inhibit detection. While real-world objects are much more complex than laboratory stimuli, knowledge of spatial and chromatic qualities that inhibit detection will assist military designers in the quest for better camouflage.

Other studies of use to military designers include the numerous studies documenting an achromatic Class-I oblique effect and the fact that it is generally found psychophysically only at high spatial frequencies. This study produced similar results with all subjects displaying an achromatic Class-I oblique effect (p-values of 0, 0, .139 and 0) at a spatial frequency of 7 cpd. Previous studies documenting a chromatic Class-I oblique effect, or lack thereof, are less useful due to conflicting results and possible problems with luminance artifacts tainting results (Kelly, 1976; Murasagi and Cavanagh, 1988). Indeed, the work done by Kelly and Murasagi and Cavanagh highlighted the problems in determining a chromatic oblique effect due to the difficulty of obtaining isoluminance for a subject. Any deviation can lead to the introduction of luminance artifacts and can corrupt the results of the experiment. The methodology used in this thesis takes advantage of the elliptical shape of the curve connecting thresholds at a fixed temporal and spatial frequency, and makes the exact determination of isoluminance unnecessary.

This thesis supports the hypothesis that a Class-I chromatic oblique does exist. At a spatial frequency of 3 cpd, a chromatic oblique effect is evident. A chromatic oblique effect is shown for three of the four subjects and, with an alpha of .05, is significant for two of the four subjects. Additionally, while the p-value for Subject Three (.057) is not less than .05, this subject conducted only three runs with 12 thresholds. An additional run would likely reduce this p-value to a value less than .05.

The main value of this study is the tool it provides for further investigation of a Class-I chromatic oblique effect without the problems associated with luminance artifacts. However, this tool does have its drawbacks. The data collection required is extremely time-intensive. A total of at least five runs at each spatial frequency is desirable due to the variability of the data. With each session lasting approximately 45 minutes to an hour and one run consisting of an oblique session and a non-oblique session, the time required for five runs is approximately 7.5 to ten hours. This time does not account for three sessions needed to determine a subject's maximum oblique and non-oblique sensitivity. This large time commitment on the part of subjects poses problems, as their motivation begins to wane. Motivation was a possible problem, as UL subjects did not run consistently; their average run time (days) was 19 and 18 versus 10 and 12 for the NPS subjects. This undoubtedly affected the variability of their data, as evidenced by the number of their p-values in Table 4.5 less than .05.

While the determination of exact isoluminance is not required, it is desirable to determine an approximate isoluminance axis. If an ellipse major to minor axis ratio is four or greater, then Sellers et al. (1986) state that the major axis is a good approximation of the equiluminous axis. Major to minor axis ratios in this study averaged 3.3 and exceeded four only one-third of the time. For Subject One at 7 cpd graphically (Figure 4.3), it appears that a Class-I chromatic oblique effect is evident. Taking into account that the highest major to minor axis ratio for this subject at this spatial frequency is 2.66, a chromatic oblique effect is even more likely since the equiluminous axis is not likely approximated that well by the major axis. In this case, the p-value of .588 does not provide much information regarding what actually occurred. The statistical test resulting from the model formulation tests the significance in the difference of the length of the axes and does not account for the fact that the true isoluminance axis may not be aligned with the major axis.

This thesis has provided an excellent tool for further research. Possible improvements include determination of a subject's equiluminous axis prior to running the experiment, thus enabling the experimenter to choose ratios that would run through this approximate axis. A spatial frequency of 3 cpd is worthy of further study with more runs and fewer confounding variables (different monitors).

## APPENDIX A. S-PLUS CODE

```

> ellipse
function(x, y, a = 2, b = 3, e = 0, theta = 0, fit.center = F, grad = T,
        is.there.hess = T, plot.it = T, chat = T)
{
# This is for a Class-I type ellipse
# Fit a least-squares ellipse centered at 0 with semi-axes (a, b)
# and angle to the origin theta, to the data in x, y. The ellipse
# is here parameterized by a, e (the eccentricity) and theta,
# in that order. a is always > b.
# a,b,e and theta are starting points
# fit.center=F pins the ellipse to the origin when this is true the
# ellipse is allowed to "float"
# grad=gradient
# .hess=hessian
# plot.it activates plot
# chat=T shows values as they are computed
#
# If a is supplied, and it's a vector, then we've been given
# starting points for all the parameters. Use 'em, first making
# sure that there is the right number (3 if we're not fitting
# the center, and 5 if we are).
#
  if(!missing(a) && length(a) > 1) {
    if((fit.center && length(a) != 5) || (!fit.center &&
length(a) != 3))
      stop(paste("Parameter vector has length", length(a),
        ", expecting ", ifelse(fit.center, 5, 3)))
    if(length(names(a[2])) == 0 || names(a[2]) == "e") {
      if(length(names(a[2])) == 0)
        warning("No param names: using e in pos. 2")
      e <- a[2]
      b <- a[1] * sqrt(1 - e^2)
    }
    else {
      b <- a[2]
      e <- sqrt(1 - (b/a[1])^2)
    }
    theta <- a[3]
    if(fit.center) {
      center.x <- a[4]
      center.y <- a[5]
    }
    a <- a[1]
  }
  else {
    if(missing(a))
      a <- 0.5 * diff(range(x))
    if(missing(b))
      b <- 0.5 * diff(range(y))
    e <- ifelse(a > b, sqrt(1 - (b/a)^2), sqrt(1 - (a/b)^2))
    if(missing(theta)) {
      ls.out <- lsfit(x, y)
      theta <- atan(ls.out$coef[2])
    }
  }
}

```

```

    }
    center.x <- mean(x)
    center.y <- mean(y)
  }
  tt <- ell.tt(x, y)
  if(plot.it) {
    graph <- dev.list()["win.graph"][1]
    if(length(graph) == 0 || all(is.na(graph)))
      win.graph()
    else dev.set(graph)
  }
  if(grad)
    grad.func <- ell.grad
  else grad.func <- NULL
  if(fit.center) {
    start.vec <- c(a = a, e = e, theta = theta, center.x =
      center.x, center.y = center.y)
    lower.vec <- c(0.0001, 0.0001, -2 * pi, - Inf, - Inf)
    upper.vec <- c(Inf, 0.999999, 2 * pi, Inf, Inf)
  }
  else {
    start.vec <- c(a = a, e = e, theta = theta)
    lower.vec <- c(0.0001, 0.0001, -2 * pi)
    upper.vec <- c(Inf, 0.999999, 2 * pi)
  }
  out <- nlminb(start = start.vec, objective = ell.res, gradient =
    grad.func, hessian = is.there.hess, lower = lower.vec, upper
    = upper.vec, tt = tt, my.x = x, my.y = y, plot.it =
    plot.it, chat = chat, is.there.hess = is.there.hess,
    fit.center = fit.center, step.min = 100 *
    .Machine$double.eps, scale.upd = 1) #
### p.names <- names(out$parameters)
### cat("In ellipse, check p.names\n")
### browser()
b <- out$parameters["a"] * sqrt(1 - out$parameters["e"]^2)
if(length(out$parameters) > 3) {
  out$parameters <- c(out$parameters["a"], b = b, out$
    parameters[3:length(out$parameters)]) #
  names(out$parameters) <- c("a", "b", "theta", "center.x",
    "center.y") # Beats me...
}
else {
  out$parameters <- c(out$parameters["a"], b = b, out$
    parameters[3]) #
  names(out$parameters) <- c("a", "b", "theta")
}
out$sigma.sq <- out$obj/length(x)
out$sigma <- sqrt(out$sigma.sq)
out$aux <- NULL
out$x <- x
out$y <- y
if(length(out$hessian) > 0) {
  if(qr(out$hessian)$rank < ncol(out$hessian))
    out$cov <- "Can't invert Hessian"
  else out$cov <- out$sigma.sq * solve(out$hessian)
}
out$tt <- tt
out$fitted.tt <- ell.tt(x - center.x, y - center.y)

```



```

    pred <- ell.pred(out$fitted.tt, out$parameters["a"],
out$parameters["b"], out$parameters["theta"],
return.unrotated.too = F, fit.center = fit.center,
    center.x = ifelse(fit.center, out$
    parameters["center.x"], 0), center.y = ifelse(fit.center,
    out$ parameters["center.y"], 0))
    out$fitted.x <- pred$x
    out$fitted.y <- pred$y
    out$fitted.r <- sqrt(pred$x^2 + pred$y^2)
    class(out) <- "ellipse"
    return(out)
}

```

### > ellipse.II

```

function(x, y, a = 2, b = 3, theta = 0, delta = 0, fit.center = F, grad
= T, is.there.hess = T, plot.it = T, chat = T, class.I = rep(T,
length(x)), which.type = 1)
{
# This is for a Class-II type ellipse
# class.I separates oblique and non-oblique data. For an x vector of
# length 160 where the first 80 points were non-oblique data the
# class.I vector should consist of a boolean vector or length 160 #
# comprised of 80 T's followed by 80 F's
# which.type=1 when testing differences in the major axes (a's or #
# chromaticity)
# which.type=2 when testing differences in the minor axes (b's
# or luminance)
# This version of ellipse works, but you must set grad=F,is.there.hess=F
# and plot.it=F
#
# Fit a least-squares ellipse centered at 0 with semi-axes (a, b)
# and angle to the origin theta, to the data in x, y. The ellipse
# is now parameterized by a, b (not e) and theta, in that order.
# a is always > b; we can enforce that at the end.
#
    if(is.matrix(x) && ncol(x) > 1) {
        if(any(dimnames(x)[[2]] == "y")) {
            y <- x[, "y"]
            if(any(dimnames(x)[[2]] == "x"))
                x <- x[, "x"]
            else x <- x[, 1]
        }
        else {
            y <- x[, 2]
            x <- x[, 1]
        }
    }
    if(is.list(x)) {
        if(any(names(x) == "y")) {
            y <- x$y
            if(any(names(x) == "x"))
                x <- x$x
            else x <- x[[1]]
        }
        else {
            y <- x[[2]]
            x <- x[[1]]
        }
    }
}

```

```

    }
  }
#
# If a is supplied, and it's a vector, then we've been given
# starting points for all the parameters. Use 'em, first making
# sure that there is the right number (3 if we're not fitting
# the center, and 5 if we are). These #'s increase 1 for every delta
# estimated.
  if(!missing(a) && length(a) > 1) {
    if((fit.center && length(a) != 5) || (!fit.center &&
length(a) != 3))
      stop(paste("Parameter vector has length", length(a),
", expecting ", ifelse(fit.center, 5, 3)))
    b <- a[2]
    e <- sqrt(1 - (b/a[1])^2)
    theta <- a[3]
    if(fit.center) {
      center.x <- a[4]
      center.y <- a[5]
    }
    a <- a[1]
  }
  else {
    if(missing(a))
      a <- 0.5 * diff(range(x))
    if(missing(b))
      b <- 0.5 * diff(range(y))
    if(a < b) {
      switcheroo <- a
      a <- b
      b <- switcheroo
    }
    e <- sqrt(1 - (b/a)^2)
    if(missing(theta)) {
      ls.out <- lsfit(x, y)
      theta <- atan(ls.out$coef[2])
    }
    center.x <- mean(x)
    center.y <- mean(y)
  }
  tt <- ell.tt(x, y)
  if(plot.it) {
    graph <- dev.list()["win.graph"][1]
    if(length(graph) == 0 || all(is.na(graph)))
      win.graph()
    else dev.set(graph)
  }
  if(grad)
    grad.func <- ell.grad.II
  else grad.func <- NULL
  if(fit.center) {
    start.vec <- c(a = a, b = b, theta = theta, center.x =
center.x, center.y = center.y, delta = delta)
    lower.vec <- c(0.00001, 0.00001, -2 * pi, - Inf, - Inf, -
Inf)
    upper.vec <- c(Inf, Inf, 2 * pi, Inf, Inf, Inf)
  }
  else {

```

```

        start.vec <- c(a = a, b = b, theta = theta, delta = delta)
        lower.vec <- c(0.00001, 0.00001, -2 * pi, - Inf)
        upper.vec <- c(Inf, Inf, 2 * pi, Inf)
    }
    out <- nlmminb(start = start.vec, objective = ell.res.II, gradient
        = grad.func, hessian = is.there.hess, lower =
        lower.vec, upper = upper.vec, tt = tt, my.x = x, my.y
        = y, plot.it = plot.it, chat = chat, is.there.hess =
        is.there.hess, fit.center = fit.center, class.I =
        class.I, which.type = which.type, step.min = 100 *
        .Machine$double.eps, scale.upd = 1) #
### p.names <- names(out$parameters)
### cat("In ellipse, check p.names\n")
### browser()
if(length(out$parameters) > 4)
    names(out$parameters) <- c("a", "b", "theta", "center.x",
        "center.y", "delta") # Beats me...
else names(out$parameters) <- c("a", "b", "theta", "delta")
out$sigma.sq <- out$obj/length(x)
out$sigma <- sqrt(out$sigma.sq)
out$aux <- NULL
out$x <- x
out$y <- y
if(length(out$hessian) > 0) {
    if(qr(out$hessian)$rank < ncol(out$hessian))
        out$cov <- "Can't invert Hessian"
    else out$cov <- out$sigma.sq * solve(out$hessian)
}
out$tt <- tt
out$fitted.tt <- ell.tt(x - center.x, y - center.y)
pred<-ell.pred(out$fitted.tt, out$parameters["a"],
    out$parameters["b"], out$parameters["theta"],
    return.unrotated.too = F, fit.center = fit.center,
    center.x = ifelse(fit.center, out$parameters["center.x"],
    0), center.y = ifelse(fit.center, out$parameters["center.y"],
    0))
out$fitted.x <- pred$x
out$fitted.y <- pred$y
out$fitted.r <- sqrt(pred$x^2 + pred$y^2)
class(out) <- "ellipse"
return(out)
}

```

### > ellipse.III

```

function(x, y, a = 2, b = 3, theta = 0, delta.a = 0, delta.b = 0,
    fit.center = F, grad = T, is.there.hess = T, plot.it = T, chat =
    T, class.I = rep(T, length(x)))
{
# This is for Class-III ellipses
# This version of ellipse works, but you must set grad=F,is.there.hess=F
# and plot.it=F
#
#
# Fit a least-squares ellipse centered at 0 with semi-axes (a, b)
# and angle to the origin theta, to the data in x, y. The ellipse
# is now parameterized by a, b (not e) and theta, in that order.
# a is always > b; we can enforce that at the end.

```

```

#
if(is.matrix(x) && ncol(x) > 1) {
  if(any(dimnames(x)[[2]] == "y")) {
    y <- x[, "y"]
    if(any(dimnames(x)[[2]] == "x"))
      x <- x[, "x"]
    else x <- x[, 1]
  }
  else {
    y <- x[, 2]
    x <- x[, 1]
  }
}
if(is.list(x)) {
  if(any(names(x) == "y")) {
    y <- x$y
    if(any(names(x) == "x"))
      x <- x$x
    else x <- x[[1]]
  }
  else {
    y <- x[[2]]
    x <- x[[1]]
  }
}

#
# If a is supplied, and it's a vector, then we've been given
# starting points for all the parameters. Use 'em, first making
# sure that there is the right number (3 if we're not fitting
# the center, and 5 if we are). These #'s increase 1 for every delta
# estimated
if(!missing(a) && length(a) > 1) {
  if((fit.center && length(a) != 5) || (!fit.center &&
length(a) != 3))
    stop(paste("Parameter vector has length", length(a),
              ", expecting ", ifelse(fit.center, 5, 3)))
  b <- a[2]
  e <- sqrt(1 - (b/a[1])^2)
  theta <- a[3]
  if(fit.center) {
    center.x <- a[4]
    center.y <- a[5]
  }
  a <- a[1]
}
else {
  if(missing(a))
    a <- 0.5 * diff(range(x))
  if(missing(b))
    b <- 0.5 * diff(range(y))
  if(a < b) {
    switcheroo <- a
    a <- b
    b <- switcheroo
  }
  e <- sqrt(1 - (b/a)^2)
  if(missing(theta)) {
    ls.out <- lsfit(x, y)

```

```

        theta <- atan(ls.out$coef[2])
    }
    center.x <- mean(x)
    center.y <- mean(y)
}
tt <- ell.tt(x, y)
if(plot.it) {
    graph <- dev.list()["win.graph"][1]
    if(length(graph) == 0 || all(is.na(graph)))
        win.graph()
    else dev.set(graph)
}
if(grad)
    grad.func <- ell.grad.III
else grad.func <- NULL
if(fit.center) {
    start.vec <- c(a = a, b = b, theta = theta, center.x =
        center.x, center.y = center.y, delta.a = delta.a,
        delta.b = delta.b)
    lower.vec <- c(0.00001, 0.00001, -2 * pi, - Inf, - Inf, 0,
        0)
    upper.vec <- c(Inf, Inf, 2 * pi, Inf, Inf, Inf, Inf)
}
else {
    start.vec <- c(a = a, b = b, theta = theta, delta.a =
        delta.a, delta.b = delta.b)
    lower.vec <- c(0.00001, 0.00001, -2 * pi, 0, 0)
    upper.vec <- c(Inf, Inf, 2 * pi, Inf, Inf)
}
out <- nlminb(start = start.vec, objective = ell.res.III, gradient
    = grad.func, hessian = is.there.hess, lower = lower.vec,
    upper = upper.vec, tt = tt, my.x = x, my.y = y, plot.it =
    plot.it, chat = chat, is.there.hess = is.there.hess,
    fit.center = fit.center, class.I = class.I, step.min = 100 *
    .Machine$double.eps, scale.upd = 1) #
### p.names <- names(out$parameters)
### cat("In ellipse, check p.names\n")
### browser()
if(length(out$parameters) > 4)
    names(out$parameters) <- c("a", "b", "theta", "center.x",
        "center.y", "delta.a", "delta.b") # Beats me...
else names(out$parameters) <- c("a", "b", "theta", "delta.a",
    "delta.b")
out$sigma.sq <- out$obj/length(x)
out$sigma <- sqrt(out$sigma.sq)
out$aux <- NULL
out$x <- x
out$y <- y
if(length(out$hessian) > 0) {
    if(qr(out$hessian)$rank < ncol(out$hessian))
        out$cov <- "Can't invert Hessian"
    else out$cov <- out$sigma.sq * solve(out$hessian)
}
out$tt <- tt
out$fitted.tt <- ell.tt(x - center.x, y - center.y) #
### pred <- ell.pred(out$fitted.tt, out$parameters["a"],
### out$parameters[
### "b"], out$parameters["theta"], return.unrotated.too = F,

```

```

###         fit.center = fit.center, center.x = ifelse(fit.center, out$
###         parameters["center.x"], 0), center.y = ifelse(fit.center,
###         out$parameters["center.y"], 0))
###         out$fitted.x <- pred$x
###         out$fitted.y <- pred$y
###         out$fitted.r <- sqrt(pred$x^2 + pred$y^2)
###         class(out) <- "ellipse"
###         return(out)
}

> ell.res
function(params, tt, my.x, my.y, is.there.hess, fit.center, plot.it,
chat)
{
#
# ell.res: Compute objective to be minimized.
#
# This computes the objective function: the sum of squared
# differences between the observed points on the ellipse
# (after transformation) and the predicted ones.
#
# "params" is the vector (a, e, theta). Get them out, and
# compute rat, the ratio a/b.
#
  a <- params[1]
  e <- params[2]
  if(e > 0.99)
    return(1000)
  b <- a * sqrt(1 - e^2)
  theta <- params[3] #
  if(fit.center == T) {
    center.x <- params[4]
    center.y <- params[5] #
    tt <- ell.tt(my.x - center.x, my.y - center.y)
  }
  else {
    center.x <- center.y <- 0
  }
  fitted.r <- ell.pred(tt, a, b, theta, fit.center = fit.center,
    center.x = center.x, center.y = center.y) #
  new.x <- fitted.r$x
  new.y <- fitted.r$y #
# Plot it: add dotted lines at x = 0 and y = 0.
#
  if(plot.it) {
    plot(my.x, my.y, xlim = range(my.x, new.x), ylim =
    range(my.y, new.y))
    abline(h = 0, lty = 2)
    abline(v = 0, lty = 2) #
    points(new.x, new.y, pch = 1, col = 4) #
    points(center.x, center.y, pch = 1, col = 2)
  }
###   for(i in 1:length(tt))
###     polar(c(0, 0.5), rep(tt[i], 2), type = "l") #
#
# Get fitted x and y; compute and return objective.
#

```

```

obj <- sum((my.x - new.x)^2) + sum((my.y - new.y)^2) #
if(chat) cat("a:", signif(a, 4), "b:", signif(b, 4), "th:",
            signif(theta, 4), ifelse(fit.center, paste(";x,y:", signif(
            center.x, 4), signif(center.y, 4)), ""), ";obj:",
            signif(obj, 4), "\n") ### cat("BTW: ")
### ell.grad(params, tt, my.x, my.y, is.there.hess)
### cat("\n")
return(obj)
}

```

> ell.res.II

```

function(params, tt, my.x, my.y, is.there.hess, fit.center, plot.it,
         chat, class.I, which.type)
{
#
# ell.res: Compute objective to be minimized. This version is the
# Class-II one.
#
# This computes the objective function: the sum of squared
# differences between the observed points on the ellipse
# (after transformation) and the predicted ones.
#
# "params" is the vector (a, b, theta).
#
  a <- params[1]
  b <- params[2]
  theta <- params[3] #
  if(is.null(class.I)) {
    class.I <- rep(T, length(my.x))
    delta <- 0
  }
  if(fit.center == T) {
    center.x <- params[4]
    center.y <- params[5] #
    delta <- params[6]
    tt <- ell.tt(my.x - center.x, my.y - center.y)
  }
  else {
    center.x <- center.y <- 0
    delta <- params[4]
  }
  if(sum(class.I) < length(my.x)) {
    fitted.r.I <- ell.pred(tt[class.I], a, b, theta, fit.center
      = fit.center, center.x = center.x, center.y =
      center.y) #
    if(which.type == 1)
      fitted.r.II <- ell.pred(tt[!class.I], a + delta, b,
        theta, fit.center = fit.center, center.x =
        center.x, center.y = center.y)
    else fitted.r.II <- ell.pred(tt[!class.I], a, b + delta,
      theta, fit.center = fit.center, center.x =
      center.x, center.y = center.y) #
  }
  else fitted.r.I <- ell.pred(tt, a, b, theta, fit.center =
    fit.center, center.x = center.x, center.y = center.y) #
  new.x <- numeric(length(my.y))
  new.y <- numeric(length(my.y))
}

```

```

new.x[class.I] <- fitted.r.I$x
new.y[class.I] <- fitted.r.I$y
if(sum(!class.I) > 0) {
  new.x[!class.I] <- fitted.r.II$x
  new.y[!class.I] <- fitted.r.II$y
}
#
#
# If plot it, add dotted lines at x = 0 and y = 0, plus points.
#
  if(plot.it) {
    plot(my.x, my.y, xlim = range(my.x, new.x), ylim =
range(my.y, new.y))
    abline(h = 0, lty = 2)
    abline(v = 0, lty = 2) #
    points(new.x, new.y, pch = 1, col = 4) #
    points(center.x, center.y, pch = 1, col = 2)
  }
#
  cat("grad.norm is ", sum(ell.grad.II(params, tt, my.x, my.y,
is.there.hess, fit.center, class.I, which.type)^2), "\n")
#
# Get fitted x and y; compute and return objective.
#
  obj <- sum((my.x - new.x)^2) + sum((my.y - new.y)^2) #
  if(chat)
    cat("a:", signif(a, 4), ", delta: ", signif(delta, 4),
",b:",signif(b, 4), ",th:", signif(theta, 4), ifelse(
fit.center, paste(";x,y:", signif(center.x, 4),
signif(center.y, 4)), ""), ";obj:", signif(obj, 4),
"\n")
  return(obj)
}

> ell.res.III
function(params, tt, my.x, my.y, is.there.hess, fit.center, plot.it,
  chat, class.I)
{
#
# ell.res: Compute objective to be minimized. This version is the
# Class-III one.
#
# This computes the objective function: the sum of squared
# differences between the observed points on the ellipse
# (after transformation) and the predicted ones.
#
# "params" is the vector (a, b, theta).
#
  a <- params[1]
  b <- params[2]
  theta <- params[3] #
  if(is.null(class.I)) {
    class.I <- rep(T, length(my.x))
    delta.a <- delta.b <- 0
  }
  if(fit.center == T) {

```



```

        center.x <- params[4]
        center.y <- params[5] #
        delta.a <- params[6]
        delta.b <- params[7]
        tt <- ell.tt(my.x - center.x, my.y - center.y)
    }
else {
    center.x <- center.y <- 0
    delta.a <- params[4]
    delta.b <- params[5]
}
if(sum(class.I) < length(my.x)) {
    fitted.r.I <- ell.pred(tt[class.I], a, b, theta, fit.center
        = fit.center, center.x = center.x, center.y =
        center.y) #
    fitted.r.II <- ell.pred(tt[!class.I], a + delta.a, b +
        delta.b, theta, fit.center = fit.center, center.x =
        center.x, center.y = center.y) #
}
else fitted.r.I <- ell.pred(tt, a, b, theta, fit.center =
    fit.center, center.x = center.x, center.y = center.y) #
new.x <- numeric(length(my.y))
new.y <- numeric(length(my.y))
new.x[class.I] <- fitted.r.I$x
new.y[class.I] <- fitted.r.I$y
if(sum(!class.I) > 0) {
    new.x[!class.I] <- fitted.r.II$x
    new.y[!class.I] <- fitted.r.II$y
}
#
#
# If plot it, add dotted lines at x = 0 and y = 0, plus points.
#
if(plot.it) {
    plot(my.x, my.y, xlim = range(my.x, new.x), ylim =
        range(my.y, new.y))
    abline(h = 0, lty = 2)
    abline(v = 0, lty = 2) #
    points(new.x, new.y, pch = 1, col = 4) #
    points(center.x, center.y, pch = 1, col = 2)
}
###
## cat("grad.norm is ", sum(ell.grad.II(params, tt, my.x, my.y,
## is.there.hess, fit.center, class.I, which.type)^2), "\n")
#
# Get fitted x and y; compute and return objective.
#
obj <- sum((my.x - new.x)^2) + sum((my.y - new.y)^2) #
if(chat)
    cat("a:", signif(a, 4), ", delta.a: ", signif(delta.a, 4),
        ",b:", signif(b, 4), "delta.b: ", signif(delta.b, 4),
        ",th:", signif(theta, 4), ifelse(fit.center, paste(
        ";x,y:", signif(center.x, 4), signif(center.y, 4)),
        ""), ";obj:", signif(obj, 4), "\n")
return(obj)
}

```

```

> ell.grad
function(params, tt, my.x, my.y, is.there.hess, fit.center)
{
  tol <- 1e-006
  a <- params[1]
  e <- params[2]
  theta <- params[3]
  if(fit.center == T) {
    center.x <- params[4]
    center.y <- params[5]
    tt <- ell.tt(my.x - center.x, my.y - center.y)
  }
  else {
    center.x <- center.y <- 0
  }
  b <- a * sqrt(1 - e^2)
  fitted <- ell.pred(tt, a, b, theta, return.unrotated.too = T,
    fit.center = fit.center, center.x = center.x, center.y =
    center.y)
  xprime <- fitted$x.prime
  yprime <- fitted$y.prime
  x <- fitted$x
  y <- fitted$y
  cos.theta <- cos(theta)
  sin.theta <- sin(theta)
  cos.2.tt.theta <- cos(2 * (tt - theta))
  sin.2.tt.theta <- sin(2 * (tt - theta))
  sinsq.tt.theta <- (sin(tt - theta))^2
  cossq.tt.theta <- (cos(tt - theta))^2
  sinsq.2.tt.theta <- (sin(2 * (tt - theta)))^2
  consq.2.tt.theta <- (cos(2 * (tt - theta)))^2
  one.minus.e.sq <- 1 - e^2
  denom <- cossq.tt.theta * one.minus.e.sq + sinsq.tt.theta
  dxprime.da <- xprime/a
  dxprime.de <- (( - a^2/(4 * xprime)) * (e *
    sinsq.2.tt.theta))/(denom^ 2)
  dxprime.de[abs(xprime) < tol] <- 0
  dyprime.da <- yprime/a
  dyprime.de <- - (one.minus.e.sq * xprime * dxprime.de + e * (a^2
    -xprime^2))/yprime
  dyprime.de[abs(yprime) < tol] <- 0
  dx.da <- cos.theta * dxprime.da - sin.theta * dyprime.da
  dx.de <- cos.theta * dxprime.de - sin.theta * dyprime.de
  dy.da <- sin.theta * dxprime.da + cos.theta * dyprime.da
  dy.de <- sin.theta * dxprime.de + cos.theta * dyprime.de
  x.diff <- my.x - x
  y.diff <- my.y - y
  ### grad.mat <- matrix(0, length(x), 3)
  ### grad.mat[, 1] <- -2 * (x.diff * dx.da + y.diff * dy.da)
  ### grad.mat[, 2] <- -2 * (x.diff * dx.de + y.diff * dy.de)
  grad.a <- -2 * sum(x.diff * dx.da + y.diff * dy.da)
  grad.e <- -2 * sum(x.diff * dx.de + y.diff * dy.de)
  num <- one.minus.e.sq * sin(2 * (tt - theta))
  dxprime.dtheta <- (a^2/(2 * xprime)) * (num/denom^2)
  dxprime.dtheta[abs(xprime) < tol] <- 0
  dyprime.dtheta <- - (one.minus.e.sq * xprime * dxprime.dtheta)/
    yprime
  dyprime.dtheta[abs(yprime) < tol] <- 0

```

```

dx.dtheta <- - (y - center.y) + cos.theta * dxprime.dtheta -
             sin.theta * dyprime.dtheta
dy.dtheta <- (x - center.x) + sin.theta * dxprime.dtheta +
             cos.theta * dyprime.dtheta
grad.theta <- -2 * sum(x.diff * dx.dtheta + y.diff * dy.dtheta)
#
### grad.mat[, 3] <- -2 * (x.diff * dx.dtheta + y.diff * dy.dtheta)
### cat("Grad mat approx. is...\n")
### print(t(grad.mat) %*% grad.mat)
if(fit.center == F)
  grad <- c(grad.a, grad.e, grad.theta)
else {
  dxprime.dt <- - dxprime.dtheta
  dyprime.dt <- - dyprime.dtheta
  R.sq <- (my.x - center.x)^2 + (my.y - center.y)^2
  dt.dx0 <- (my.y - center.y)/R.sq
  dt.dy0 <- - (my.x - center.x)/R.sq
  dxprime.dx0 <- dxprime.dt * dt.dx0
  dxprime.dy0 <- dxprime.dt * dt.dy0
  dyprime.dx0 <- dyprime.dt * dt.dx0
  dyprime.dy0 <- dyprime.dt * dt.dy0 #
  dyprime.dprime <- one.minus.e.sq * ( - xprime/yprime)
  dyprime.dprime[abs(yprime) < tol] <- 0 #
  dx.dx0 <- (cos.theta * dxprime.dx0) - (sin.theta *
        dyprime.dx0) + 1
  dy.dx0 <- (sin.theta * dxprime.dx0) + (cos.theta *
        dyprime.dx0)
  dx.dy0 <- (cos.theta * dxprime.dy0) - (sin.theta *
        dyprime.dy0)
  dy.dy0 <- (sin.theta * dxprime.dy0) + (cos.theta *
        dyprime.dy0) + 1
  grad.x0 <- -2 * sum(x.diff * dx.dx0 + y.diff * dy.dx0)
  grad.y0 <- -2 * sum(x.diff * dx.dy0 + y.diff * dy.dy0)
  grad <- c(grad.a, grad.e, grad.theta, grad.x0, grad.y0)
}
if(is.there.hess == F)
  return(grad)
d2xprime.da2 <- d2yprime.da2 <- 0
d2xprime.dade <- dxprime.de/a
d2yprime.dade <- dyprime.de/a
d2xprime.dadtheta <- dxprime.dtheta/a
d2yprime.dadtheta <- dyprime.dtheta/a
ddenom.de <- -2 * e * cossq.tt.theta
ddenom.dtheta <- - e^2 * sin(2 * (tt - theta))
term1 <- ( - a^2 * sinsq.2.tt.theta)/4
xprime.denom.sq <- xprime * denom^2
d2xprime.de2 <- xprime.denom.sq - e * (dxprime.de * denom^2 + 2 *
  xprime * denom * ddenom.de)
d2xprime.de2 <- (term1/xprime.denom.sq^2) * d2xprime.de2
d2xprime.de2[abs(xprime) < 1e-006] <- 0
d2yprime.de2 <- one.minus.e.sq * (-2 * xprime * d2xprime.de2 - 2 *
  dxprime.de^2) + 8 * e * xprime * dxprime.de - 2 * (a^2 -
  xprime^2)
term1 <- - a^2 * e
d2xprime.dedtheta <- - xprime.denom.sq * sin(4 * (tt - theta)) -
  sinsq.2.tt.theta * (xprime * denom * ddenom.dtheta +
  dxprime.dtheta * denom^2)
d2xprime.dedtheta <- (( - a^2 * e)/xprime.denom.sq^2) *

```

```

d2xprime.dedtheta
d2xprime.dedtheta[abs(xprime) < 1e-006] <- 0
d2yprime.dedtheta <- (-1/yprime^2) * (yprime * ((one.minus.e.sq *
(
  xprime * d2xprime.dedtheta + dxprime.dtheta * dxprime.de)) -
  2 * e * xprime * dxprime.dtheta) - one.minus.e.sq * xprime *
  dxprime.dtheta * dxprime.de)
d2yprime.dedtheta[abs(yprime) < 1e-006] <- 0
dnum.dtheta <- -2 * one.minus.e.sq * cos(2 * (tt - theta))
d2xprime.dtheta2 <- xprime.denom.sq * dnum.dtheta - num * (2 *
  xprime * denom * ddenom.dtheta + denom^2 * dxprime.dtheta)
d2xprime.dtheta2 <- (d2xprime.dtheta2 * a^2)/(2 *
  xprime.denom.sq^2)
d2xprime.dtheta2[abs(xprime) < 1e-006] <- 0
d2yprime.dtheta2 <- - (one.minus.e.sq/yprime) * (yprime * (xprime
  * d2xprime.dtheta2 + dxprime.dtheta^2) - dyprime.dtheta * (
  xprime * dxprime.dtheta))
d2yprime.dtheta2[abs(yprime) < 1e-006] <- 0
d2x.dade <- cos.theta * d2xprime.dade - sin.theta * d2yprime.dade
d2y.dade <- sin.theta * d2xprime.dade + cos.theta * d2yprime.dade
d2x.de2 <- cos.theta * d2xprime.de2 - sin.theta * d2yprime.de2
d2y.de2 <- sin.theta * d2xprime.de2 + cos.theta * d2yprime.de2
grad.a2 <- 2 * sum(dx.da^2 + dy.da^2)
grad.ae <- 2 * sum(- x.diff * d2x.dade + dx.da * dx.de - y.diff *
  d2y.dade + dy.da * dy.de)
d2x.dadtheta <- cos.theta * d2xprime.dadtheta - sin.theta *
  d2yprime.dadtheta - dy.da
d2y.dadtheta <- sin.theta * d2xprime.dadtheta + cos.theta *
  d2yprime.dadtheta + dx.da
d2x.dedtheta <- cos.theta * d2xprime.dedtheta - sin.theta *
  d2yprime.dedtheta - dy.de
d2y.dedtheta <- sin.theta * d2xprime.dedtheta + cos.theta *
  d2yprime.dedtheta + dx.de
d2x.dtheta2 <- cos.theta * d2xprime.dtheta2 - sin.theta *
  d2yprime.dtheta2 - 2 * dy.dtheta + x
d2y.dtheta2 <- sin.theta * d2xprime.dtheta2 + cos.theta *
  d2yprime.dtheta2 + 2 * dx.dtheta + y
grad.atheta <- 2 * sum(- x.diff * d2x.dadtheta + dx.da *
  dx.dtheta - y.diff * d2y.dadtheta + dy.da * dy.dtheta)
grad.e2 <- 2 * sum(- x.diff * d2x.de2 + dx.de^2 - y.diff *
  d2y.de2 + dy.de^2)
grad.etheta <- 2 * sum(- x.diff * d2x.dedtheta + dx.de *
  dx.dtheta - y.diff * d2y.dedtheta + dy.de * dy.dtheta)
grad.theta2 <- 2 * sum(- x.diff * d2x.dtheta2 + dx.dtheta^2 -
  y.diff * d2y.dtheta2 + dy.dtheta^2) #
### grad.mat <- matrix(c(grad.a2, grad.ae, grad.atheta, grad.ae,
  grad.e2, grad.etheta, grad.atheta, grad.etheta,
  grad.theta2), 3, 3, T)
### cat("Hessian approx. is...\n")
### print(solve(grad.mat))
if(fit.center == F)
  hessian <- c(grad.a2, grad.ae, grad.e2, grad.atheta,
    grad.etheta, grad.theta2)
else {
#
#
# Second derivatives: a and x0, a and y0
#
d2xprime.dadx0 <- dxprime.dx0/a

```

```

d2yprime.dadx0 <- dyprime.dx0/a
d2xprime.dady0 <- dxprime.dy0/a
d2yprime.dady0 <- dyprime.dy0/a
d2x.dadx0 <- cos.theta * d2xprime.dadx0 - sin.theta *
  d2yprime.dadx0
d2y.dadx0 <- sin.theta * d2xprime.dadx0 + cos.theta *
  d2yprime.dadx0 #
# and the gradient
grad.ax0 <- 2 * sum( - x.diff * d2x.dadx0 + dx.da * dx.dx0 -
  y.diff * d2y.dadx0 + dy.da * dy.dx0)
d2x.dady0 <- cos.theta * d2xprime.dady0 - sin.theta *
  d2yprime.dady0
d2y.dady0 <- sin.theta * d2xprime.dady0 + cos.theta *
  d2yprime.dady0 #
#
grad.ay0 <- 2 * sum( - x.diff * d2x.dady0 + dx.da * dx.dy0 -
  y.diff * d2y.dady0 + dy.da * dy.dy0) #
#
#
ddenom.dx0 <- e^2 * sin.2.tt.theta * dt.dx0
ddenom.dy0 <- e^2 * sin.2.tt.theta * dt.dy0
A <- xprime * denom^2
dA.dx0 <- denom * (2 * xprime * ddenom.dx0 + denom *
  dxprime.dx0)
dA.dy0 <- denom * (2 * xprime * ddenom.dy0 + denom *
  dxprime.dy0)
out.front <- - (a^2 * e)/4
z <- sinsq.2.tt.theta/A #
z[abs(A) < tol] <- 0
d2xprime.dedx0 <- out.front * ((2 * sin(4 * (tt - theta)) *
  dt.dx0)/A - ((dA.dx0 * z)/A))
d2xprime.dedy0 <- out.front * ((2 * sin(4 * (tt - theta)) *
  dt.dy0)/A - ((dA.dy0 * z)/A))
d2xprime.dedx0[abs(A) < tol] <- 0
d2xprime.dedy0[abs(A) < tol] <- 0 #
# Here's one from Mathematica.
#
d2yprime.dedx0 <- ( - (3 * e)/2 * yprime * dt.dx0 *
  sin.2.tt.theta)/denom^2
d2yprime.dedx0[abs(yprime) < tol] <- 0
d2x.dedx0 <- cos.theta * d2xprime.dedx0 - sin.theta *
  d2yprime.dedx0
d2y.dedx0 <- sin.theta * d2xprime.dedx0 + cos.theta *
  d2yprime.dedx0
grad.ex0 <- 2 * sum( - x.diff * d2x.dedx0 + dx.de * dx.dx0 -
  y.diff * d2y.dedx0 + dy.de * dy.dx0)
d2yprime.dedy0 <- ( - (3 * e)/2 * yprime * dt.dy0 *
  sin.2.tt.theta)/denom^2
d2yprime.dedy0[abs(yprime) < tol] <- 0
d2x.dedy0 <- cos.theta * d2xprime.dedy0 - sin.theta *
  d2yprime.dedy0
d2y.dedy0 <- sin.theta * d2xprime.dedy0 + cos.theta *
  d2yprime.dedy0
grad.ey0 <- 2 * sum( - x.diff * d2x.dedy0 + dx.de * dx.dy0 -
  y.diff * d2y.dedy0 + dy.de * dy.dy0) #
#
# Here's another from Mathematica.
#

```

```

out.front <- (xprime * (1 - 2 * e^2 + e^2 *
              cos.2.tt.theta))/ denom^2
out.front[abs(denom) < tol] <- 0
d2xprime.dthetadx0 <- out.front * dt.dx0
d2yprime.dthetady0 <- out.front * dt.dy0 #
out.front <- ((one.minus.e.sq) * yprime * (3 - 2 * denom))/
              denom^2
out.front[abs(denom) < tol] <- 0
d2yprime.dthetadx0 <- out.front * dt.dx0
d2yprime.dthetady0 <- out.front * dt.dy0 #

#
#

d2x.dthetadx0 <- - dy.dx0 + cos.theta * d2xprime.dthetadx0
              - sin.theta * d2yprime.dthetadx0
d2y.dthetadx0 <- (dx.dx0 - 1) + sin.theta *
              d2xprime.dthetadx0 + cos.theta * d2yprime.dthetadx0
grad.thetax0 <- 2 * sum( - x.diff * d2x.dthetadx0 +
dx.dtheta * dx.dx0 - y.diff * d2y.dthetadx0 +
              dy.dtheta * dy.dx0)
d2x.dthetady0 <- - (dy.dy0 - 1) + cos.theta *
              d2xprime.dthetady0 - sin.theta * d2yprime.dthetady0
d2y.dthetady0 <- dx.dy0 + sin.theta * d2xprime.dthetady0 +
              cos.theta * d2yprime.dthetady0
grad.thetay0 <- 2 * sum( - x.diff * d2x.dthetady0 +
dx.dtheta * dx.dy0 - y.diff * d2y.dthetady0 +
              dy.dtheta * dy.dy0)
#

#
#

d2t.dx02 <- -2 * (dt.dx0 * dt.dy0)
d2t.dx0dy0 <- -1/R.sq + 2 * (dt.dx0)^2
d2t.dy02 <- - d2t.dx02
d2xprime.dx02 <- - dxprime.dtheta * d2t.dx02 -
              d2xprime.dthetadx0 * dt.dx0
d2yprime.dx02 <- - dyprime.dtheta * d2t.dx02 -
              d2yprime.dthetadx0 * dt.dx0
d2x.dx02 <- cos.theta * d2xprime.dx02 - sin.theta *
              d2yprime.dx02
d2y.dx02 <- sin.theta * d2xprime.dx02 + cos.theta *
              d2yprime.dx02
grad.x02 <- 2 * sum( - x.diff * d2x.dx02 + dx.dx0^2 - y.diff
              * d2y.dx02 + dy.dx0^2) #

#

d2xprime.dx0dy0 <- - dxprime.dtheta * d2t.dx0dy0 -
              d2xprime.dthetady0 * dt.dx0
d2yprime.dx0dy0 <- - dyprime.dtheta * d2t.dx0dy0 -
              d2yprime.dthetady0 * dt.dx0
d2x.dx0dy0 <- cos.theta * d2xprime.dx0dy0 - sin.theta *
              d2yprime.dx0dy0
d2y.dx0dy0 <- sin.theta * d2xprime.dx0dy0 + cos.theta *
              d2yprime.dx0dy0
grad.x0y0 <- 2 * sum( - x.diff * d2x.dx0dy0 + dx.dx0 *
              dx.dy0 - y.diff * d2y.dx0dy0 + dy.dx0 * dy.dy0) #

#

d2xprime.dy02 <- - dxprime.dtheta * d2t.dy02 -
              d2xprime.dthetady0 * dt.dy0
d2yprime.dy02 <- - dyprime.dtheta * d2t.dy02 -
              d2yprime.dthetady0 * dt.dy0

```

```

d2x.dy02 <- cos.theta * d2xprime.dy02 - sin.theta *
  d2yprime.dy02
d2y.dy02 <- sin.theta * d2xprime.dy02 + cos.theta *
  d2yprime.dy02
grad.y02 <- 2 * sum( - x.diff * d2x.dy02 + dx.dy0^2 - y.diff
  * d2y.dy02 + dy.dy0^2)
hessian <- c(grad.a2, grad.ae, grad.e2, grad.atheta,
  grad.etheta, grad.theta2, grad.ax0, grad.ex0,
  grad.thetax0, grad.x02, grad.ay0, grad.ey0,
  grad.thetay0, grad.x0y0, grad.y02) #
### print(hessian)
}
thing <- list(gradient = grad, hessian = hessian)
return(thing)
}

```

> ell.grad.II

```

function(params, tt, my.x, my.y, is.there.hess, fit.center, class.I,
  which.type)
{
  tol <- 1e-006 #
  a <- params[1]
  b <- params[2]
  e <- sqrt(1 - (b/a)^2)
  theta <- params[3]
  if(fit.center == T) {
    center.x <- params[4]
    center.y <- params[5]
    delta <- params[6]
    tt <- ell.tt(my.x - center.x, my.y - center.y)
  }
  else {
    delta <- params[4]
    center.x <- center.y <- 0
  }
  if(sum(class.I) == length(my.x)) {
    fitted <- ell.pred(tt, a, b, theta, return.unrotated.too =
      T, fit.center = fit.center, center.x = center.x, center.y =
        center.y)
    xprime <- fitted$x.prime
    yprime <- fitted$y.prime
    x <- fitted$x
    y <- fitted$y
  }
  else {
    fitted.I <- ell.pred(tt[class.I], a, b, theta,
      return.unrotated.too = T, fit.center = fit.center,
      center.x = center.x, center.y = center.y)
    if(which.type == 1)
      fitted.II <- ell.pred(tt[!class.I], a + delta, b,
        theta, return.unrotated.too = T, fit.center
          = fit.center, center.x = center.x, center.y
            = center.y)
    else fitted.II <- ell.pred(tt[!class.I], a, b + delta,
      theta,
      return.unrotated.too = T, fit.center =
        fit.center, center.x = center.x, center.y =

```

```

        center.y)
xprime <- yprime <- x <- y <- numeric(length(my.x))
xprime[class.I] <- fitted.I$x.prime
xprime[!class.I] <- fitted.II$x.prime
yprime[class.I] <- fitted.I$y.prime
yprime[!class.I] <- fitted.II$y.prime
x[class.I] <- fitted.I$x
x[!class.I] <- fitted.II$x
y[class.I] <- fitted.I$y
y[!class.I] <- fitted.II$y
}
if(which.type == 1) {
  a <- rep(a, length(my.x))
  a[!class.I] <- a[!class.I] + delta
}
else {
  b <- rep(b, length(my.x))
  b[!class.I] <- b[!class.I] + delta
}
cos.theta <- cos(theta)
sin.theta <- sin(theta)
cos.2.tt.theta <- cos(2 * (tt - theta))
sin.2.tt.theta <- sin(2 * (tt - theta))
sinsq.tt.theta <- (sin(tt - theta))^2
cossq.tt.theta <- (cos(tt - theta))^2
sinsq.2.tt.theta <- (sin(2 * (tt - theta)))^2
consq.2.tt.theta <- (cos(2 * (tt - theta)))^2
one.minus.e.sq <- 1 - e^2
denom <- cossq.tt.theta * one.minus.e.sq + sinsq.tt.theta
dxprime.da <- xprime/a
dxprime.de <- (( - a^2/(4 * xprime)) * (e *
sinsq.2.tt.theta))/(denom^2)
dxprime.de[abs(xprime) < tol] <- 0
dyprime.da <- yprime/a
dyprime.de <- - (one.minus.e.sq * xprime * dxprime.de + e * (a^2
- xprime^2))/yprime
dyprime.de[abs(yprime) < tol] <- 0 #
#
# Okay. Here's where we go from "e" to "b". We still need dx/y.de.
#
de.db <- - b/(a^2 * e)
dx.da <- cos.theta * dxprime.da - sin.theta * dyprime.da #
dx.de <- cos.theta * dxprime.de - sin.theta * dyprime.de
dx.db <- cos.theta * dxprime.de * de.db - sin.theta * dyprime.de *
de.db
dy.da <- sin.theta * dxprime.da + cos.theta * dyprime.da #
dy.de <- sin.theta * dxprime.de + cos.theta * dyprime.de
dy.db <- sin.theta * dxprime.de * de.db + cos.theta * dyprime.de *
de.db
x.diff <- my.x - x
y.diff <- my.y - y
grad.a.indiv <- -2 * (x.diff * dx.da + y.diff * dy.da) #
grad.a <- sum(grad.a.indiv)
### grad.e <- -2 * sum(x.diff * dx.de + y.diff * dy.de)
grad.b.indiv <- -2 * (x.diff * dx.db + y.diff * dy.db)
grad.b <- sum(grad.b.indiv)
if(which.type == 1)
  grad.delta <- sum(grad.a.indiv[!class.I])

```



```

else grad.delta <- sum(grad.b.indiv[!class.I])
num <- one.minus.e.sq * sin(2 * (tt - theta))
dxprime.dtheta <- (a^2/(2 * xprime)) * (num/denom^2)
dxprime.dtheta[abs(xprime) < tol] <- 0
dyprime.dtheta <- - (one.minus.e.sq * xprime * dxprime.dtheta)/
  yprime
dyprime.dtheta[abs(yprime) < tol] <- 0
dx.dtheta <- - (y - center.y) + cos.theta * dxprime.dtheta -
  sin.theta * dyprime.dtheta
dy.dtheta <- (x - center.x) + sin.theta * dxprime.dtheta +
  cos.theta * dyprime.dtheta
grad.theta <- -2 * sum(x.diff * dx.dtheta + y.diff * dy.dtheta)

#   if(!exists("killme", frame = 0))
#   browser()
if(fit.center == F)
  grad <- c(grad.a, grad.b, grad.theta, grad.delta)
else {
  dxprime.dt <- - dxprime.dtheta
  dyprime.dt <- - dyprime.dtheta
  R.sq <- (my.x - center.x)^2 + (my.y - center.y)^2
  dt.dx0 <- (my.y - center.y)/R.sq
  dt.dy0 <- - (my.x - center.x)/R.sq
  dxprime.dx0 <- dxprime.dt * dt.dx0
  dxprime.dy0 <- dxprime.dt * dt.dy0
  dyprime.dx0 <- dyprime.dt * dt.dx0
  dyprime.dy0 <- dyprime.dt * dt.dy0 #
  dyprime.dprime <- one.minus.e.sq * ( - xprime/yprime)
  dyprime.dprime[abs(yprime) < tol] <- 0 #
  dx.dx0 <- (cos.theta * dxprime.dx0) - (sin.theta *
    dyprime.dx0) + 1
  dy.dx0 <- (sin.theta * dxprime.dx0) + (cos.theta *
    dyprime.dx0)
  dx.dy0 <- (cos.theta * dxprime.dy0) - (sin.theta *
    dyprime.dy0)
  dy.dy0 <- (sin.theta * dxprime.dy0) + (cos.theta *
    dyprime.dy0) + 1
  grad.x0 <- -2 * sum(x.diff * dx.dx0 + y.diff * dy.dx0)
  grad.y0 <- -2 * sum(x.diff * dx.dy0 + y.diff * dy.dy0)
  grad <- c(grad.a, grad.b, grad.theta, grad.x0, grad.y0,
    grad.delta)
}
if(is.there.hess == F) {
  print(grad)
  return(grad)
}
d2xprime.da2 <- d2yprime.da2 <- 0
d2xprime.dade <- dxprime.de/a
d2yprime.dade <- dyprime.de/a
d2xprime.dadtheta <- dxprime.dtheta/a
d2yprime.dadtheta <- dyprime.dtheta/a
ddenom.de <- -2 * e * cossq.tt.theta
ddenom.dtheta <- - e^2 * sin(2 * (tt - theta))
term1 <- ( - a^2 * sinsq.2.tt.theta)/4
xprime.denom.sq <- xprime * denom^2
d2xprime.de2 <- xprime.denom.sq - e * (dxprime.de * denom^2 + 2 *
  xprime * denom * ddenom.de)
d2xprime.de2 <- (term1/xprime.denom.sq^2) * d2xprime.de2

```

```

d2xprime.de2[abs(xprime) < 1e-006] <- 0
d2yprime.de2 <- one.minus.e.sq * (-2 * xprime * d2xprime.de2 - 2 *
  dxprime.de^2) + 8 * e * xprime * dxprime.de - 2 * (a^2 -
  xprime^2)
term1 <- - a^2 * e
d2xprime.dedtheta <- - xprime.denom.sq * sin(4 * (tt - theta)) -
  sinsq.2.tt.theta * (xprime * denom * ddenom.dtheta +
  dxprime.dtheta * denom^2)
d2xprime.dedtheta <- (( - a^2 * e)/xprime.denom.sq^2) *
  d2xprime.dedtheta
d2xprime.dedtheta[abs(xprime) < 1e-006] <- 0
d2yprime.dedtheta <- (-1/yprime^2) * (yprime * ((one.minus.e.sq *
(
  xprime * d2xprime.dedtheta + dxprime.dtheta * dxprime.de) -
  2 * e * xprime * dxprime.dtheta) - one.minus.e.sq * xprime *
  dxprime.dtheta * dxprime.de)
d2yprime.dedtheta[abs(yprime) < 1e-006] <- 0
dnum.dtheta <- -2 * one.minus.e.sq * cos(2 * (tt - theta))
d2xprime.dtheta2 <- xprime.denom.sq * dnum.dtheta - num * (2 *
  xprime * denom * ddenom.dtheta + denom^2 * dxprime.dtheta)
d2xprime.dtheta2 <- (d2xprime.dtheta2 * a^2)/(2 *
  xprime.denom.sq^2)
d2xprime.dtheta2[abs(xprime) < 1e-006] <- 0
d2yprime.dtheta2 <- - (one.minus.e.sq/yprime) * (yprime * (xprime
  * d2xprime.dtheta2 + dxprime.dtheta^2) - dyprime.dtheta * (
  xprime * dxprime.dtheta))
d2yprime.dtheta2[abs(yprime) < 1e-006] <- 0 #
d2e.db2 <- (b * de.db - e)/(a * e)^2
d2e.dadb <- (2 * b)/(a^3 * e) #
### d2x.dade <- cos.theta * d2xprime.dade - sin.theta * d2yprime.dade
d2x.dadb <- cos.theta * (dxprime.de * d2e.dadb + d2xprime.dade *
  de.db) - sin.theta * (dyprime.de * d2e.dadb + d2yprime.dade
  * de.db) #
### d2y.dade <- sin.theta * d2xprime.dade + cos.theta * d2yprime.dade
d2y.dadb <- sin.theta * (dxprime.de * d2e.dadb + d2xprime.dade *
  de.db) + cos.theta * (dyprime.de * d2e.dadb + d2yprime.dade
  * de.db) #
### d2x.de2 <- cos.theta * d2xprime.de2 - sin.theta * d2yprime.de2
### d2y.de2 <- sin.theta * d2xprime.de2 + cos.theta * d2yprime.de2
d2x.dadb <- cos.theta * (dxprime.de * d2e.dadb + d2xprime.dade *
  de.db) - sin.theta * (dyprime.de * d2e.dadb + d2yprime.dade
  * de.db)
d2y.dadb <- sin.theta * (dxprime.de * d2e.dadb + d2xprime.dade *
  de.db) + cos.theta * (dyprime.de * d2e.dadb + d2yprime.dade
  * de.db)
d2xprime.dedb <- d2xprime.de2 * de.db
d2yprime.dedb <- d2yprime.de2 * de.db
d2x.db2 <- cos.theta * (dxprime.de * d2e.db2 + d2xprime.dedb *
  de.db) - sin.theta * (dyprime.de * d2e.db2 + d2yprime.dedb *
  de.db)
d2y.db2 <- sin.theta * (dxprime.de * d2e.db2 + d2xprime.dedb *
  de.db) + cos.theta * (dyprime.de * d2e.db2 + d2yprime.dedb *
  de.db)
grad.a2 <- 2 * sum(dx.da^2 + dy.da^2) #
### grad.ae <- 2 * sum( - x.diff * d2x.dade + dx.da * dx.de - y.diff *
### d2y.dade + dy.da * dy.de)
grad.ab <- 2 * sum( - x.diff * d2x.dadb + dx.da * dx.db - y.diff *
  d2y.dadb + dy.da * dy.db)

```

```

d2x.dadtheta <- cos.theta * d2xprime.dadtheta - sin.theta *
  d2yprime.dadtheta - dy.da
d2y.dadtheta <- sin.theta * d2xprime.dadtheta + cos.theta *
  d2yprime.dadtheta + dx.da #
###
d2x.dedtheta <- cos.theta * d2xprime.dedtheta - sin.theta *
  d2yprime.dedtheta - dy.de
###
d2y.dedtheta <- sin.theta * d2xprime.dedtheta + cos.theta *
  d2yprime.dedtheta + dx.de
###
d2x.dbdtheta <- cos.theta * d2xprime.dedtheta * de.db - sin.theta
  * d2yprime.dedtheta * de.db - dy.db
d2y.dbdtheta <- sin.theta * d2xprime.dedtheta * de.db + cos.theta
  * d2yprime.dedtheta * de.db + dx.db
d2x.dtheta2 <- cos.theta * d2xprime.dtheta2 - sin.theta *
  d2yprime.dtheta2 - 2 * dy.dtheta + x
d2y.dtheta2 <- sin.theta * d2xprime.dtheta2 + cos.theta *
  d2yprime.dtheta2 + 2 * dx.dtheta + y
grad.atheta <- 2 * sum( - x.diff * d2x.dadtheta + dx.da *
  dx.dtheta - y.diff * d2y.dadtheta + dy.da * dy.dtheta) #
###
grad.e2 <- 2 * sum( - x.diff * d2x.de2 + dx.de^2 - y.diff * ###
  d2y.de2 + dy.de^2)
###
grad.etheta <- 2 * sum( - x.diff * d2x.dedtheta + dx.de * dx.dtheta
  - y.diff * d2y.dedtheta + dy.de * dy.dtheta)
###
grad.b2 <- 2 * sum( - x.diff * d2x.db2 + dx.db^2 - y.diff *
  d2y.db2 + dy.db^2)
grad.btheta <- 2 * sum( - x.diff * d2x.dbdtheta + dx.db *
  dx.dtheta - y.diff * d2y.dbdtheta + dy.db * dy.dtheta)
grad.theta2 <- 2 * sum( - x.diff * d2x.dtheta2 + dx.dtheta^2 -
  y.diff * d2y.dtheta2 + dy.dtheta^2)
if(fit.center == F)
  hessian <- c(grad.a2, grad.ab, grad.b2, grad.atheta,
    grad.btheta, grad.theta2)
else {
#
#
# Second derivatives: a and x0, a and y0
#
  d2xprime.dadx0 <- dxprime.dx0/a
  d2yprime.dadx0 <- dyprime.dx0/a
  d2xprime.dady0 <- dxprime.dy0/a
  d2yprime.dady0 <- dyprime.dy0/a
  d2x.dadx0 <- cos.theta * d2xprime.dadx0 - sin.theta *
    d2yprime.dadx0
  d2y.dadx0 <- sin.theta * d2xprime.dadx0 + cos.theta *
    d2yprime.dadx0 #
# and the gradient
  grad.ax0 <- 2 * sum( - x.diff * d2x.dadx0 + dx.da * dx.dx0 -
    y.diff * d2y.dadx0 + dy.da * dy.dx0)
  d2x.dady0 <- cos.theta * d2xprime.dady0 - sin.theta *
    d2yprime.dady0
  d2y.dady0 <- sin.theta * d2xprime.dady0 + cos.theta *
    d2yprime.dady0 #
#
  grad.ay0 <- 2 * sum( - x.diff * d2x.dady0 + dx.da * dx.dy0 -
    y.diff * d2y.dady0 + dy.da * dy.dy0) #
#
#
  ddenom.dx0 <- e^2 * sin.2.tt.theta * dt.dx0
  ddenom.dy0 <- e^2 * sin.2.tt.theta * dt.dy0

```

```

A <- xprime * denom^2
dA.dx0 <- denom * (2 * xprime * ddenom.dx0 + denom *
  dxprime.dx0)
dA.dy0 <- denom * (2 * xprime * ddenom.dy0 + denom *
  dxprime.dy0)
out.front <- - (a^2 * e)/4
z <- sinsq.2.tt.theta/A #
z[abs(A) < tol] <- 0
d2xprime.dedx0 <- out.front * ((2 * sin(4 * (tt - theta)) *
  dt.dx0)/A - ((dA.dx0 * z)/A))
d2xprime.dedy0 <- out.front * ((2 * sin(4 * (tt - theta)) *
  dt.dy0)/A - ((dA.dy0 * z)/A))
d2xprime.dedx0[abs(A) < tol] <- 0
d2xprime.dedy0[abs(A) < tol] <- 0 #
# Here's one from Mathematica.
#
d2yprime.dedx0 <- ( - (3 * e)/2 * yprime * dt.dx0 *
  sin.2.tt.theta)/denom^2
d2yprime.dedx0[abs(yprime) < tol] <- 0 #
###
d2x.dedx0 <- cos.theta * d2xprime.dedx0 - sin.theta *
  d2yprime.dedx0
###
d2y.dedx0 <- sin.theta * d2xprime.dedx0 + cos.theta *
  d2yprime.dedx0
###
grad.ex0 <- 2 * sum( - x.diff * d2x.dedx0 + dx.de * dx.dx0 -
  y.diff * d2y.dedx0 + dy.de * dy.dx0)
d2x.dbdx0 <- cos.theta * d2xprime.dedx0 * de.db - sin.theta
  * d2yprime.dedx0 * de.db
d2y.dbdx0 <- sin.theta * d2xprime.dedx0 * de.db + cos.theta
  * d2yprime.dedx0 * de.db
grad.bx0 <- 2 * sum( - x.diff * d2x.dbdx0 + dx.db * dx.dx0 -
  y.diff * d2y.dbdx0 + dy.db * dy.dx0)
d2yprime.dedy0 <- ( - (3 * e)/2 * yprime * dt.dy0 *
  sin.2.tt.theta)/denom^2
d2yprime.dedy0[abs(yprime) < tol] <- 0 #
###
d2x.dedy0 <- cos.theta * d2xprime.dedy0 - sin.theta *
  d2yprime.dedy0
###
d2y.dedy0 <- sin.theta * d2xprime.dedy0 + cos.theta *
  d2yprime.dedy0
###
d2x.dbdy0 <- cos.theta * d2xprime.dedy0 * de.db - sin.theta
  * d2yprime.dedy0 * de.db
d2y.dbdy0 <- sin.theta * d2xprime.dedy0 * de.db + cos.theta
  * d2yprime.dedy0 * de.db
grad.by0 <- 2 * sum( - x.diff * d2x.dbdy0 + dx.db * dx.dy0 -
  y.diff * d2y.dbdy0 + dy.db * dy.dy0) #
#
# Here's another from Mathematica.
#
out.front <- (xprime * (1 - 2 * e^2 + e^2 *
  cos.2.tt.theta))/denom^2
out.front[abs(denom) < tol] <- 0
d2xprime.dthetadx0 <- out.front * dt.dx0
d2xprime.dthetady0 <- out.front * dt.dy0 #
out.front <- ((one.minus.e.sq) * yprime * (3 - 2 * denom))/
  denom^2
out.front[abs(denom) < tol] <- 0
d2yprime.dthetadx0 <- out.front * dt.dx0
d2yprime.dthetady0 <- out.front * dt.dy0 #
#

```

```

#
d2x.dthetadx0 <- - dy.dx0 + cos.theta * d2xprime.dthetadx0
- sin.theta * d2yprime.dthetadx0
d2y.dthetadx0 <- (dx.dx0 - 1) + sin.theta *
d2xprime.dthetadx0 + cos.theta * d2yprime.dthetadx0
grad.thetax0 <- 2 * sum( - x.diff * d2x.dthetadx0 +
dx.dtheta * dx.dx0 - y.diff * d2y.dthetadx0 +
dy.dtheta * dy.dx0)
d2x.dthetady0 <- - (dy.dy0 - 1) + cos.theta *
d2xprime.dthetady0 - sin.theta * d2yprime.dthetady0
d2y.dthetady0 <- dx.dy0 + sin.theta * d2xprime.dthetady0 +
cos.theta * d2yprime.dthetady0
grad.thetay0 <- 2 * sum( - x.diff * d2x.dthetady0 +
dx.dtheta * dx.dy0 - y.diff * d2y.dthetady0 +
dy.dtheta * dy.dy0)
#
#
d2t.dx02 <- -2 * (dt.dx0 * dt.dy0)
d2t.dx0dy0 <- -1/R.sq + 2 * (dt.dx0)^2
d2t.dy02 <- - d2t.dx02
d2xprime.dx02 <- - dxprime.dtheta * d2t.dx02 -
d2xprime.dthetadx0 * dt.dx0
d2yprime.dx02 <- - dyprime.dtheta * d2t.dx02 -
d2yprime.dthetadx0 * dt.dx0
d2x.dx02 <- cos.theta * d2xprime.dx02 - sin.theta *
d2yprime.dx02
d2y.dx02 <- sin.theta * d2xprime.dx02 + cos.theta *
d2yprime.dx02
grad.x02 <- 2 * sum( - x.diff * d2x.dx02 + dx.dx0^2 - y.diff
*d2y.dx02 + dy.dx0^2) #
#
d2xprime.dx0dy0 <- - dxprime.dtheta * d2t.dx0dy0 -
d2xprime.dthetady0 * dt.dx0
d2yprime.dx0dy0 <- - dyprime.dtheta * d2t.dx0dy0 -
d2yprime.dthetady0 * dt.dx0
d2x.dx0dy0 <- cos.theta * d2xprime.dx0dy0 - sin.theta *
d2yprime.dx0dy0
d2y.dx0dy0 <- sin.theta * d2xprime.dx0dy0 + cos.theta *
d2yprime.dx0dy0
grad.x0y0 <- 2 * sum( - x.diff * d2x.dx0dy0 + dx.dx0 *
dx.dy0 - y.diff * d2y.dx0dy0 + dy.dx0 * dy.dy0) #
#
d2xprime.dy02 <- - dxprime.dtheta * d2t.dy02 -
d2xprime.dthetady0 * dt.dy0
d2yprime.dy02 <- - dyprime.dtheta * d2t.dy02 -
d2yprime.dthetady0 * dt.dy0
d2x.dy02 <- cos.theta * d2xprime.dy02 - sin.theta *
d2yprime.dy02
d2y.dy02 <- sin.theta * d2xprime.dy02 + cos.theta *
d2yprime.dy02
grad.y02 <- 2 * sum( - x.diff * d2x.dy02 + dx.dy0^2 - y.diff
*d2y.dy02 + dy.dy0^2)
hessian <- c(grad.a2, grad.ab, grad.b2, grad.atheta,
grad.btheta, grad.theta2, grad.ax0, grad.bx0,
grad.thetax0, grad.x02, grad.ay0, grad.by0,
grad.thetay0, grad.x0y0, grad.y02) #
###
hessian <- c(grad.a2, grad.ae, grad.e2, grad.atheta,

```

```

###          grad.etheta, grad.theta2, grad.ax0, grad.ex0,
###          grad.thetax0, grad.x02, grad.ay0, grad.ey0,
###          grad.thetay0, grad.x0y0, grad.y02) #
### print(hessian)
}
thing <- list(gradient = grad, hessian = hessian)
return(thing)
}

> ell.pred
function(tt, a, b, theta = 0, return.unrotated.too = F, fit.center = F,
        center.x = 0, center.y = 0)
{
#
# Get fitted x and y for ellipse with points at angles "tt",
# with eccentricity = e and a = a. Rotate by theta afterwards,
# if asked. Finally, if fit.center = T, move everything by
# center.x in the x direction and by center.y in the y direction.
#
# A little algebra shows that
#
# 
$$x^2 = \frac{a^2 \sin^2(\pi/2 - tt) (1 - e^2)}{\sin^2(tt) + \sin^2(\pi/2 - tt) (1 - e^2)}$$

# if a > b.
#
# (If a < b, that's y^2, except you have to switch the tt's and the
# (pi/2 - tt)'s.). The sin^2(pi/2-tt) term is "thang." So take
# x (if a > b) to be the positive square root of that for the
# moment. Then y^2 = (a - ex)^2 - (ae - x)^2. So get that, too.
#
    new.tt <- tt - theta
    if(a > b) {
        e <- sqrt(1 - (b/a)^2) #
###      if(e > 0.99) return(1000 * length(x))
        thang <- (sin(pi/2 - new.tt)^2) * (1 - e^2) #
        x <- sqrt((a^2 * thang)/(sin(new.tt)^2 + thang))
        yy <- (a - e * x)^2 - (a * e - x)^2 #
# Make sure y^2 is always positive (round-off errors can hurt here);
# then get y.
#
        yy[yy < 0] <- 0
        y <- sqrt(yy) #
    }
    else {
###      e <- sqrt(1 - (a/b)^2) #
        if(e > 0.99) return(1000 * length(x))
        thang <- (sin(new.tt)^2) * (1 - e^2) #
        y <- b * sqrt(thang/(sin(pi/2 - new.tt)^2 + thang))
        xx <- (b - e * y)^2 - (b * e - y)^2 #
        xx[xx < 0] <- 0
        x <- sqrt(xx) #
    }
    quad <- new.tt %% (2 * pi)
    quad.2.3 <- quad > pi/2 & quad < (3 * pi)/2
    x[quad.2.3] <- - x[quad.2.3]
    quad.3.4 <- quad > pi
    y[quad.3.4] <- - y[quad.3.4]
    rotated.data <- matrix(c(cos(theta), - sin(theta), sin(theta),

```

```

cos( theta)), 2, 2, T) %*% rbind(x, y)
if(fit.center == F) {
  center.x <- 0
  center.y <- 0
}
if(return.unrotated.too == T)
  return(list(x = rotated.data[1, ] + center.x, y =
    rotated.data[2, ] + center.y, x.prime = x, y.prime
    = y))
else return(list(x = rotated.data[1, ] + center.x, y =
rotated.data[2, ] + center.y))
}

```

> ell.tt

```

function(x, y)
{
#
# ell.tt: get angle values for data. It's acos(x/r)
# in the first quadrant, etc.
#
  tt <- numeric(length(x))
  ratio <- x/sqrt(x^2 + y^2)
  ratio[ratio > 1] <- 1
  ratio[ratio < -1] <- -1
  ind <- x >= 0 & y >= 0
  tt[ind] <- acos(ratio[ind])
  ind <- x < 0 & y >= 0
  tt[ind] <- pi - acos( - ratio[ind])
  ind <- x < 0 & y < 0
  tt[ind] <- pi + acos( - ratio[ind])
  ind <- x >= 0 & y < 0
  tt[ind] <- 2 * pi - acos(ratio[ind])      #
  tt
}

```





## APPENDIX B. EXAMPLES

**pc1ss1** = **pc** is subject 1's initials  
the **1** is the spatial frequency  
**ss1** means sum of squares obtained from ellipse (vice ellipse.**II** or ellipse.**III**)

**pc1all** = a data frame containing all of the data at 1 cpd for **pc**  
this data always consists of non-oblique data followed by oblique data.  
For this subject the first 80 (x,y) pairs are non-oblique and 81-160 are oblique data

**fit.center=T** lets the ellipse center "float" vice being pinned to the origin

```
> pc1ss1_ellipse(pc1all[,1], pc1all[,2], fit.center=T)
a: 0.0615 ,b: 0.05194 ,th: -0.005236 ;x,y: 0.001551 0.00008819 ;obj: 0.06455
a: 0.02742 ,b: 0.02742 ,th: -0.07295 ;x,y: 0.01894 -0.001528 ;obj: 0.07366
removed middle output to save space
a: 0.04698 ,b: 0.03466 ,th: -0.02604 ;x,y: 0.004495 0.0006379 ;obj: 0.02068
a: 0.04698 ,b: 0.03466 ,th: -0.02605 ;x,y: 0.004495 0.0006379 ;obj: 0.02068
a: 0.04698 ,b: 0.03466 ,th: -0.02605 ;x,y: 0.004495 0.0006379 ;obj: 0.02068
> pc1ss1
```

Message was

RELATIVE FUNCTION CONVERGENCE

a b theta center.x center.y

0.04698378 0.03466318 -0.02604936 0.004495335 0.0006378881

```
> pc1ss1[2]
```

\$objective:

```
[1] 0.02068425
```

**pc1ss2.III** = **pc** is subject 1's initials  
the **1** is the spatial frequency  
**ss2** means sum of squares obtained from ellipse.**II** or ellipse.**III**  
**.III** lets us know this is from ellipse.**III**

```
> pc1ss2.III_ellipse.III(pc1all[,1], pc1all[,2], grad=F,
+ is.there.hess=F, fit.center=T, class.I = (1:160) < 81, plot=F)
a: 0.07282 , delta.a: 0 ,b: 0.0615 delta.b: 0 ,th: -0.005236 ;x,y: 0.001551
0.00008819 ;obj: 0.1364
a: 0.07283 , delta.a: 0 ,b: 0.0615 delta.b: 0 ,th: -0.005236 ;x,y: 0.001551
0.00008819 ;obj: 0.1364
removed middle output to save space
6 ;x,y: 0.004467 0.0006382 ;obj: 0.02067
a: 0.04703 , delta.a: -0.0001285 ,b: 0.03424 delta.b: 0.0008527 ,th: -0.0266
6 ;x,y: 0.004467 0.0006382 ;obj: 0.02067
```

```
a: 0.04703 , delta.a: -0.0001281 ,b: 0.03424 delta.b: 0.000853 ,th: -0.02666
;x,y: 0.004467 0.0006382 ;obj: 0.02067
a: 0.04703 , delta.a: -0.0001281 ,b: 0.03424 delta.b: 0.0008523 ,th: -0.0266
6 ;x,y: 0.004467 0.0006382 ;obj: 0.02067
```

Warning messages:

```
1: singularity encountered in: nlminb.0(temp, p, liv, lv, objective, bounds,
scale)
removed identical warnings numbered 2 and 3
4: singularity encountered in: nlminb.0(temp, p, liv, lv, objective, bounds,
scale)
```

```
> pc1ss2.III
```

Message was

```
RELATIVE FUNCTION CONVERGENCE
a      b      theta center.x center.y delta.a
0.04703421 0.03424435 -0.0266577 0.004466774 0.0006382473 -0.0001281251
delta.b
0.0008526696
```

**this is the objective function value which the program minimizes**

```
> pc1ss2.III[2]
```

\$objective:

```
[1] 0.02067104
```

**p-values for the ellipses being different?**

```
> 1-pf(((pc1ss1[[2]]-pc1ss2.III[[2]])/2)/(pc1ss1[[2]]/(160-5)),2,155)
```

```
[1] 0.9517269
```

```
> 1-pf(((pc3ss1[[2]]-pc3ss2.III[[2]])/2)/(pc3ss1[[2]]/(160-5)),2,155)
```

```
[1] 0.07660905
```

```
> 1-pf(((pc7ss1[[2]]-pc7ss2.III[[2]])/2)/(pc7ss1[[2]]/(160-5)),2,155)
```

```
[1] 1.822829e-007
```

**are the b's significant**

```
> 1-pf((pc1ss2.II[[2]]-pc1ss2.III[[2]])/(pc1ss2.III[[2]]/153),1,153)
```

```
[1] 0.7693711
```

```
> 1-pf((pc3ss2.II[[2]]-pc3ss2.III[[2]])/(pc3ss2.III[[2]]/153),1,153)
```

```
[1] 0.837154
```

```
> 1-pf((pc7ss2.II[[2]]-pc7ss2.III[[2]])/(pc7ss2.III[[2]]/153),1,153)
```

```
[1] 2.110824e-008
```

**changing which.type to 2 forces the non-oblique and oblique ellipses to have the same major axis.**

```

> pc1ss2.II.which.type.2_ellipse.II(pc1all[,1],pc1all[,2],fit.center=T,class.I = (1:160) <
  81,which.type=2,grad=F,is.there.hess=F,plot.it=F)
>pc3ss2.II.which.type.2_ellipse.II(pc3all[,1],pc3all[,2],fit.center=T,class.I = (1:160) <
  81,which.type=2,grad=F,is.there.hess=F,plot.it=F)
>pc7ss2.II.which.type.2_ellipse.II(pc7all[,1],pc7all[,2],fit.center=T,class.I = (1:160) <
  81,which.type=2,grad=F,is.there.hess=F,plot.it=F)

```

**are the a's significant ?**

**subject 1 at 7 cpd**

```

> 1-pf((pc7ss2.II.which.type.2[[2]]-pc7ss2.III[[2]])/(pc7ss2.III[[2]]/153),1,153)
[1] 0.5883988

```

**subject 1 at 3 cpd**

```

> 1-pf((pc3ss2.II.which.type.2[[2]]-pc3ss2.III[[2]])/(pc3ss2.III[[2]]/153),1,153)
[1] 0.02835718

```

**subject 1 at 1 cpd**

```

> 1-pf((pc1ss2.II.which.type.2[[2]]-pc1ss2.III[[2]])/(pc1ss2.III[[2]]/153),1,153)
[1] 0.9753455

```



## LIST OF REFERENCES

- Annis, R. C. and Frost, B. (1973). Human visual ecology and orientation anisotropies in Science, 182, 729-731.
- Appelle, S. (1972). Perception and discrimination as a function of stimulus orientation: The "oblique effect" in man and animals. Psychological Bulletin, 78, 266-278.
- Attneave, F. and Olsen, R. K. (1967). Discriminability of stimuli varying in physical and retinal orientation. Journal of Experimental Psychology, 74, 149-157.
- Attneave, F. and Reid, K. W. (1968). Voluntary control of frame of reference and slope equivalence under head rotation. Journal of Experimental Psychology, 78, 153-159.
- Bates, D. M. and Watts, D. G. (1988). Nonlinear regression analysis and its applications. New York : Wiley, 1988.
- Berkley, M. A., Kitterle, F. and Watkins, D. W. (1975). Grating visibility as a function of orientation and retinal eccentricity. Vision Research, 15, 239-244.
- Bradley, A., Switkes, E. and De Valois, K. K. (1988). Orientation and spatial frequency selectivity of adaptation to color and luminance gratings. Vision Research, 28, 841-856.
- Brown, W.R. and MacAdam, D. L. (1949). Visual sensitivities to combined chromaticity and luminance differences. Journal of the Optical Society of America, 39, 808-834.
- Camisa, J. M., Blake, R. and Lema, S. (1977). The effects of temporal modulation on the oblique effect in humans. Perception, 6, 165-171.
- Campbell, F. W., Kulikowski, J. J. and Levinson, J. (1966a). The effect of orientation on the visual resolution of gratings. Journal of Physiology, 187, 427-436.
- Campbell, F. W. and Kulikowski, J. J. (1966b). Orientation selectivity of the human visual system. Journal of Physiology, 187 437-445.
- Cecala, A. J. and Garner, W. R. (1986). Internal frame of reference as a determinant of the oblique effect. Journal of Experimental Psychology: Human Perception and Performance, 12, 314-323.
- De Valois, R., Smith, C. J., Kitai, S. T. and Karoly, J. (1958). Response of single cells in monkey lateral geniculate nucleus to monochromatic light. Science, 127(32), 238-239.

- De Valois, K. K. and Switkes, E. (1983). Simultaneous masking interactions between chromatic and luminance gratings. Journal of the Optical Society of America, 73, 11-18.
- De Valois, R. L. and De Valois, K. K. (1988). Spatial Vision. New York: Oxford Science Publications.
- Essock, E. A. (1980). The oblique effect of stimulus identification considered with respect to two classes of oblique effects. Perception, 9, 37-46.
- Graham, N. V. (1989). Visual pattern analyzers. New York: Oxford University Press.
- Hartline, H. K. (1938). The response of single optic nerve fibers of the vertebrate eye to illumination of the retina. American Journal of Physiology, 121, 400-415.
- Kaiser, P. K. and Boynton, R. M. (1996). Human Color Vision (2nd ed.). Washington, D. C.: Optical Society of America.
- Kelly, D. H. (1975). No oblique effect in chromatic pathways. Journal of the Optical Society of America, 65, 1512-1514.
- Krebs, W. K. (1992). The investigation of tunnel vision. Does stimulus orientation and location in a peripheral display influence the effects of tunnel vision? Doctoral Thesis. University of Louisville, KY.
- Koenderink, J. J. and Van Doorn, A. J. (1980). Spatial summation for complex bar patterns. Vision Research, 20, 169-176.
- Larsen, R. J. and Marx, M. L. (1986). An introduction to mathematical statistics and its applications (2nd ed.). Englewood, NJ: Prentice-Hall.
- Lasaga, M. I. and Garner, W. R. (1983). Effect of line orientation on various information-processing tasks. Journal of Experimental Psychology: Human Perception and Performance, 9, 215-225.
- Leehy, S. C. Moskowitz-Cook, A., Brill, S. and Held, R. (1975). Orientation anisotropy in infant vision. Science, 190, 900-902.
- Lennie, P. (1974). Head orientation and meridional variations in acuity. Vision Research, 14, 107-111.
- Livingstone, M. and Hubel, D. (1984). Anatomy and physiology of a color system in a primate primary visual cortex. Journal of Neuroscience, 4, 309-356.

- MacAdam, D. L. (1942). Visual sensitivities to color differences in daylight. Journal of the Optical Society of America, 32, 247-274.
- Maffei, L. and Campbell, F. W. (1970). Neurophysical localization of the vertical and horizontal visual coordinates in man. Science, 167, 386-387.
- Maffei, L. and Fiorentini, A. (1973). The visual cortex of a spatial frequency analyzer. Vision Research, 13, 1255-1267.
- Mayer, M. J. (1983). Practice improves adults sensitivity to diagonals. Vision Research, 23, 547-550.
- McIlwain, J. T. (1996). An introduction to the biology of vision. Cambridge: Cambridge University Press.
- Merigan, W. H. (1989). Chromatic and achromatic vision of macaques: Role of the P pathway. The Journal of Neuroscience, 9, 776-783.
- Michael, C. R. (1978). Color vision mechanisms in monkey striate cortex: Simple cells with dual opponent-color receptive fields. Journal of Neurophysiology, 41, 1233-1249.
- Mitchell, D. E. and Muir, D. W. (1976). Does the tilt after-effect occur in the oblique meridian? Vision Research, 16, 609-613.
- Mullen, K. T. (1985). The contrast sensitivity of human colour vision to red-green and blue-yellow chromatic gratings. Journal of Physiology, 359, 381-400.
- Murasugi, C. M. and Cavanagh, P. (1989). Anisotropy in the chromatic channel: A horizontal-vertical effect. Spatial Vision, 3(4), 281-291.
- Noorlander, C., Heuts, M. J. and Koenderink, J. J. (1980). Influence of the target size on the detection threshold for luminance and chromaticity contrast," Journal of the Optical Society of America, 70, 1116-1121.
- Noorlander, C., Heuts, M. J. and Koenderink, J. J. (1981). Sensitivity to spatiotemporal combined luminance and chromaticity contrast. Journal of the Optical Society of America, 71, 453-459.
- Noorlander, C. and Koenderink, J. J. (1983). Spatial and temporal discrimination ellipsoids in color space. Journal of the Optical Society of America, 73, 1533-1543.

- Poggio, G. F., Baker, F. H., Mansfield, R. J. , Sillito, A. and Grigg, P. ( 1975). Spatial and chromatic properties of neurons subserving foveal and parafoveal vision in rhesus monkey. Brain Research, 100, 25-59.
- Rabin, J., Adams, J. A and Switkes, E. (1992). Perceptual ambiguity and the short wavelength sensitive visual pathway. Vision Research, 32, 399-401.
- Rabin, J., Switkes, E., Crognale, M., Schneck, M.E. and Adams, A. J. (1994). Visual evoked potentials in three-dimensional color space: correlates of spatio-chromatic processing. Vision Research, 34, 2657-2671.
- Rock, I. and Heimer, W. (1957). The effect of retinal and phenomental orientation on the perception of form. The American Journal of Psychology, 70, 493-511.
- Schiffman, H. R. (1996). Sensation and Perception (4th ed.). New York: John Wiley and Sons.
- Sekuler, R. and Blake, R. (1994). Perception (3rd ed.). New York: McGraw-Hill.
- Sellers, K. L., Chioran, G. M., Dain, S. J., Benes, S. C., Lubow, M., Rammohan, K. and King-Smith, P.E. (1986). Red-green mixture thresholds in congenital and acquired color defects. Vision Research, 26, 1083-1097.
- Silberstein, L. and MacAdam, D. L. (1945). The distribution of color matchings around a color center. Journal of the Optical Society of America, 35, 32-39.
- Switkes, E., Bradley, A. and De Valois, K. K. (1988). Contrast dependence and mechanisms of masking interactions among chromatic and luminance gratings. Journal of the Optical Society of America A, 5, 1149-1162.
- Thorell, L. G., De Valois, R. L. and Albrecht, D. G. (1984). Spatial mapping of monkey V1 cells with pure color and luminance stimuli. Vision Research, 24, 751-769.
- Tovee, M. J. (1996). An introduction to the visual system. Cambridge: Cambridge University Press.
- Wandell, B. A. (1985). Color measurement and discrimination. Journal of the Optical Society of America A, 2, 62-71.
- Ware, C. and Mitchell, D. E. (1974). The spatial selectivity of the tilt aftereffect. Vision Research, 14, 735-737.



Watson, A. B. and Pelli, D.G. (1983). QUEST: A Bayesian adaptive psychometric method. Perception and Psychophysics, 33(2), 113-120.

Webster, M. A., De Valois, K. K. and Switkes, E. (1990). Orientation and spatial-frequency discrimination for luminance and chromatic gratings. Journal of the Optical Society of America A, 7, 1034-1049.

Who is Fourier? (1995). Belmont, MA: Language Research Foundation.



## BIBLIOGRAPHY

- Burbeck, C.A. and Kelly, D. H. (1980). Spatiotemporal characteristics of visual mechanisms: excitatory-inhibitory model. Journal of the Optical Society of America, 70, 1121-1126.
- Burbeck, C. A. and Regan, D. (1983). Independence of orientation and size in spatial discriminations. Journal of the Optical Society of America, 73, 1691-1694.
- Cavanagh, P., MacLeod, D. I. and Anstis, S. M. (1987). Equiluminance: Spatial and temporal factors and the contribution of blue-sensitive cones. Journal of the Optical Society of America A, 4(8), 1428-1438.
- Cavanagh, P., Tyler, C. W. and Favreau, O. E. (1984). Perceived velocity of moving chromatic gratings. Journal of the Optical Society of America A, 1, 893-899.
- Cavonius, C.R. and Estevez, O. (1975). Sensitivity of human color mechanisms to gratings and flicker. Journal of the Optical Society of America, 65, 966-968.
- Coletta, N. J., Segu, P. and Tiana, C. L. (1993). An oblique effect in parafoveal motion perception. Vision Research, 33, 2747-2756.
- Cook, T. D. and Campbell, D. T. (1979). Quasi-experimentation design and analysis issues for field settings. Boston: Houghton Mifflin.
- De Valois, R. L., Albrecht, D. G. and Thorell, L. G. (1982). Spatial frequency selectivity of cells in macaque visual cortex," Vision Research, 22, 545-559.
- Elsner, A. E. (1978). Hue difference contours can be used in processing orientation information. Perception and Psychophysics, 24, 451-456.
- Elsner, A. E., Pokorny, J. and Burns, S. A. (1986). Chromaticity discrimination: Effects of luminance contrast and spatial frequency. Journal of the Optical Society of America A, 3, 916-920.
- Essock, E. A. (1982). Anisotropies of perceived contrast and detection speed. Vision Research, 22, 1185-1191.
- Essock, E. A. (1990). The influence of stimulus length on the oblique effect of contrast sensitivity. Vision Research, 30, 1243-1246.

- Favreau, O.E. and Cavanagh, P. (1983). Interocular transfer of a chromatic frequency shift. Vision Research, 23, 951-957.
- Fisher, C. B. (1980). Children's memory for line orientation: A reexamination of the 'oblique effect'. Journal of Experimental Child Psychology, 29, 446-459.
- Flanagan, P., Cavanagh, P. and Favreau, O.E. (1987). Orientation is processed in chromatic channels. Journal of the Optical Society of America A, 4 (13), 115.
- Flanagan, P., Cavanagh, P. and Favreau, O. E. (1990). Independent orientation-selective mechanisms for the cardinal directions of colour space. Vision Research, 30, 769-778.
- Flitcroft, D. I. (1989). The interactions between chromatic aberration, defocus and stimulus chromaticity: Implications for visual physiology and colorimetry. Vision Research, 34, 349-360.
- Granger, E.M. and Heurtley, J. C. (1973). Visual chromaticity-modulation transfer function. Journal of the Optical Society of America, 63, 1173-1174.
- Guth, S. L. and Lodge, H. R. (1973). Heterochromatic additivity, foveal spectral sensitivity, and a new color model. Journal of the Optical Society of America, 63, 450-462.
- Heeley, D. W. and Buchanan-Smith, H. M. (1990). Recognition of Stimulus Orientation. Vision Research, 30, 1429-1437.
- Heeley, D. W. and Timney, B. (1988). Meridional anisotropies of orientation discrimination for sine wave gratings. Vision Research, 28, 337-344.
- Heeley, D. W. and Timney, B. (1989). Spatial frequency discrimination at different orientations. Vision Research, 29, 1221-1228.
- Hirsch, J. and Hylton, R. (1985). Spatial-frequency discrimination at low frequencies: evidence for position quantization by receptive fields. Journal of the Optical Society of America A, 2, 128-135.
- Hoekstra, J., Van Der Goot, D. P., Van Der Brink, G. and Bilsen, F. A., The influence of the number of cycles upon the visual contrast threshold for spatial sine wave patterns. Vision Research, 14, 365-3684.
- Howarth, P. A. and Bradley, A. (1986). The longitudinal chromatic aberration of the human eye and its correction. Vision Research, 26, 361-366.

- Howell, E. R. and Hess, R. F. (1978). The functional area for summation to threshold for sinusoidal gratings. Vision Research, 18, 369-374.
- Ingling, C. R., Jr. and Martinez-Uriegas, E. (1985). The spatiotemporal properties of the r-g x-cell channel. Vision Research, 25, 33-38.
- Jouen, F. (1985). The influence of body position on perception of orientation in infants. Behavioural Brain Research, 15, 241-245.
- Kelly, D. H. (1974). Spatio-temporal frequency characteristics of color-vision mechanisms. Journal of the Optical Society of America, 64, 983-990.
- Kelly, D. H. (1975). Luminous and chromatic flickering patterns have opposite effects. Science, 188, 371-372.
- Kelly, D. H. (1981). Nonlinear visual responses to flickering sinusoidal gratings. Journal of the Optical Society of America, 71, 1051-1055.
- Kelly, D. H. (1983). Spatiotemporal variation of chromatic and achromatic contrast thresholds. Journal of the Optical Society of America, 73, 1051-1055.
- Kelly, D. H. and Burbeck, C. A. (1980). Motion and vision. III. Stabilized pattern adaptation. Journal of the Optical Society of America, 70, 1283-1289.
- Kelly, D. H. and Van Norren, D. (1977). Two-band model of heterochromatic flicker. Journal of the Optical Society of America, 67, 1081-1091.
- King-Smith, P. E. (1975). Visual detection analysed in terms of luminance and chromatic signals. Nature, 255, 69-70.
- King-Smith, P. E. and Carden, D. (1976). Luminance and opponent-color contributions to visual detection and adaptation to temporal and spatial integration. Journal of the Optical Society of America, 66, 709-717.
- King-Smith, P. E., Chioran, G. M., Sellers, K. L. and Alvarez, S. A. (1983). Normal and deficient colour discrimination analysed by colour television. Colour Vision, 167-172.
- Kranda, K. and King-Smith, P. E. (1979). Detection of coloured stimuli by independent linear systems. Vision Research, 19, 733-745.
- Krauskopf, J. and Farell, B. (1991). Vernier acuity: Effects of chromatic content, blur and contrast. Vision Research, 31, 735-749.

- Krauskopf, J., Williams, D. R., Mandler, M. B. and Brown, A.M. (1986). Higher order color mechanisms. Vision Research, 26, 23-32.
- Larsen, R. J. and Marx, M. L. (1986). An introduction to mathematical statistics and its applications (2nd ed.). Englewood, NJ: Prentice-Hall.
- Lasaga, M. I. and Garner, W. R. (1983). Effect of line orientation on various information-processing tasks. Journal of Experimental Psychology: Human Perception and Performance, 9, 215-225.
- Lennie, P. (1980). Parallel visual pathways: A review. Vision Research, 20, 561-594.
- Lindsey, D. T. and Teller, D. Y. (1990). Motion at isoluminance: Discrimination/detection ratios for moving isoluminant gratings. Vision Research, 30, 1751-1761.
- Livingstone, M. and Hubel, D. (1986). Segregation of form, color, movement and depth: Anatomy, physiology, and perception. Science, 240, 740-749.
- MacLeod, D. I. and Boynton, R. M. (1979). Chromaticity diagram showing cone excitation by stimuli of equal luminance. Journal of the Optical Society of America, 69, 1183-1186.
- Mansfield, R. J. (1974). Neural basis of orientation perception in primate vision. Science, 186, 1133-1135.
- Marimont, D. H. and Wandell, B. A. (1994). Matching color images: the effects of axial chromatic aberration. Journal of the Optical Society of America A, 11, 3113-3122.
- Matin, E., Rubsamen, C. and Vannata, D. (1987). Orientation discrimination as a function of orientation and spatial frequency. Perception and Psychophysics, 41, 303-307.
- Mayer, M. J. (1983). Non-astigmatic children's contrast sensitivities differ from anisotropic patterns of adults. Vision Research, 23, 551-559.
- McIlwain, J. T. (1996). An introduction to the biology of vision. Cambridge: Cambridge University Press.
- Mitchell, D. E., Freeman, R. D. and Westheimer, G. (1967). Effect of orientation on the modulation sensitivity for interference fringes on the retina. Journal of the Optical Society of America, 57, 246-249.
- Nagy, A. L., Eskew, R. T., Jr. and Boynton, R. M. (1987). Analysis of color-matching ellipses in a cone-excitation space. Journal of the Optical Society of America A, 4, 756-768.

Nelson, J. I., Kupersmith, M. J., Seiple, W. H., Weiss, P. A. and Carr, R. E. (1984). Spatiotemporal conditions which elicit or abolish the oblique effect in man: Direct measurements with swept evoked potential. Vision Research, 24, 579-586.

Orban, G. A., Vandebussche, E. and Vogels, R. (1984). Human orientation discrimination tested with long stimuli. Vision Research, 24, 121-128.

Palmer, J., Mobley, L. A. and Teller, D. Y. (1993). Motion at isoluminance: discrimination/detection ratios and the summation of luminance and chromatic signals, Journal of the Optical Society of America A, 10, 1353-1362.

Parker, J. E., Krebs, W. K., Marsh, J. S., Still, D. L. and Temme, L. A. (1994). The Sharper Image: Implementing a Fast Fourier Transformation (FFT) to Enhance a Video-Captured Image. (NAMRL Special Report 94-1). Pensacola, FL: Naval Aerospace Medical Research Laboratory.

Quinn, P. C. and Lehmkuhle, S. (1983). An oblique effect of spatial summation. Vision Research, 23, 655-658.

Regan, D. (1977). Steady-state evoked potentials. Journal of the Optical Society of America, 67, 1475-1489.

Regan, D. and Price, P. (1994). Periodicity in orientation discrimination and the unconfounding of visual information. Vision Research, 34, 2657-2671.

Regan, B. C., Reffin, J. P. and Mollon, J. D. (1994). Luminance noise and the rapid determination of discrimination ellipses in colour deficiency," Vision Research, 34, 1279-1299.

Reisbeck, T. E. and Gegenfurtner, K. R. (1996). Effects of contrast, temporal Frequency and chromatic content on orientation discrimination (Technical Report No. 32). Max-Planck-Institut.

Robson, J. G. (1966). Spatial and temporal contrast-sensitivity functions of the visual system. Journal of the Optical Society of America, 56, 1141-1142.

Saarinen, J. and Levi, D. M. (1995). Orientation anisotropy in vernier acuity. Vision Research, 35, 2449-2461.

Savoy, R. L. and McCann, J. J. (1965). Visibility of low-spatial-frequency sine-wave targets: Dependence on number of cycles. Journal of the Optical Society of America, 65, 343-350.

- Sekiguchi, N., Williams, D. R. and Brainard, D. H. (1993). Aberration-free measurements of the visibility of isoluminant gratings. Journal of the Optical Society of America A, 10, 1121-1126.
- Stromeyer, C. F., III, Klein, S., Dawson, B. M. and Spillman, L. (1982). Low spatial-frequency channels in human vision: Adaptation and masking. Vision Research, 22, 225-233.
- Stromeyer, C. F., III, Kranda, K. and Sternheim, C. E. (1978). Selective chromatic adaptation at different spatial frequencies. Vision Research, 18, 427-437
- Stromeyer III, C. F., Kronauer, R. E., Madsen, J. C. and Klein, S. A. (1984). Opponent-Movement Mechanisms in Human Vision. Journal of the Optical Society of America A, 1, 876-884.
- Tansley, B. W. and Boynton, R. M. (1978). Chromatic border perception: The role of red- and green-sensitive cones. Vision Research, 18, 683-697.
- Thomas, J. P. and Gille, J. (1979). Bandwidth of orientation channels in human vision. Journal of the Optical Society of America, 69, 652-660.
- Thornton, J. E. and Pugh, E.N., Jr. (1983). Red/green color opponency at detection threshold. Science, 219, 191-193.
- Tootle, J. S. and Berkley, M. A. (1983). Contrast sensitivity for vertically and obliquely oriented gratings as a function of grating area. Vision Research, 23, 907-910.
- Ts'o, D. Y. and Gilbert, C. D. (1988). The organization of chromatic and spatial interactions in the primate striate cortex. The Journal of Neuroscience, 8, 1712-1727.
- Van Der Horst, G. J. and Bouman, M. A. (1969). Spatiotemporal chromaticity discrimination. Journal of the Optical Society of America, 59, 1482-1488.
- Valle, V., Rivera, R. M. and Matin, E. (1984). Effects of intertrial interval orientation, and adaptation on orientation discrimination measured with a yes-no signal detection paradigm. Perceptual and Motor Skills, 59, 743-748.
- Vogels, R. and Orban, G. A. (1986). Decision processes in visual discrimination of line orientation. Journal of Experimental Psychology: Human Perception and Performance, 12, 115-132.
- Vogels, R. and Orban, G. A. (1985). The effect of practice on the oblique effect in line orientation judgements. Vision Research, 25, 1679-1687.



Williams, L. J. (1982). The oblique effect: A new slant on things. Perceptual and Motor Skills, vol. 54, 992-994.

Wyszecki, G. and Fielder, G. H. (1971). New color-matching ellipses. Journal of the Optical Society of America, 61, 1135-1152.

Zulauf, M., Flammer, J. and Signer, C. (1988). Spatial brightness contrast sensitivity measured with white, green, red and blue light. Ophthalmologica, 196, 43-48.

Zeki, S. (1993). A Vision of the Brain. London: Blackwell Scientific Publications.



## INITIAL DISTRIBUTION LIST

1. Defense Technical Information Center ..... 2  
 8725 John J. Kingman Rd, STE 0944  
 Ft. Belvoir, Virginia 22060-6218
  
2. Dudley Knox Library ..... 2  
 Naval Postgraduate School  
 411 Dyer Rd.  
 Monterey, California 93943-5101
  
3. Director Training and Education ..... 1  
 MCCDC, Code C46  
 1019 Elliot Rd.  
 Quantico, Virginia 22134-5027
  
4. Director, Marine Corps Research Center ..... 2  
 MCCDC, Code C40RC  
 2040 Broadway Street  
 Quantico, Virginia 22134-5107
  
5. Director Studies and Analysis Division ..... 1  
 MCCDC, Code C45  
 300 Russel Road  
 Quantico, Virginia 22134-5130
  
6. Marine Corps Representative ..... 1  
 Naval Postgraduate School  
 Code 037, Bldg. 234, HA-220  
 699 Dyer Road  
 Monterey, CA 93940
  
7. Marine Corps Tactical Systems Support Activity ..... 1  
 Technical Advisory Branch  
 Attn: Maj J.C. Cummiskey  
 Box 555171  
 Camp Pendleton, CA 92055-5080
  
8. W. K. Krebs, Code OR/Kw ..... 1  
 Naval Postgraduate School  
 Monterey, CA 93943-5000

- 9. S. E. Buttrey, Code OR/Sb ..... 1  
Naval Postgraduate School  
Monterey, CA 93943-5000
  
- 10. P. G. Curran ..... 1  
202 Speight Street  
Havelock, NC 28532

WUDLEY KNOW LIBRARY  
NAVAL POSTGRADUATE SCHOOL  
MONTEREY CA 93943-5101

DUDLEY KNOX LIBRARY



3 2768 00338552 7